

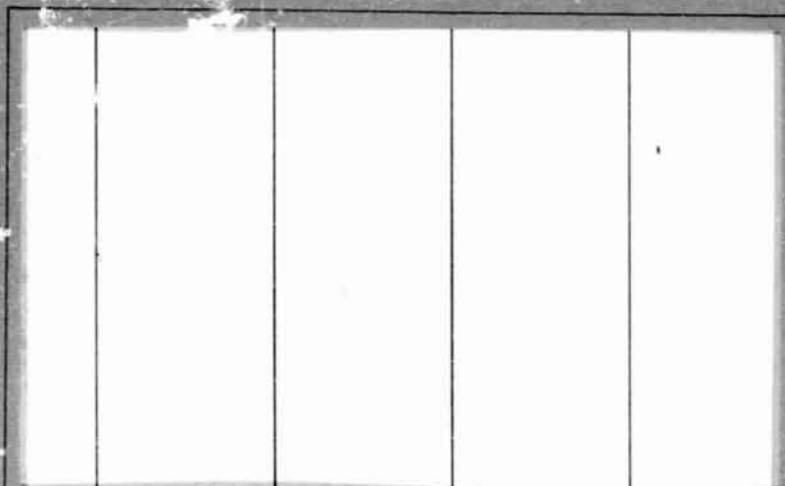
(NASA-CR-144171) VEHICLE SYSTEMS AND  
PAYLOAD REQUIREMENTS EVALUATION Final  
Report, Oct. 1970 - Dec. 1975 (Battelle  
Columbus Labs., Ohio.) 167 p HC \$6.75

N76-17187

CSCL 22B G3/18

Unclass  
14151

## RESEARCH REPORT



# Battelle

Columbus Laboratories



FINAL REPORT

on

VEHICLE SYSTEMS AND PAYLOAD  
REQUIREMENTS EVALUATION  
(October, 1970 - December, 1975)

Prepared for


NATIONAL AERONAUTICS AND SPACE ADMINISTRATION  
GEORGE C. MARSHALL SPACE FLIGHT CENTER  
MARSHALL SPACE FLIGHT CENTER, ALABAMA 35812


Contract No. NAS8-26491

December 23, 1975

by

F. G. Rea, J. L. Pittenger, R. J. Conlon, and J. D. Allen

  
F. G. Rea, Study Manager

  
Approved by: B. W. Davis, Manager  
Space Systems and Applications Section

BATTELLE  
Columbus Laboratories  
505 King Avenue  
Columbus, Ohio 43201

### ABSTRACT

This report summarizes work done on "Vehicle Systems and Payload Requirements Evaluation" during the five years of the study. Reference is made to specific previous Interim Scientific Reports. Work done since the last Interim Scientific Report is reported on in more detail. This includes the analysis of Redundant Systems. An investigation of potential problems with the Gravitational Red Shift mission, and development of the Interactive Graphic Orbit Selection computer program.

## TABLE OF CONTENTS

	<u>Page</u>
INTRODUCTION . . . . .	1
Program Objectives. . . . .	1
Project Tasks . . . . .	1
SUMMARY. . . . .	3
Update and Maintain Computer Codes (Task 1). . . . .	3
HEAO . . . . .	3
Investigate Astrionics for OSS Missions (Task 2) . . . . .	4
Investigate Scout Astrionics Requirements (Task 3) . . . . .	4
Perform Mission Requirements Assignments (Task 4). . . . .	4
BACKGROUND . . . . .	5
Related Prior Work. . . . .	5
Techniques for Evaluating Astrionics for Interplanetary Missions. . . . .	6
Techniques for Evaluating Integrated Avionics. . . . .	6
Battelle's Navigation Error Analysis Program (NEAP) . . . . .	8
Concurrent Related Projects . . . . .	8
NASA Launch Vehicle Project (NLVP) . . . . .	8
Delta Inertial Guidance System (DIGS) Project. . . . .	8
TECHNICAL DISCUSSION . . . . .	9
Task 1 Development and Maintenance of Techniques and Computer Codes for the Evaluation and Analysis of Astrionics Systems. . . . .	9
Task 2 Investigate Astrionics Requirements for OSS Missions. . . . .	11
Modular Redundant System Reliability . . . . .	11
Development of an Analytic Method . . . . .	11

TABLE OF CONTENTS  
(Continued)

	<u>Page</u>
Sample Calculation . . . . .	16
Task 3 Investigate Scout Astrionics Requirements . . . . .	28
Spun Stage Simulation and Error Model. . . . .	28
Investigation of the Dynamic Behavior of the Red Shift Probe. . . . .	28
Eddy Current Damping . . . . .	29
Spinning Stage Simulation. . . . .	31
Equation of Motion. . . . .	35
Six Degree of Freedom Simulation . . . . .	37
Error Sources Considered . . . . .	44
Ammonia Venting . . . . .	44
Fourth-Stage Tipoff . . . . .	44
Thrust Misalignment . . . . .	44
Fourth-Stage Burnout Unbalance. . . . .	48
Payload Unbalances . . . . .	48
Thrust Misalignment and Tipoff. . . . .	48
Concluding Remarks . . . . .	54
Task 4 Perform Mission Requirements Assessments. . . . .	55
IGOS Program Description . . . . .	57
Earth-Observation Coverage . . . . .	60
Radiation Environment . . . . .	60
Orbit to Sun Precession. . . . .	61
Orbit Decay and Launch-Vehicle Injection Accuracy. . . . .	61
Launch-Vehicle Payload Capabilities. . . . .	64
IGOS Mathematical Models . . . . .	69
Earth Coverage Model . . . . .	69

TABLE OF CONTENTS  
(Continued)

	<u>Page</u>
Earth-Observation Sensor Model . . . . .	70
Longitude Viewed . . . . .	76
Distribution of Gaps . . . . .	84
Combined Coverage Model. . . . .	93
Radiation Environment . . . . .	97
Orbit-to-Sun Precession . . . . .	97
Orbit Decay . . . . .	98
Launch Vehicle Injection Error Model. . . . .	102
Scout Error Model . . . . .	102
Launch Vehicle Performance Model. . . . .	102
CONCLUSIONS AND RECOMMENDATIONS . . . . .	106
Task 1 . . . . .	106
EOMP-I. . . . .	106
IGOS . . . . .	106
Specific Site Coverage . . . . .	107
Side Looking and Multiple Sensors. . . . .	107
Elliptical Orbits . . . . .	107
Shuttle Performance Calculations . . . . .	107
Other Computer Codes . . . . .	108
EOMP-II . . . . .	108
Monte Carlo. . . . .	108
ABBACUS . . . . .	109
Spun Stage Simulation. . . . .	109
Task 2 . . . . .	109
Task 3 . . . . .	109
Task 4 . . . . .	110
REFERENCES . . . . .	111

TABLE OF CONTENTS  
(Continued)

	<u>Page</u>
APPENDIX A	
IGOS USERS GUIDE . . . . .	A-1

APPENDIX B	
SAMPLE IGOS WORK SESSION . . . . .	B-1

<u>LIST OF TABLES</u>	
Table 1. VSPRE Project Tasks . . . . .	2
Table 2. VSPRE Computer Codes . . . . .	10
Table 3. Summary of Roll Rate Decay Calculations. . . . .	33
Table 4. Values Used in Simulation . . . . .	39
Table 5. Prestored INCLINATIONS FOR IGOS PERFORMANCE TABLES . . . . .	105

<u>LIST OF FIGURES</u>	
Figure 1. Block Diagram of Integrated Astrionics . . . . .	7
Figure 2. Performance and Reliability Specifications. . . . .	17
Figure 3. Component Requirements of Individual Tasks. . . . .	19
Figure 4. Equipment Allocation and Reliability State Propagation. . .	20
Figure 5. Nominal [No-Failures] Equipment Utilization . . . . .	27
Figure 6. Distance of Payload From Center of Earth . . . . .	32
Figure 7. Spin Decay Due to Eddy Currents . . . . .	34
Figure 8a. Several Nozzles of Infinitesimal Area . . . . .	36
Figure 8b. One Large Nozzle . . . . .	36
Figure 9. Integration Over Nozzle Area. . . . .	36

LIST OF FIGURES  
(Continued)

	<u>Page</u>
Figure 10. Sample Graphic Output. . . . .	41
Figure 11. Definition of Graphical . . . . .	42
Figure 12. Example of Graphic Output Illustrating Burnout Anomaly . .	43
Figure 13. Effect of Ammonia Venting for First 100 Seconds After Fourth-Stage Ignition . . . . .	45
Figure 14. Effect of Tipoff ( $t=0-40$ sec). . . . .	46
Figure 15. Effect of Thrust Misalignment ( $t=0-30$ sec) . . . . .	47
Figure 16. Effect of Worst-Case Combination of Thrust Misalignment and Tipoff ( $t=0-30$ sec) . . . . .	49
Figure 17. Thrust Models Used . . . . .	50
Figure 18. Final Coning With Single-Segment Fuel Model. . . . .	51
Figure 19. Final Coning With Three-Segment Fuel Model . . . . .	52
Figure 20. Final Coning With Eight-Segment Fuel Model . . . . .	53
Figure 21. IGOS Operation . . . . .	58
Figure 22. Typical IGOS Graphical Output. . . . .	59
Figure 23. Sun-Orbit Precession Limit . . . . .	62
Figure 24. Orbit Decay and Launch-Vehicle Injection Accuracy. . . . .	63
Figure 25. Launch Vehicle Payload Weight Contours . . . . .	65
Figure 26. Sample Problem Coverage, Radiation, and Sun-Orbit Precession Requirements . . . . .	67
Figure 27. Sample Problem With Trial Orbit and Launch Vehicle . . . .	68
Figure 28. Model Parameters . . . . .	73
Figure 29. Flow Diagram for Sensor Model. . . . .	74
Figure 30. Field-of-View Half-Angle as a Function of Altitude. . . . .	75
Figure 31. Single Pass Earth Coverage . . . . .	77
Figure 32. Longitude Viewed (V) Versus Inclination. . . . .	80



LIST OF FIGURES  
(Continued)

	<u>Page</u>
Figure 33. View Versus Inclination and Altitude . . . . .	81
Figure 34. Successive Ground Tracks . . . . .	82
Figure 35. Locus of Constant Shift (S) Versus Inclination and Altitude . . . . .	85
Figure 36. Successive Modes . . . . .	86
Figure 37. Gap Sizes Versus Shift . . . . .	87
Figure 38. Resonant Points Versus Orbit Shift . . . . .	90
Figure 39. Maximum Gap Versus Orbit Shift . . . . .	91
Figure 40. Resonant Points Versus Orbit Shift . . . . .	92
Figure 41. Maximum Gaps Versus Orbit Shift. . . . .	92
Figure 42. Maximum Gap Versus Altitude and Inclination. . . . .	94
Figure 43. Combined View and Maximum Gap Versus Inclinationa and Altitude . . . . .	95
Figure 44. Typical Coverage Model Output. . . . .	96
Figure 45. $f_1(h)$ , The Normalized Life Time . . . . .	100
Figure 46. $f_1(I)$ , The Inclination Factor . . . . .	100
Figure 47. Solar Activity Time Factor $f_t(t)$ . . . . .	101
Figure 48. One Sigma Scout Altitude Dispersions . . . . .	103

VEHICLE SYSTEMS AND PAYLOAD REQUIREMENTS EVALUATION  
(October 1970 - December 1975)

by

F. G. Rea, J. L. Pittenger, R. J. Conlon, and J. D. Allen

INTRODUCTION

This report presents the results of the work on "Vehicle Systems and Payload Requirements Evaluation" (VSPRE) for NASA Marshall Space Flight Center (MSFC) under Contract Number NAS 8-26491 between October, 1970 and December, 1975. Background information and a summary of the study results are presented for the entire project along with detailed technical discussion, recommendations, and conclusions of the past 18 months. Details of the first four years have been published earlier in Interim Reports (Reference 1, 2, and 3\*).

Program Objectives

The objective of this program was to develop techniques for identifying launch vehicle system requirements for NASA automated space missions, and to conduct analyses to assist NASA OSS in the management of its related Supporting Research and Technology (SR&T) programs. Achievement of this overall objective required development of various computer programs. These include extensions of previously developed system analysis and evaluation programs for the analysis of a broader scope of vehicle systems. In addition, these programs were applied to the analysis of several NASA mission astrionics requirements. For these missions, trade-off evaluation of competitive systems and analysis of operational requirements were performed.

Project Tasks

The efforts of this study have been conducted under specific tasks. The contract modification of April, 1974 redefined the task numbers from those in use since 1970. For convenience in referring to earlier reports, Table 1 shows the old and new task number definitions. All tasks discussed in this report are under the new numbers.

\*References are listed at the end of this report.

TABLE 1. VSPRE PROJECT TASKS

Task Description	Old Task No. (Prior to April, 1974)	New Task No. (After April, 1974)
Update and Maintain Computer Codes	1	1
Investigate HEAO Astrionics Requirements	2	--
Investigate Astrionics for OSS Missions	3	2
Investigate Scout Astrionics Requirements	4	3
Perform Mission Requirements Assessments	**	4

\*\* This effort was begun in 1973 under Old Task 3.

### SUMMARY

The following paragraphs summarize the effort on each of the project tasks. Detailed discussions appear in the Technical Discussion Section of this report.

#### Update and Maintain Computer Codes (Task 1)

Several computer programs have been developed under this task and delivered to MSFC. Most significant of these are:

- EOMP-I (Earth Orbit Mission Program - I) which performs linear error analysis of launch vehicle dispersions for both vehicle and navigation system factors, and
- IGOS (Interactive Graphic Orbit Selection) program which allows the user to select orbits which satisfy mission requirements and to evaluate the necessary injection accuracy. This program was written as part of the Task 4 investigation of mission requirements for astronics improvements.

### HEAO

The High Energy Astronomical Observatory (HEAO) mission was investigated under the original VSPRE Task 2. At that time it was proposed that HEAO be launched on a Titan IIID with a Lockheed Orbit Adjust Stage (OAS) for final orbit placement. VSPRE efforts were:

- Calculation of the Titan IIID open loop guidance system injection errors,
- Analysis of the probability of obtaining sufficient parking orbit life time to adequately track the vehicle, and
- Development of an optional OAS thrusting policy.

Results of these studies (References 1, 2 and 3) indicated the Titan IIID/OAS vehicle was feasible.

Subsequently the HEAO payload weight was reduced, and the payload was reassigned to an Atlas vehicle.

### Investigate Astrionics for OSS Missions (Task 2)

A number of specific analysis studies have been directed by the COR (Contracting Officer's Representative). Astrionics requirements for HEAO and LAGEOS, have been discussed in previous reports (Reference 1, 2 and 3). The Red Shift mission requirements for Scout are discussed under Task 3 in this report.

Recent Task 2 activity has concentrated on an evaluation of the requirements for a high reliability computer, specifically the ARMMS (Automatically Reconfigurable Modular Multiprocessor System) computer under development at MSFC. The evaluation of ARMMS resulted in the writing of a preliminary version of a generalized computer program, ABBACUS for the analysis of a reconfigurable astrionics system.

### Investigate Scout Astrionics Requirements (Task 3)

Several potential modifications to Scout astrionics have been evaluated and the results previously published in References 2 and 3. No conclusive recommendations regarding the need for the modifications could be made due to a lack of firm mission requirements for increased injection accuracy.

Most recently, Task 3 effort concentrated on the application of Scout for the Gravitational Red Shift mission. This mission is a sub-orbital launch with the payload attached to the spinning, depleted, fourth stage. The results of the study indicate no problems are encountered due to the operation of the payload while attached to the spinning fourth stage.

### Perform Mission Requirements Assignments (Task 4)

When establishing mission requirements, the planners frequently stated, as a requirement, the known accuracy of the vehicle they assume would be assigned to their mission. In other cases, arbitrarily small errors are specified to minimize the chance of failure without regard to the implied increased astrionics costs.

This situation led to the development of the Interactive Graphics Orbit Selection (IGOS) programs. IGOS displays both the mission requirements (orbits which met the requirements) and the various launch vehicle capabilities

(payload weight and injection accuracy). The program serves as the basis for concise dialog between mission and vehicle oriented specialists. IGOS is a tool for either orbit selection (mission design), or for the evaluation of launch vehicle accuracy requirements. In addition to the details presented in the Technical Discussion, a users manual and a sample work session are presented in Appendices A and B.

## BACKGROUND

### Related Prior Work

The astrionics/avionics evaluation techniques extended under the contract were originally developed by Battelle for NASA/OSSA under contract with the NASA Electronics Research Center (ERC), Contract Number NAS12-550, and for the U. S. Air Force (USAF) Avionics Laboratory, Contract Number F33615-69-C-1402. The ERC contract was originally initiated to develop an evaluation technique for inertial sensors to be included in strapdown inertial navigation systems. To effectively evaluate sensors for strapdown application, it was determined that a more comprehensive systems level study including other astrionics subsystems was necessary.

The systems evaluation techniques developed under the ERC contract were extended to cover avionics under the USAF Avionics Laboratory contract. In analyzing integrated avionics systems, the assumption that each item of hardware is associated with a particular function (such as navigation or target acquisition) is too restrictive. For this reason, a more general technique was developed in which a total system is considered as an assembly of subsystems. The operational objectives of the combined system are then defined in terms of functions such as navigation and flight control. Any hardware subsystem might be involved in satisfying one or more functions. The ERC and Avionics Laboratory studies are described in more detail in the following paragraphs.

### Techniques for Evaluating Astrionics for Interplanetary Missions

Techniques for evaluating astrionics systems for interplanetary probe missions were developed under Contract NAS 12-550 over a 3 year period. The objective of the study was to develop a technique for evaluating strapdown guidance systems. The technique utilizes system parameters describing the reliability, power, weight, and performance of the strapdown guidance system in determining a measure (or index) of guidance system performance. This work is discussed in detail in References 4 through 10.

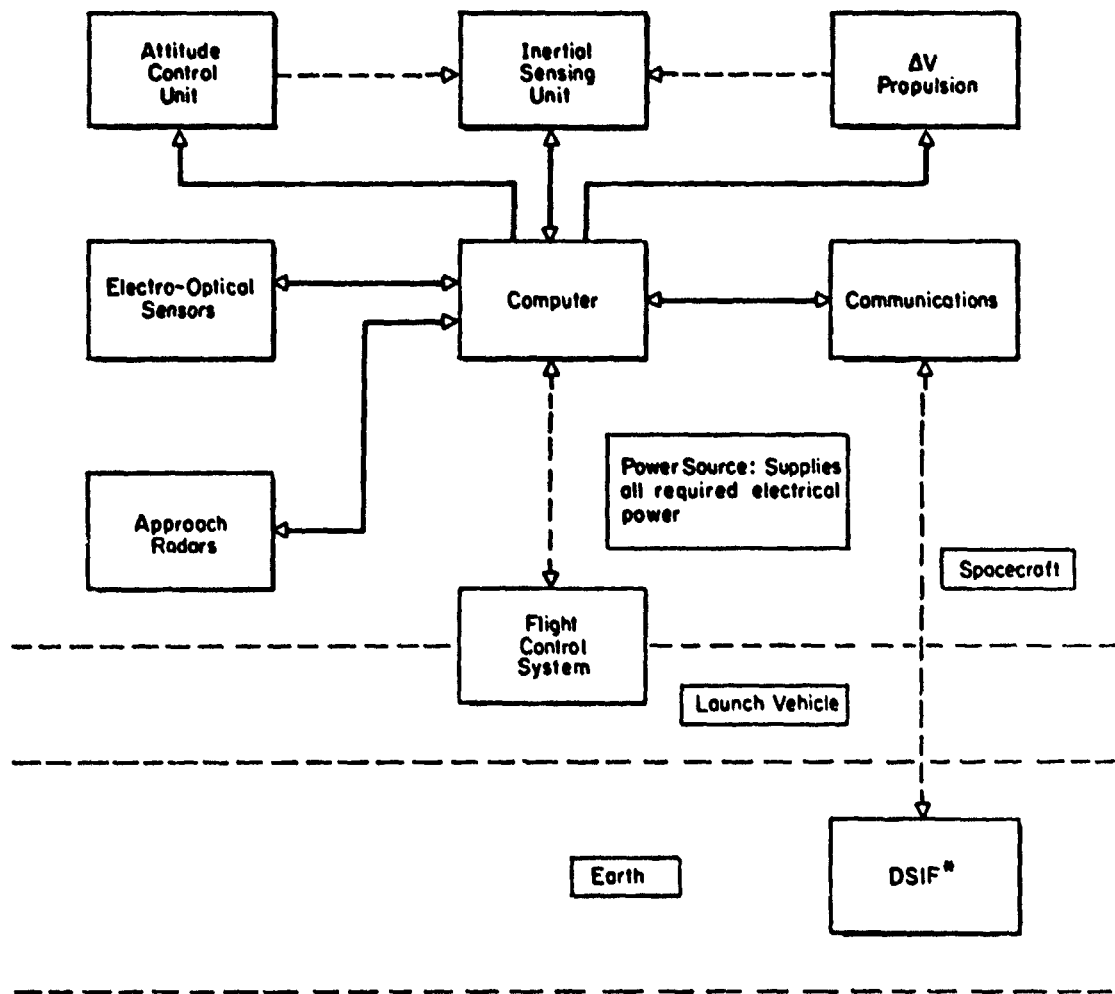
During the work performed for ERC it was assumed that the astrionics being considered were an integral part of the spacecraft as shown in Figure 1. In using this program, it would not be necessary for the astrionics to be an integral part of the spacecraft if only launch vehicle navigation and guidance were being considered. In this case, certain subsystems such as the spacecraft attitude control would not be considered in the analyses.

Techniques for evaluating astrionics for interplanetary missions require definition of a baseline set of inertial sensors, computers, and other onboard hardware items that are not designed internally by the program. In addition, parameters that describe the mission must be provided to generate the appropriate flight trajectory.

One limitation of these evaluation techniques is that no provision is made for consideration of backup modes for the various functions, e.g., navigation. The user must specify those subsystems he wishes to use to perform each function. The evaluation yields measures of the penalty for including those subsystems. Work initiated under USAF contract in 1969 allows consideration of backup modes for various functions. This work is described in the following section.

### Techniques for Evaluating Integrated Avionics

The objective of this study (performed under Contract Number F33615-C-1402) was to develop techniques and associated computer programs for evaluating the effectiveness of integrated avionics for USAF aircraft on appropriate missions. Further discussions of this work are contained in References 11 and 12.



\* Deep Space Instrumentation Facility

FIGURE 1. BLOCK DIAGRAM OF INTEGRATED ASTRIONICS



Battelle's Navigation Error  
Analysis Program (NEAP)

The technique of performing linear sensitivity analysis used under the ERC contract to determine strapdown navigation errors was generalized to include all possible navigation mechanizations and extended to cover open-loop vehicle dispersions under a Battelle-funded study described in detail in Reference 13. Experience gained from this Battelle-funded study was used in writing the Earth Orbital Mission Program-I (EOMP-I).

Concurrent Related Projects

Concurrently with performance of Contract Number NAS 8-26491, Battelle personnel were involved in two related projects funded by NASA OSS which provide valuable data and practical experience.

NASA Launch Vehicle Project (NLVP)

This project (Contract Number NASw-2018) provides extensive launch-vehicle and trajectory data for present and future NASA expendable launch vehicles. Model formulations and computer programs are structured to maintain compatibility with NLVP data. In addition, consultations with NLVP personnel on the subjects of propulsion and vehicle capability provided valuable support for this study.

Delta Inertial Guidance  
System (DIGS) Project

Battelle assisted the Delta Project Office (DPO, Goddard Space Flight Center) in the technical evaluation of the Delta inertial guidance system. Work under this contract (NAS 7-786) has included the development of a FORTRAN program to simulate the Delta launch vehicle, its control systems, and on-board computer software. This provided VSPRE personnel with a very detailed description of the NASA OSS launch vehicle, onboard systems, and software. As discussed in Reference 3, the DIGS project has also provided an opportunity for an independent check of results obtained by using EOMP-I.

## TECHNICAL DISCUSSION

The Technical Discussion section of this report is divided into discussions of the four current project tasks. The recommendations resulting from each of the tasks are presented separately in the Recommendations section later in this report.

### Task 1 Development and Maintenance of Techniques and Computer Codes for the Evaluation and Analysis of Astrionics Systems

Several computer codes are used in the analysis of astrionics systems. These programs are summarized in Table 2. The table includes reference to prior reports for programs developed and/or used during earlier reporting periods.

The Interactive Graphics Orbit Selection (IGOS) program has been written during this reporting period and has recently been delivered to MSFC for operation on the UNIVAC 1108. This program operates interactively from a remote graphics terminal such as a Tektronix 4010/4012.

A complete users manual is included in Appendix A and a sample work session is included in Appendix B. Technical details of the program are described under Task 4 of this report.

TABLE 2. VSPRE COMPUTER CODES

PROGRAM NAME	DESCRIPTION	STATUS*
EOMP-I	Generates Launch Vehicle injection dispersions (References 1, and 2)	Delivered to MSFC. Converted to 1108
EOMP-II	Compares Launch Vehicle injection dispersions to mission requirements (Reference 2)	Inactive due to lack of adequate mission requirements.
MONTE CARLO	Computes statisfied distribution of orbital elements from Guassian injection covariance (References 2, and 3)	Delivered to MSFC. Operational on 1108
Performance Code	Generates optimal nominal trajectory from vehicle weight statement (Reference 3)	Not developed on VSPRE contract.
ABBACUS	Modular Redundant System Reliability Analysis (Task 2 of this report)	Preliminary version only. Development dropped.
SPUN STAGE SIMULATION	Simulates a generalized spinning body with mass flow and thrusting. (Reference 3 and Task 3 of this report)	Preliminary program for specific applications. Not delivered.
IGOS	Interactive Graphics Orbit Selection (IGOS) program. Generates mission accuracy requirements. (Task 4 of this report)	Delivered to MSFC. Operational on 1108

\* All programs are operational on Battelle's CDC 6400/Cyber computer system.

## Task 2 Investigate Astrionics Requirements for OSS Missions

High reliability modular computer development has received considerable funding under the NASA OSS Launch Vehicle and Propulsion Programs SR&T program. In particular, the Automatically Reconfigurable Modular Multiprocessor Systems (ARMMS) project at MSFC was the prime reason for most of the effort. The VSPRE project team was directed by the COR to review the ARMMS project and to evaluate the concept particularly in terms of its impact on vehicle reliability. VSPRE memoranda (References 14 and 15) were published as the result of attendance at an ARMMS design review and a study of ARMMS documents.

### Modular Redundant System Reliability

The evaluation of modular redundant systems is a more general subject than the ARMMS reliability study. The insight gained and the analytic tools developed for the ARMMS-related investigations are applicable to many launch vehicle systems and subsystems, including redundant astrionics hardware. Therefore, the analysis was carried through to the development of a computer code. Its use and its integration with other techniques are presented below.

### Development of an Analytic Method

In order to evaluate the reliability of a modular redundant system, it is necessary to know the loading on the various pieces of hardware. A nominal mission is deterministic. If no hardware failures occur, then the on-off history of every component is known a priori. Thus, the on and off failure rates can be used as appropriate in a system simulation. Analytical problems arise because, in any real situation, the on-off histories are not deterministic. Generally, the evaluation of reliability must be accomplished in a multi-dimensional space. The on-off histories are correlated in a very complex way. Every component state is propagated as a function of the dynamic states of all the system modules. This kind of problem can be handled by means of convolution integrals in which the final probabilities of failure for the spare modules are dependent upon both the on and off failure rates of the modules which are nominally planned for use. An active

module which has a very high failure rate would tend to decrease the reliability of a back-up module near the end of the mission, since there is a higher probability that it has been used at that point.

The predicted reliability of any module in the system is dependent upon the previous history and records of failures and use rates of every module in the system. The analysis necessary to handle this problem is exceedingly complex, and one is finally forced to use a Monte Carlo type of approach. For many applications this would be too expensive and, therefore, some simplifying assumptions have to be made.

During the course of the ARMMS study, one of the parameters of interest was the ratio between the active and dormant failure rates of modules. If, as has been indicated by a recent study (Reference 16), failure rates for active and dormant modules differ not by orders of magnitude but only by a factor of two or less, then - in terms of numbers one normally deals with and accuracies which are required for reliability computations - it is not necessary to include in the model separate failure rates for the modules in their active and passive states. The inclusion of an extra module might improve reliability by two or three orders of magnitude; whereas, accounting for different on-off failure rates would not affect the calculation nearly this much.

Another problem common to this area of reliability analysis is the large number of individual component reliability states which must be propagated. For a system with  $N$  modules, there are  $2^N$  different failure states the system may be in. For a system of only 20 modules, this number is already in the neighborhood of a million, and certainly far beyond anything that could reasonably be treated on an independent state basis. It is necessary to view the problem in such a way that fewer states are encountered. This is possible because, for purposes of the reliability analysis, we only need to know how many of a given type of module have failed - not specifically which ones. It is assumed that the executive system will correctly keep track of which modules are operable. Let us define, for each set of  $N$  modules of a given class,  $N + 1$  states. We define a zero-state in which all modules of this given class are operable, a one-state in which one module is no longer working, and so on through the  $N$ -state which indicates all modules of this class have failed. It is possible to calculate, from original occupation numbers of each of the states, what the occupation numbers for each state at any time in the future will be. If one starts with a zero-state completely occupied -

that is, probability of being in zero state is equal to one and probability for each of the other states up through the N-state is zero - and waits long enough, the probability approaches zero for all the states except the N-state, which approaches one. The probability that, at time t, one will be able to assemble from the N components of a given class a set of  $M \leq N$  modules to perform a given task or set of tasks at that time is simply the probability that no units have failed, plus the probability that one unit has failed, plus ... and so on through the probability of a maximum number of failures which still provides the required hardware. It is possible then, by forming the sums, to determine the probability of having the necessary modules of a given class. If we further assume that the failures of modules in different classes are independent, it is possible to write down the probability that one can assemble at any point in time, a complete set of hardware required by the task load at that time, as a product of sums. It is necessary only to propagate individual class probabilities, the number of which is linear with the total number of modules in the system, rather than  $2^N$ . If there are  $N_k$  modules of type k and  $M_k(t)$  are required for the task load being considered at time t, then the work can be performed only if  $M_k(t) \leq N_k$  for all k. The sets  $\{M_k(t)\}$  and  $\{N_k\}$  define the requirements and total available hardware. The probability that the necessary hardware is available is

$$P(t) = \prod_k \sum_{i=0}^{N_k - M_k} P_{ik}(t) \quad , \quad (1)$$

where  $P_{ik}(t)$  is the probability that exactly i of the type k modules have failed by time t. The individual  $P_{ik}(t)$ 's may be calculated as shown in the following derivation.

Assume  $N_k$  indistinguishable modules of type k with failure rate  $\lambda_k$  during the time interval  $t_1 \leq t \leq t_2$ . Define  $P_{ik}$  as the probability that i of the modules have failed (and only i). Then

$$0 \leq P_{ik}(t) \leq 1 \text{ for all } 0 \leq i \leq N_k \text{ for given } t \quad (2)$$

and

$$\sum_{i=0}^{N_k} P_{ik}(t) = 1 \text{ for given } t \quad .$$

Suppose that all  $N_k + 1$  of the  $P_{ik}$ 's are known at time  $t_1$ . Any  $P_{ik}$  is then calculable at time  $t_2 \geq t_1$  since the probability of being in the given state at  $t_2$  is simply a sum of products. The sum runs over all states  $j$  which the occupants of state  $i$  at  $t_2$  could possibly have occupied at  $t_1$  (i.e., all  $j \leq i$ ). The products are the probabilities that the  $j$  state degenerates to the  $i$  state during the interval  $t_1 \leq t \leq t_2$ , times the probability that the set of  $N_k$  modules was in state  $j$  at time  $t_1$ .

Given that the set was in state  $j \leq i$  at  $t_1$ , the probability that it is in state  $i$  at  $t_2$  is

$$C_{N-i}^{N-j} e^{-\lambda_k(N_k - i)(t_2 - t_1)} [1 - e^{-\lambda_k(t_2 - t_1)}]^{(i-j)},$$

where

(3)

$$C_{N-i}^{N-j} = \frac{(N-j)!}{(i-j)!(N-i)!}, \text{ the binomial coefficient.}$$

The probability that the set was in state  $j$  at  $t_1$  is  $P_{jk}(t_1)$ , thus

$$P_{ik}(t_2) = e^{-\lambda_k(N_k - i)(t_2 - t_1)} \sum_{0 \leq j \leq i \leq N} P_{jk}(t_1) C_{N-i}^{N-j} [1 - e^{-\lambda_k(t_2 - t_1)}]^{(i-j)}.$$

(4)

Finally then

$$P(t) = \prod_k \sum_{i=0}^{N_k - M_k(t)} e^{-\lambda_k(N_k - i)(t - t_0)} \sum_{0 \leq j \leq i} P_{jk}(t_0) C_{N_k - i}^{N_k - j} [1 - e^{-\lambda_k(t - t_0)}]^{(i-j)},$$

(5)

where  $P(t)$  is the probability of having the required hardware, defined by  $\{M_k(t)\}$ , at time  $t$ . It is assumed that the complete set of  $P_{jk}(t_0)$ 's is known at some earlier time  $t_0$ .

The problem of computing the reliability of performing a mission (that is, of successfully completing all tasks necessary for the successful completion of the mission) reduces to two parts. One part consists of finding the definition, for all points in time, of the minimal hardware set which will accomplish the task load required at that time. The second part consists of calculating the probability of having the necessary hardware available when it is required. To illustrate how one might use some of these concepts and techniques, it is perhaps best to describe the input and the output of a computer program which accomplishes the first step.

The input to the program which calculates the hardware requirements as a function of time during the mission consists of three parts. The first part is a listing of what hardware is available, how many copies of each type, its power and weight, and initial reliability and the performance characteristics of that particular kind of module. In order to be as general as necessary for the treatment of many different kinds of systems, all modules are characterized by a set of four performance parameters. These are: (1) receiving rate, (2) processing rate, (3) storage capacity, and (4) transmitting rate. For some modules, one or more of these parameters may be inapplicable and, therefore, ignored by the program. A memory, for example, has a receiving rate, a storage capacity, and a transmittal rate, but no processing rate. A data bus has a receiving and transmitting rate (the same, of course) but no storage capacity and no processing rate. The processors have receiving, processing, and transmitting rates but no storage capacity. There follows, in the input, a list of tasks which may be required at some point in the mission. Tasks normally have certain hardware requirements which include, not just a list of hardware, but also performance characteristics required for the hardware. For example, a given task might have a certain memory requirement, or a certain minimum transmittal rate for data. These numbers are associated with the task together with the required modules. The program, in associating requirements with equipment actually available, allocates resources to best fulfill the needs of the mission. The third section of data names the tasks and when they are to be initiated and completed. The output warns of any situation which may arise in which the tasks called for cannot be performed due to insufficient hardware and will inform the user of excess hardware (if any) which is carried and the consequences in terms of excess weight and power requirements. The program reads the tasks sequentially and assigns hardware based on the requirements of each task. The algorithm for the allocation of hardware is somewhat arbitrary and must be designed for whatever executive system is being used. The algorithm employed for the sample calculation adopts the following guidelines:



- (1) If a task requires more than one of a given module type, only currently unassigned units may be considered. If a sufficient number of such units can be found to accommodate the task requirements, the load is divided equally among such units. Considering only unassigned modules minimizes the number of units allocated to a particular task.
- (2) If only one of a given module type is required by a task, then no more than one of a given type can be assigned to that task. A task may not be allocated, for example, ten percent of each of two memory modules.
- (3) All tasks are allocated the necessary hardware in the order in which the tasks are specified in the data deck, subject always to the restrictions given by (1) and (2) above.

#### Sample Calculation

Figure 2 shows the suite of modules chosen for this exercise. Along with the module names and unit designators (A, B, C, ... etc.) the active and dormant failure rates, the four performance specifications previously discussed, and weight and power are given.

The hardware specifications given do not correspond to any real, specific hardware. Since the purpose of this example is merely to demonstrate a capability rather than to analyze a given hardware suite, all numbers are reported in arbitrary units rather than pounds, hours, watts, bits per second, etc.

MODULE SPECIFICATIONS									
MODULE	FR-ON	FR-OFF	RTR	RTP	PERFORMANCE MAXIMA				
					CAP	RTT	WEIGHT	POWER	
PROCESSOR (PROC) A	.000050	.000050	4000000	4000000	120.	40000000	.5000	10.0000	
ON-LINE MEMORY (OLM) A	.000020	.000020	4000000	4000000	16000.	40000000	5.0000	1.0000	
TELEMETRY (TELE) A	.000000	.000000	1000.	1000.	100.	1000.	15.0000	200.0000	
BULK MEMORY (BLK)	.000000	.000000	1600000	1600000	100.	80000000	5.0000	20.0000	
EXP SENSOR (SENS) A	.000004	.000004	5000.	5000.	100.	5000.	50.0000	70.0000	
INNER MEAS UNIT (IU) A	.000000	.000000	10000.	10000.	100.	10000.	6.0000	5.0000	
PROCESSOR (PROC) B	.000050	.000050	4000000	4000000	120.	40000000	.5000	10.0000	
ON-LINE MEMORY (OLM) B	.000020	.000020	4000000	4000000	16000.	40000000	5.0000	1.0000	
TELEMETRY (TELE) B	.000000	.000000	1000.	1000.	100.	1000.	15.0000	200.0000	
BULK MEMORY (BLK) B	.000000	.000000	1600000	1600000	100.	80000000	5.0000	20.0000	
EXP SENSOR (SENS) B	.000004	.000004	5000.	5000.	100.	5000.	50.0000	70.0000	
INNER MEAS UNIT (IU) B	.000000	.000000	10000.	10000.	100.	10000.	6.0000	5.0000	
PROCESSOR (PROC) C	.000050	.000050	4000000	4000000	120.	40000000	.5000	10.0000	
ON-LINE MEMORY (OLM) C	.000020	.000020	4000000	4000000	16000.	40000000	5.0000	1.0000	
TELEMETRY (TELE) C	.000000	.000000	1000.	1000.	100.	1000.	15.0000	200.0000	
BULK MEMORY (BLK) C	.000000	.000000	1600000	1600000	100.	80000000	5.0000	20.0000	
EXP SENSOR (SENS) C	.000004	.000004	5000.	5000.	100.	5000.	50.0000	70.0000	
INNER MEAS UNIT (IU) C	.000000	.000000	10000.	10000.	100.	10000.	6.0000	5.0000	
PROCESSOR (PROC) D	.000050	.000050	4000000	4000000	120.	40000000	.5000	10.0000	
ON-LINE MEMORY (OLM) D	.000020	.000020	4000000	4000000	16000.	40000000	5.0000	1.0000	
TELEMETRY (TELE) D	.000000	.000000	1000.	1000.	100.	1000.	15.0000	200.0000	
BULK MEMORY (BLK) D	.000000	.000000	1600000	1600000	100.	80000000	5.0000	20.0000	
EXP SENSOR (SENS) D	.000004	.000004	5000.	5000.	100.	5000.	50.0000	70.0000	
INNER MEAS UNIT (IU) D	.000000	.000000	10000.	10000.	100.	10000.	6.0000	5.0000	
PROCESSOR (PROC) E	.000050	.000050	4000000	4000000	120.	40000000	.5000	10.0000	
ON-LINE MEMORY (OLM) E	.000020	.000020	4000000	4000000	16000.	40000000	5.0000	1.0000	
TELEMETRY (TELE) E	.000000	.000000	1000.	1000.	100.	1000.	15.0000	200.0000	
BULK MEMORY (BLK) E	.000000	.000000	1600000	1600000	100.	80000000	5.0000	20.0000	
EXP SENSOR (SENS) E	.000004	.000004	5000.	5000.	100.	5000.	50.0000	70.0000	
INNER MEAS UNIT (IU) E	.000000	.000000	10000.	10000.	100.	10000.	6.0000	5.0000	
SYSTEM WEIGHT IS	253.5000								
SYSTEM POWERED-DOWN FAILURE RATE IS	.00034								
SYSTEM ALL-ON WARMUP-CHECKOUT FAILURE RATE IS	.00034								

FIGURE 2. PERFORMANCE AND RELIABILITY SPECIFICATIONS

Figure 3 illustrates the demands on the hardware. For each task, there is a list of the necessary modules and the performance required. In the first task, titled Receive Ground Update (Recv Gnd Updt), the telemetry is required to accept 400 units of information per unit time. The On-line Memory must store 64000 units of information.

Figure 4 shows the mission load (that is, the number of modules of each type required at discrete times in the mission). At these times, it also shows the failure state probabilities, the  $P_{jk}$ 's of Equation 5. At 4999.90 time units into the mission the Control System Monitor (Control Sys.-Mon) task is initiated.

The system requires a single Inertial Measurement Unit (IMU). Since two such units are onboard, there are three possible states: (1) both are still working (probability = 0.6065); (2) one has failed (probability = 0.3445); or (3) both have failed (probability = 0.0489). The probability that the need for an IMU can be satisfied at 4999.90 time units into the mission is 0.9510 (0.6065 + 0.3445).

Figure 5 provides a summary of the utilization of available modules in the case of no failures. It provides no direct reliability information but is useful in planning.

REPRODUCIBILITY : THE  
ORIGINAL PAGE IS POOR

MODULES REQUIRED FOR THE VARIOUS TASKS				
	RTR	RTP	CAP	RTT
RECV GND UPDT				
PROCESSOR(PROC)	2000.	0.	0.	2000.
ON-LINE MEMORY(OLM)	2000.	0.	64000.	0.
TELEMETRY(TELE)	400.	0.	0.	400.
INER NAV				
PROCESSOR(PROC)	4000.	54000.	0.	4000.
ON-LINE MEMORY(OLM)	2000.	0.	6400.	2000.
BULK MEMORY(BLK)	4000.	0.	128000.	4000.
INER MEAS UNIT(IMU)	1000.	0.	0.	1000.
EXP SENS-STO				
BULK MEMORY(BLK)	0.	0.	500000.	500.
EXP SENSOR(SENS)	400.	0.	0.	500.
EXP SENS-PROC-STO				
PROCESSOR(PROC)	500.	500.	0.	500.
ON-LINE MEMORY(OLM)	20.	0.	4000.	0.
EXP SENSOR(SENS)	50.	0.	0.	500.
EXP PROC-STO				
PROCESSOR(PROC)	500.	500.	0.	500.
ON-LINE MEMORY(OLM)	500.	0.	55000.	500.
BULK MEMORY(BLK)	500.	0.	50000.	0.
EXP PROC-TRANSMIT				
PROCESSOR(PROC)	10000.	4000.	0.	5000.
TELEMETRY(TELE)	0.	0.	0.	500.
BULK MEMORY(BLK)	0.	0.	44000.	500.
CONTROL SYS-MON				
PROCESSOR(PROC)	46000.	46000.	0.	563000.
ON-LINE MEMORY(OLM)	5000.	0.	44000.	400.
INER MEAS UNIT(IMU)	0.	0.	0.	1000.

FIGURE 3. COMPONENT REQUIREMENTS OF INDIVIDUAL TASKS

MODULE TYPE	NO. REQUIRED	FAILURE STATE PROBABILITIES									
		0	1	2	3	4	5	6	7	8	9
4). FAILED =											
PROCESSOR(P3C)	0	1.0000	0.0000	0.0000	0.0000						
ON-LINE MEMORY(M4)	0	1.0000	0.0000	0.0000	0.0000	0.0000	0.0000	0.0000	0.0000	0.0000	
TELEMETRY(TE)	0	1.0000	0.0000	0.0000	0.0000						
BULK MEMORY(MK)	0	1.0000	0.0000								
EXP. SENSOR(SEM)	0	1.0000	0.0000	0.0000	0.0000						
INER MEAS UNIT(IMU)	0	1.0000	0.0000	0.0000							

[illegible]

CONTROL SYS-MON			WAS INITIATED AT C.OO									
MODULE TYPE		NO. REQUIRED	FAILURE STATE PROBABILITIES									
	NO. FAILED =		1	2	3	4	5	6	7	8	9	10
PROCESSOR(PROC)	1	1.0000	.0000	.0000	.0000							
ON-LINE MEMORY(OLM)	1	1.0000	.0000	.0000	.0000	.0000	.0000	.0000	.0000	.0000	.0000	.0000
TELEMEMORY(TEL)	0	.0000	.0000	.0000	.0000							
BULK MEMORY(BLK)	1	1.0000	.0000									
EXP SENSORS(SENS)	0	1.0000	.0000	.0000	.0000							
INER MEAS UNIT(INU)	1	1.0000	.0000	.0000	.0000							

[illegible]

#### FIGURE 4. EQUIPMENT ALLOCATION AND RELIABILITY STATE PROPAGATION

NO. FAILED =										
	0	1	2	3	4	5	6	7	8	9
PROCESSOR(ROC)	1	.9925	.0075	.0000	.0000					
ON-LINE MEMORY(OLM)	1	.9945	.0055	.0000	.0000	.0000	.0000	.0000	.0000	.0000
TELEMETRY(TEL)	0	.9275	.0725	.0000	.0000					
BULK MEMORY(BLK)	0	1.0000	.0000							
EXP SENSOR(SENS)	0	.9994	.0006	.0000	.0000					
INER MEAS UNIT(IMU)	1	.9512	.0488	.0000						
EXP SENS-STO WAS INITIATED AT 500.50										
MODULE TYPE NO. REQUIRED FAILURE STATE PROBABILITIES										
	0	1	2	3	4	5	6	7	8	9
PROCESSOR(ROC)	1	.9925	.0075	.0000	.0000					
ON-LINE MEMORY(OLM)	1	.9945	.0055	.0000	.0000	.0000	.0000	.0000	.0000	.0000
TELEMETRY(TEL)	0	.9275	.0725	.0000	.0000					
BULK MEMORY(BLK)	1	1.0000	.0000							
EXP SENSOR(SENS)	1	.9994	.0006	.0000	.0000					
INER MEAS UNIT(IMU)	1	.9511	.0489	.0000						
EXP SENS-STO TERMINATED AT 501.50										
MODULE TYPE NO. REQUIRED FAILURE STATE PROBABILITIES										
	0	1	2	3	4	5	6	7	8	9
PROCESSOR(ROC)	1	.9925	.0075	.0000	.0000					
ON-LINE MEMORY(OLM)	1	.9945	.0055	.0000	.0000	.0000	.0000	.0000	.0000	.0000
TELEMETRY(TEL)	0	.9275	.0725	.0000	.0000					
BULK MEMORY(BLK)	0	1.0000	.0000							
EXP SENSOR(SENS)	0	.9994	.0006	.0000	.0000					
INER MEAS UNIT(IMU)	1	.9511	.0489	.0000						
EXP PROC-TRANSMIT WAS INITIATED AT 501.51										
MODULE TYPE NO. REQUIRED FAILURE STATE PROBABILITIES										
	0	1	2	3	4	5	6	7	8	9
PROCESSOR(ROC)	1	.9925	.0075	.0000	.0000					
ON-LINE MEMORY(OLM)	1	.9945	.0055	.0000	.0000	.0000	.0000	.0000	.0000	.0000
TELEMETRY(TEL)	1	.9275	.0725	.0000	.0000					
BULK MEMORY(BLK)	1	1.0000	.0000							
EXP SENSOR(SENS)	0	.9994	.0006	.0000	.0000					
INER MEAS UNIT(IMU)	1	.9511	.0489	.0000						

FIGURE 4. EQUIPMENT ALLOCATION AND RELIABILITY STATE PROPAGATION  
(Continued)

EXP PROC-TRANS:IT TERMINATED AT 501.03									
MODULE TYPE	NO. REQUIRED	FAILURE STATE PROBABILITIES	1	2	3	4	5	6	7
NO. FAILED =									
PROCESSOR(PROC)	1	.0925 .0375 .0000 .0000 .0000 .0000 .0000 .0000 .0000							
ON-LINE MEMORY(OLM)	1	.0645 .0349 .0000 .0000 .0000 .0000 .0000 .0000 .0000							
TELEMETRY(TELE)	0	.0275 .0707 .0010 .0000 .0000 .0000 .0000 .0000 .0000							
BULK MEMORY(BLK)	0	1.0000 .0000 .0000 .0000 .0000 .0000 .0000 .0000 .0000							
EXP SENSOR(SENS)	0	.0994 .0000 .0000 .0000 .0000 .0000 .0000 .0000 .0000							
INFR MEAS UNIT(IMU)	1	.0511 .0493 .0000 .0000 .0000 .0000 .0000 .0000 .0000							
REC'D GND UPDT WAS INITIATED AT 501.03									
MODULE TYPE	NO. REQUIRED	FAILURE STATE PROBABILITIES	1	2	3	4	5	6	7
NO. FAILED =									
PROCESSOR(PROC)	1	.0925 .0375 .0000 .0000 .0000 .0000 .0000 .0000 .0000							
ON-LINE MEMORY(OLM)	1	.0645 .0349 .0000 .0000 .0000 .0000 .0000 .0000 .0000							
TELEMETRY(TELE)	1	.0275 .0707 .0010 .0000 .0000 .0000 .0000 .0000 .0000							
BULK MEMORY(BLK)	0	1.0000 .0000 .0000 .0000 .0000 .0000 .0000 .0000 .0000							
EXP SENSOR(SENS)	0	.0994 .0000 .0000 .0000 .0000 .0000 .0000 .0000 .0000							
INFR MEAS UNIT(IMU)	1	.0511 .0493 .0000 .0000 .0000 .0000 .0000 .0000 .0000							
REC'D GND UPDT TERMINATED AT 501.97									
MODULE TYPE	NO. REQUIRED	FAILURE STATE PROBABILITIES	1	2	3	4	5	6	7
NO. FAILED =									
PROCESSOR(PROC)	1	.0925 .0375 .0000 .0000 .0000 .0000 .0000 .0000 .0000							
ON-LINE MEMORY(OLM)	1	.0645 .0349 .0000 .0000 .0000 .0000 .0000 .0000 .0000							
TELEMETRY(TELE)	0	.0275 .0707 .0010 .0000 .0000 .0000 .0000 .0000 .0000							
BULK MEMORY(BLK)	0	1.0000 .0000 .0000 .0000 .0000 .0000 .0000 .0000 .0000							
EXP SENSOR(SENS)	0	.0994 .0000 .0000 .0000 .0000 .0000 .0000 .0000 .0000							
INFR MEAS UNIT(IMU)	1	.0511 .0493 .0000 .0000 .0000 .0000 .0000 .0000 .0000							
CONTROL SYS-MON TERMINATED AT 505.00									
MODULE TYPE	NO. REQUIRED	FAILURE STATE PROBABILITIES	1	2	3	4	5	6	7
NO. FAILED =									
PROCESSOR(PROC)	0	.0706 .0291 .0000 .0000 .0000 .0000 .0000 .0000 .0000							
ON-LINE MEMORY(OLM)	0	.0605 .0253 .0000 .0000 .0000 .0000 .0000 .0000 .0000							
TELEMETRY(TELE)	0	.0719 .0329 .0000 .0000 .0000 .0000 .0000 .0000 .0000							
BULK MEMORY(BLK)	0	1.0000 .0000 .0000 .0000 .0000 .0000 .0000 .0000 .0000							
EXP SENSOR(SENS)	0	.0994 .0000 .0000 .0000 .0000 .0000 .0000 .0000 .0000							

FIGURE 4. EQUIPMENT ALLOCATION AND RELIABILITY STATE PROPAGATION  
(Continued)

REPRODUCTION OF THIS  
ORIGINAL





EXP PROC-TRANSPIR										
TERMINATED AT 2320.21										
MODULE TYPE	NO. REQUIRED	FAILURE STATE PROBABILITIES								
NO. FAILED	0	1	2	3	4	5	6	7	8	9
PROCESSOR(LOC)	1	.9731	.0296	.0003	.0000	.0000	.0000	.0000	.0000	.0000
ON-LINE MEMORY(OLM)	1	.9646	.0270	.0042	.0003	.0000	.0000	.0000	.0000	.0000
TELEMETRY(TEL)	0	.7385	.2356	.0251	.0099	.0000	.0000	.0000	.0000	.0000
BULK MEMORY(BLK)	0	1.0000	.0000	.0000	.0000	.0000	.0000	.0000	.0000	.0000
EXP SENSOR(SENS)	0	.5976	.0024	.0021	.0000	.0000	.0000	.0000	.0000	.0000
INER MEAS UNIT(IMU)	1	.8171	.1737	.0092	.0000	.0000	.0000	.0000	.0000	.0000
EXP PROC-TRANSPIR										
TERMINATED AT 2320.21										
MODULE TYPE	NO. REQUIRED	FAILURE STATE PROBABILITIES								
NO. FAILED	0	1	2	3	4	5	6	7	8	9
PROCESSOR(LOC)	0	.9277	.0705	.0018	.0000	.0000	.0000	.0000	.0000	.0000
ON-LINE MEMORY(OLM)	0	.9777	.0259	.0014	.0034	.0002	.0036	.0000	.0000	.0000
TELEMETRY(TEL)	0	.4724	.4025	.1143	.0108	.0000	.0000	.0000	.0000	.0000
BULK MEMORY(BLK)	0	1.0000	.0000	.0000	.0000	.0000	.0000	.0000	.0000	.0000
EXP SENSOR(SENS)	0	.5940	.0060	.0000	.0000	.0000	.0000	.0000	.0000	.0000
INER MEAS UNIT(IMU)	0	.6055	.3445	.0499	.0000	.0000	.0000	.0000	.0000	.0000
CONTROL SYS-MON										
TERMINATED AT 2021.21										
MODULE TYPE	NO. REQUIRED	FAILURE STATE PROBABILITIES								
NO. FAILED	0	1	2	3	4	5	6	7	8	9
PROCESSOR(LOC)	1	.9277	.0705	.0018	.0000	.0000	.0000	.0000	.0000	.0000
ON-LINE MEMORY(OLM)	1	.9777	.0259	.0014	.0034	.0002	.0036	.0000	.0000	.0000
TELEMETRY(TEL)	0	.4724	.4025	.1143	.0108	.0000	.0000	.0000	.0000	.0000
BULK MEMORY(BLK)	0	1.0000	.0000	.0000	.0000	.0000	.0000	.0000	.0000	.0000
EXP SENSOR(SENS)	0	.5940	.0060	.0000	.0000	.0000	.0000	.0000	.0000	.0000
INER MEAS UNIT(IMU)	1	.8171	.1737	.0092	.0000	.0000	.0000	.0000	.0000	.0000
CONTROL SYS-MON										
WAS INITIATED AT 6999.90										
MODULE TYPE	NO. REQUIRED	FAILURE STATE PROBABILITIES								
NO. FAILED	0	1	2	3	4	5	6	7	8	9
PROCESSOR(LOC)	1	.9277	.0705	.0018	.0000	.0000	.0000	.0000	.0000	.0000
ON-LINE MEMORY(OLM)	1	.9777	.0259	.0014	.0034	.0002	.0036	.0000	.0000	.0000
TELEMETRY(TEL)	0	.4724	.4025	.1143	.0108	.0000	.0000	.0000	.0000	.0000
BULK MEMORY(BLK)	0	1.0000	.0000	.0000	.0000	.0000	.0000	.0000	.0000	.0000
EXP SENSOR(SENS)	0	.5940	.0060	.0000	.0000	.0000	.0000	.0000	.0000	.0000
INER MEAS UNIT(IMU)	1	.8171	.1737	.0092	.0000	.0000	.0000	.0000	.0000	.0000
EXP SENS-PROC-SIG										
WAS INITIATED AT 5000.00										

FIGURE 4. EQUIPMENT ALLOCATION AND RELIABILITY STATE PROPAGATION  
(Continued)





## PRE-FLIGHT NOMINAL PLANNING

MODULE	TOTAL TIME ON	NUMBER OF TURN-ONS
PROCESSOR(PROC) A	461.510	5
ON-LINE MEMORY(OLM)A	461.510	5
TELEMETRY(TELE) A	4.765	6
BULK MEMORY(BLK)	6.100	6
EXP SENSOR(SENS) A	130.300	4
INER MEAS UNIT(IMU)A	461.510	5
PROCESSOR(PROC) B	0.000	0
PROCESSOR(PROC) C	0.000	0
ON-LINE MEMORY(OLM)B	0.000	0
ON-LINE MEMORY(OLM)C	0.000	0
ON-LINE MEMORY(OLM)D	0.000	0
ON-LINE MEMORY(OLM)E	0.000	0
ON-LINE MEMORY(OLM)F	0.000	0
ON-LINE MEMORY(OLM)G	0.000	0
ON-LINE MEMORY(OLM)H	0.000	0
TELEMETRY(TELE) B	0.000	0
TELEMETRY(TELE) C	0.000	0
EXP SENSOR(SENS) B	0.000	0
EXP SENSOR(SENS) C	0.000	0
INER MEAS UNIT(IMU)B	0.000	0

## USE RATES (MAXIMUM AVERAGE)

MODULE	RTR	RTP	CAP	RTT
PROCESSOR(PROC) A (.00, .00) (.00, .00) (.00, .00) (.00, .00)				
ON-LINE MEMORY(OLM)A (.00, .00) (.00, .00) (.00, .00) (.00, .00)				
TELEMETRY(TELE) A (.00, .00) (.00, .00) (.00, .00) (.00, .00)				
BULK MEMORY(BLK) (.00, .00) (.00, .00) (.00, .00) (.00, .00)				
EXP SENSOR(SENS) A (.00, .00) (.00, .00) (.00, .00) (.00, .00)				
INER MEAS UNIT(IMU)A (.00, .00) (.00, .00) (.00, .00) (.00, .00)				

FIGURE 5. NOMINAL [NO-FAILURES] EQUIPMENT UTILIZATION

### Task 3 Investigate Scout Astrionics Requirements

The current Scout launch vehicle utilizes an open loop autopilot for guidance during lower stage actions and a spinning fourth stage. Without a closed loop navigation system, Scout injection errors are considerably larger than for other current launch vehicles.

Over recent years, VSPRE has investigated a number of possible modifications to the Scout guidance (References 2 and 3). These modifications have ranged from an onboard closed loop inertial navigation system as part of the proposed new vehicle (ASLV) to relatively simple modifications such as a velocity meter and velocity vernier and/or active steering of the spinning fourth stage.

The desirability of any of these modifications hinged on the mission requirements for accuracy. To properly assess the situation, accuracy requirements must be known for both currently planned launches, and even more importantly, any missions which might be reassigned to Scout from a higher performance vehicle. As explained in more detail under Task 4, adequate mission requirement data were not available for this last purpose. This, coupled with constraints on funding for launch vehicle modification, have left the decision regarding major improvements to Scout accuracy open at this time.

#### Spun Stage Simulation and Error Model

In the course of investigating alternative guidance approaches for the spun fourth stage, a spinning stage simulation, and a spun stage linear error model were developed. The simulation involves a separate FORTRAN program that considers only the fourth stage. The linear error model is compatible with EOMP and can easily be added to EOMP when the need arises (Reference 3).

#### Investigation of the Dynamic Behavior of the Red Shift Probe

VSPRE was directed by the COR to aid MSFC in assessing certain potentially significant error sources of the spun Scout fourth stage when applied to the Gravitational Red Shift Probe.

The Gravitational Red shift payload is scheduled to be launched by a Scout vehicle in 1975. The payload will remain attached to the burned-out fourth stage of the Scout and is supposed to rotate at about 10 radians per second while describing a ballistic trajectory with a coast time out of the atmosphere of approximately 10,000 seconds [Reference 19]. Because of the long coast time, effects that are usually ignored for short-life missions required investigation. BCL was requested to investigate the effects of several potential disturbing forces on dynamic stability and angular rate of the Red shift payload attached to the burned-out Scout fourth stage. The error sources investigated included

- (1) Eddy currents induced by Earth's magnetic field
- (2) Venting of ammonia from the side of the payload
- (3) Fourth-stage tipoff
- (4) Fourth-stage thrust misalignment
- (5) Fourth-stage burn-out mass unbalance
- (6) Payload static and dynamic unbalance.

The eddy current problem was handled analytically; the remaining error sources were investigated by using a computer simulation of the Scout fourth stage with the Red shift payload attached.

#### Eddy Current Damping

Because of the long ballistic coast time, the effect of spin rate damping due to eddy currents induced by the Earth's magnetic field was investigated. Reference 18 gives the following formula for the damping torque induced in a cylinder spinning about its axis of symmetry:

$$T = 2J^2 \left( \frac{f^2}{1+f} \right) \pi \omega \gamma \tau r^4 \quad \text{dyne-cm} \quad (6)$$

where;

- J = magnetic field component perpendicular to the spin axis in Oersteds
- f = fineness ratio (length/diameter)
- $\omega$  = spin rate in radians per second
- $\gamma$  = conductivity of vehicle skin in abmhos/cm
- $\tau$  = skin thickness in cm
- r = radius of the cylinder in cm.

The following formula for magnetic field intensity is given in Reference 19 and describes the Earth's magnetic field within about 10 percent accuracy:

$$J = J_0 \left( \frac{R_E}{A} \right)^3 \sin \theta \quad (7)$$

where;

- $J_0$  = horizontal intensity at the Equator = 0.31 Oersted
- $R_E$  = radius of the Earth
- A = distance from the center of the Earth to the point of interest
- $\theta$  = polar angle.

When Equation (7) is substituted into Equation (6), the result is

$$T = 2 \pi J_0^2 \left( \frac{R_E}{A} \right)^6 \frac{f^2}{1+f} \omega \gamma \tau r^4 \quad (8)$$

when  $\theta$  is assumed to be 90 degrees.

The model of the Red shift payload used with Equation (8) was taken from drawings of the payload and the Scout fourth-stage information from References 20 and 21. It was assumed that the combined package was an aluminum cylinder 17 inches in diameter and 104 inches long, spinning at 100 revolutions per minute. Skin thickness,  $\tau$ , was chosen conservatively at one-half centimeter. Using these numbers, Equation (8) reduces to

$$T = 1180 \left( \frac{R_E}{A} \right)^6 \quad \text{lb-ft.} \quad (9)$$

According to Reference 22, the coast starts at 196.50 seconds at a geocentric radius of  $22.75 \times 10^6$  feet (with Earth's radius being  $20.9 \times 10^6$  feet). At this altitude,  $\left(\frac{R_E}{A}\right)^6 = 0.61$ , and  $T = 6.4 \times 10^{-3}$  lb-ft. Decay of the body's angular rate is given by

$$\omega = \omega_0 e^{-\left(\frac{T}{H}\right) t} \quad (10)$$

where  $H$  is the angular momentum of the body about the spin axis. At the start of coast,  $H = 27.5$  lb-ft-sec for the modeled Red shift payload. Figure 6 shows the geocentric radius ( $A$ ) of the payload as a function of time. It also shows the stair-step approximation to  $A$  used incrementally in Equation (9) to obtain an approximation to the roll rate damping torque during coast. Equation (10) may be rewritten for piecewise solution as:

$$\omega_{n+1} = \omega_n e^{-\left(\frac{T_n}{H_n}\right) (t_{n+1} - t_n)} \quad (11)$$

where

$$T_n = 1.05 \times 10^{-3} \left(\frac{R_E}{A_n}\right)^6$$

and 
$$H_n = 2.63 \omega_n .$$

Results of applying Equation (11) to the stair-step approximation of  $A$  are given in Table 3. The decay of the roll rate is plotted in Figure 7. It is readily seen that the decay due to eddy current damping is predicted to be less than one percent for the 10,000 seconds of the experiment.

#### Spinning Stage Simulation

Previous work for VSPRE included derivation of equations of motion and development of a 6 degree-of-freedom simulation for spinning stages (Reference 3). The pertinent portions of this effort are repeated here for convenience.



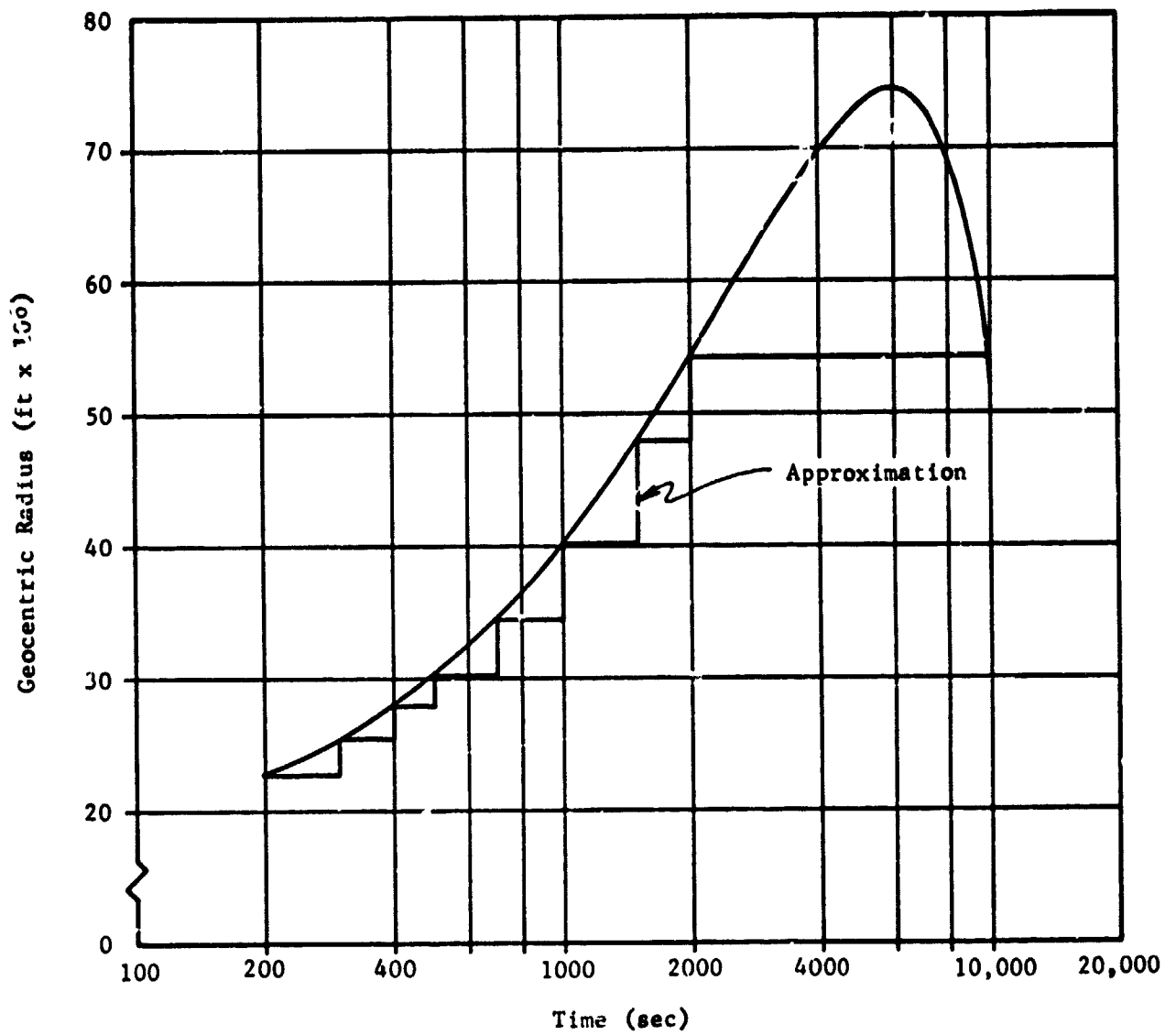


FIGURE 6. DISTANCE OF PAYLOAD FROM CENTER OF EARTH

TABLE 3. SUMMARY OF ROLL RATE DECAY CALCULATIONS

Segment Times (sec after liftoff)		Geocentric Altitude (ft)	Torque due to Eddy Currents (lb-ft)	Roll Axis Spin Rate (rev/min)	
Start	Stop			Start of Segment	End of Segment
0	196.6	$20.9 \times 10^6$	0	0	100
196.6	300.	$22.75 \times 10^6$	$6.4 \times 10^{-4}$	100	99.76
300.	400.	$25.5 \times 10^6$	$3.2 \times 10^{-4}$	99.76	99.65
400.	500.	$28.0 \times 10^6$	$1.85 \times 10^{-4}$	99.65	99.58
500.	700.	$30.3 \times 10^6$	$1.13 \times 10^{-4}$	99.58	99.49
700.	1000.	$34.6 \times 10^6$	$.504 \times 10^{-4}$	99.49	99.44
1000.	1500.	$40.2 \times 10^6$	$.208 \times 10^{-4}$	99.44	99.40
1500.	2000.	$48.0 \times 10^6$	$.072 \times 10^{-4}$	99.40	99.38
2000.	10000.	$54.4 \times 10^6$	$.034 \times 10^{-4}$	99.38	99.28

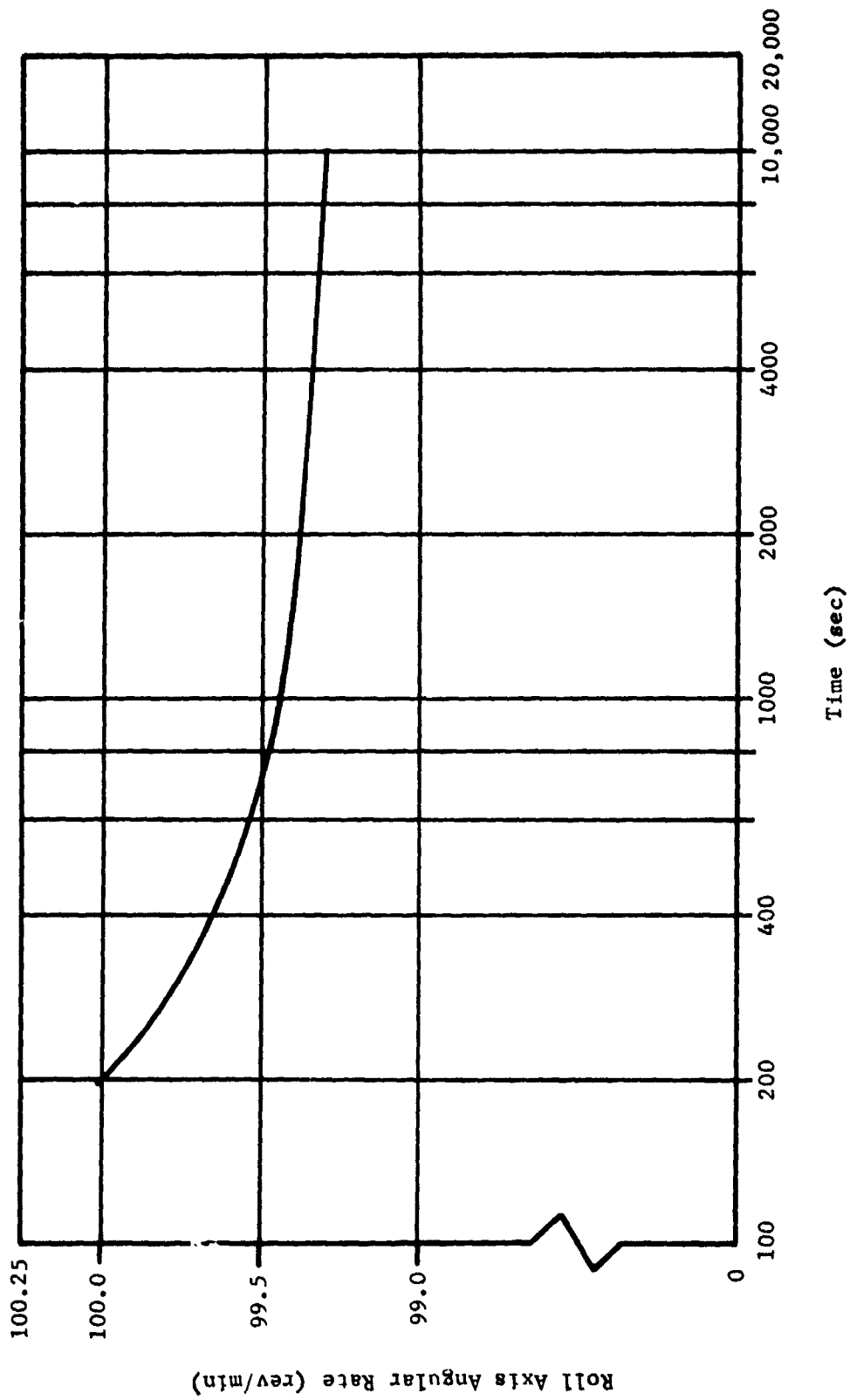


FIGURE 7. SPIN DECAY DUE TO EDDY CURRENTS

### Equations of Motion

The general equations of rotational motion, presented in Reference 23, are expressed for our notation in Equation 12:

$$\tau = J \dot{\omega} + S(\omega) J \omega + \dot{J} \omega + \sum_i \dot{m}_i S^2(r_{ei}) \omega \quad (12)$$

where

- $\tau$  = the applied torque vector,
- $J$  = the moment of inertia about the center of gravity, a 3 by 3 matrix,
- $\omega$  = the vector of angular rates,
- $S(\ )$  = the skew symmetric operator, a 3 by 3 matrix,\*
- $\dot{m}_i$  = the  $i$ th engine flow rate, and
- $r_{ei}$  = the location vector of the  $i$ th engine, relative to the c.g.

Equation 12 can be rewritten as a differential equation for the angular rates:

$$\dot{\omega} = J^{-1} \left[ \tau - S(\omega) J \omega - D \omega \right] \quad (13)$$

The three-by-three matrix  $D$  is used to represent the last two terms of Equation 12:

$$D = \dot{J} + \sum_i \dot{m}_i S^2(r_{ei}) \quad (14)$$

---

\*  $S(y)x = y$  cross  $x$ , the vector cross product.

Equation 14 has terms for the time rate of change of the moment of inertia,  $\dot{J}$ , and the angular momentum loss due to mass expulsion, jet damping. As written, Equation 14 assumes nozzles of zero area. Figure 8a represents a stage with four nozzles of zero area, each located away from the roll axis. If the nozzles are not on the roll axis, the jet damping effect is significant, even for zero area nozzles. For a more practical development, especially for the case of one nozzle on the roll axis, represented by Figure 8b, an integral over the exit area of the nozzle(s) is required. Consider a nozzle of area  $A$ , located with its centroid at  $l$  relative to the vehicle c.g. as shown in Figure 9.

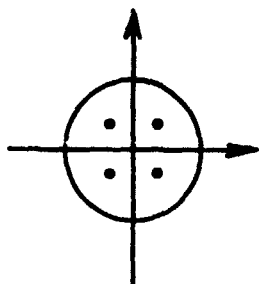


FIGURE 8a. SEVERAL NOZZLES OF INFINITESIMAL AREA

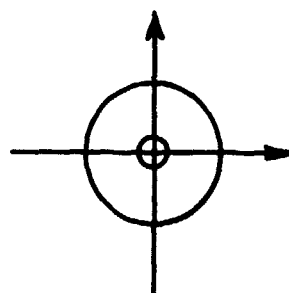


FIGURE 8b. ONE LARGE NOZZLE

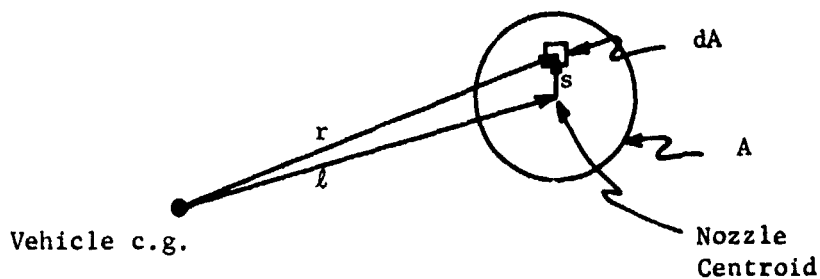


FIGURE 9. INTEGRATION OVER NOZZLE AREA

Let  $\rho$  be the mass flow per unit area, and  $s$  the vector from the nozzle centroid to an element of area,  $dA$ :

$$\dot{m}_i S^2(r_{ei}) = \int_A \rho S^2(l + s) dA \quad (15)$$

Expanding the skew squared gives

$$\dot{m}_i S^2(r_{ei}) = \int_A \rho \left[ S^2(l) + S(l)S(s) + S(s)S(l) + S^2(s) \right] dA \quad (16)$$

If the mass flow density,  $\rho$ , is independent of the location,  $s$ , the first term of Equation 11 can be expressed in terms of the total mass flow rate  $\dot{m}$ . Since  $s$  is relative to the centroid of the area,

$$\int_A S(s) dA = 0 \quad (17)$$

and the two middle terms are zero. The last term is a function of the planar moment of the area. Therefore,

$$D = J + \sum_i \dot{m}_i (S^2(l_i) + S^2(s_i)) \quad (18)$$

where  $l_i$  is the location of the  $i$ th nozzle and  $S^2(s_i)$  is a function of nozzle area and orientation.

### Six Degree of Freedom Simulation

To perform analyses, and to provide a basis for evaluating linear analysis assumptions, a general spun stage six-degree-of-freedom (6 DOF) simulation was written. The simulation performs a fourth-order Runge-Kutta-Gill integration of the position, velocity and angular rate equations:

$$\begin{aligned} \dot{r} &= v, \\ \dot{v} &= B f/m, \text{ and} \\ \dot{\omega} &= J^{-1} \left[ \tau - S(\omega) J \omega - J \omega - \sum_i \dot{m}_i \left\{ S^2(l_i) + S^2(s_i) \right\} \omega \right] \end{aligned} \quad (19)$$

where  $r$  and  $v$  are inertial position and velocity vectors,  $B$  is the three by three direction cosine transformation from body to inertial space,  $f$  is the applied force in body coordinates, and  $m$  is the vehicle mass. The attitude equation,

$$\dot{B} = B S(\omega),$$

is not integrated. A closed form solution, developed for use in error analysis, is used. This solution is valid over any time interval for periods of simultaneous constant angular rates. While only an approximation for this problem (due to time-varying rates), the error is extremely small. Its use insures maintenance of the orthogonality of B, and its execution efficiency is excellent.

The time-varying coefficient arrays are computed from data describing the vehicle on a piece part basis. Each piece part is considered a hollow cylinder with its axis parallel to the roll axis. For each of these cylinders, the following data must be provided:

1. Length
2. Inside diameter
3. Outside diameter
4. Initial weight
- 5,6,7. Location of cylinder c.g. in body coordinates
8. Ignition time
9. Mass flow rate
10. Nozzle exit area, and
- 11,12,13. Thrust vector in body coordinates.

For inert masses, items 8 through 13 are not used. Fuel masses are assumed to burn from the inside out. This approximates the burning of many solid fuel engines.\* The simulation computes the system moment of inertia, c.g. location, damping terms, etc., by summing the appropriate data for each piece part. Analysis of a Scout fourth stage and its payload, using this cylindrical model, produces parameters that agree well with published values (Reference 24).

Information used in simulating the Red shift payload was taken from References 25 - 28. Mass property data were contained in Reference 25, but these data were modified. The weight given in this reference was 144.1 lb; late information\*\* gave the weight as 165 lb. The moments of inertia given in Reference 25 were increased by the ratio  $\frac{165}{144.1}$ .

---

\* Any assumed burning pattern can be simulated with minor coding changes.

\*\* Telephone conversation with Mr. Ernest Nathan of MSFC.

The Scout fourth stage was modeled after information taken from References 20, 21 and 29. The model of the stage consisted of four pieces:

1. Engine case
2. Fuel
3. Nozzle
4. Upper D section.

The parameters used to describe these pieces and the payload are shown in Table 4.

TABLE 4. VALUES USED IN SIMULATION

	<u>Payload</u>	<u>Engine</u>	<u>Nozzle</u>	<u>Fuel</u>	<u>Upper D Section</u>
Length (in.)	35.0	48.0	34.0	36.7	35.2
Inside Dia. (in.)	4.0	8.4	8.4	3.0	9.6
Outside Dia. (in.)	8.0	8.6	8.6	9.04	10.8
Initial Wt. (lb.)	165.0	30.0	21.2	613.9	16.48
cg X (in.)	26.9	58.3	89.0	67.18	91.33
cg Y (in.)	0.0	0.0	0.0	0.0	0.0
cg Z (in.)	0.0	0.0	0.0	0.0	0.0
Ignition time (sec.)				0.0	
Mass flow rate ( $\frac{\text{lb}}{\text{sec}}$ )				-21.2	
Nozzle exit area (ft <sup>2</sup> )				2.25	
Thrust X (lb.)				5925.0	
Y (lb.)				0.0	
Z (lb.)				0.0	



The simulation program is written to provide graphic output. An example is shown in Figure 10. The Y-Z plane is defined as being normal to the vehicle roll axis at the start of the simulation. It then translates with the vehicle center-of-gravity. The trace on the Y-Z plane, then, is a function of the angular motion of the vehicle's roll axis, as shown in Figure 11. The dimensions on the Y and Z axes correspond to the sines of the angles that the roll axis makes with respect to the Y and Z directions on the Y-Z plane.

Discrete events are shown as triangles on the output. Each plot has a triangle at the origin corresponding to ignition of the fourth-stage engine. In order to avoid putting too much data on a single plot, a number of plots may be used, each covering a distinct time period. The triangle at the origin is shown for reference on all plots, including those that start at a time greater than that of fourth-stage ignition. When a multiple-segment burn is used to approximate the engine, a triangle is printed at the start of each segment's burn.

Although results obtained by the simulation appear to be reasonable during the powered flight portion of the mission, an unwelcome anomaly was found to occur at burnout. The pattern in Figure 12 is typical for Scout fourth stage with thrust misalignment during powered flight; however, the "tail" seen in the lower left of the figure is definitely not to be expected. The pattern should be a circle with diameter about .068 (or about 4 degrees) after termination of powered flight. This discontinuity is apparently due to assuming a rectangular burn with constant thrust and flow rate for the burn interval. When an eight-segment staircase approximation to the burn was used, this effect was minimized. Further discussion of this modification and its results is contained later in this section.

In order to obtain appropriate tipoff response, it was necessary to modify the fourth-stage exit area to 2.25 square feet rather than the 1.5 square feet given in Reference 20.

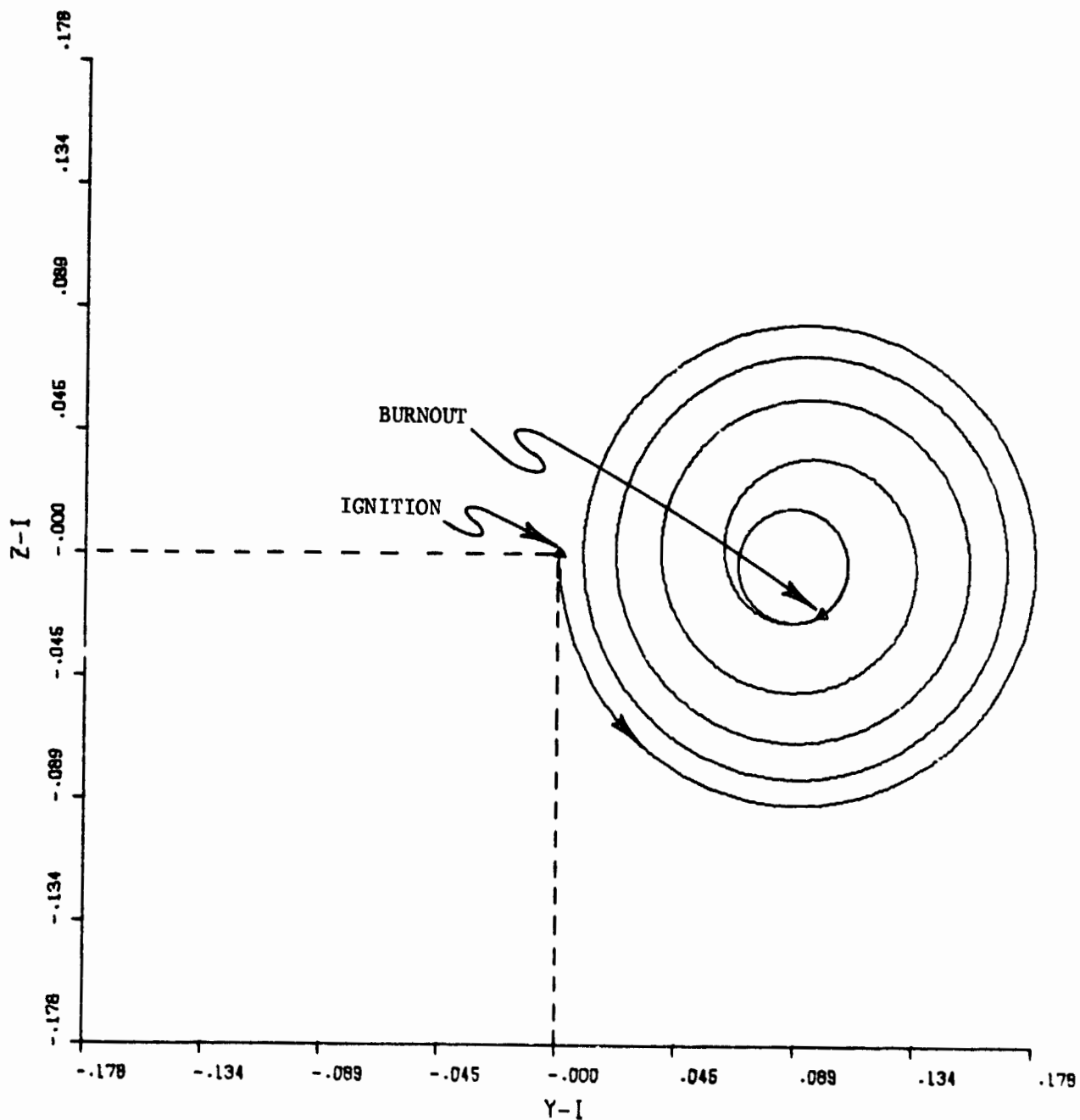


FIGURE 10. SAMPLE GRAPHIC OUTPUT

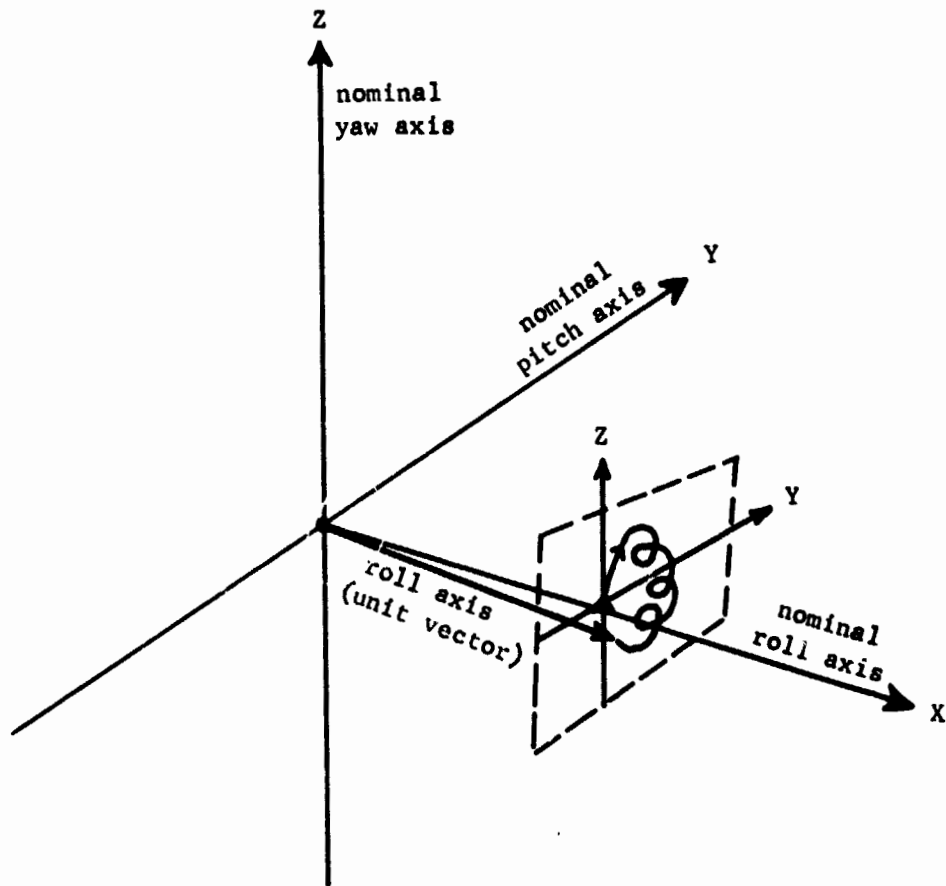


FIGURE 11. DEFINITION OF GRAPHICAL OUTPUT

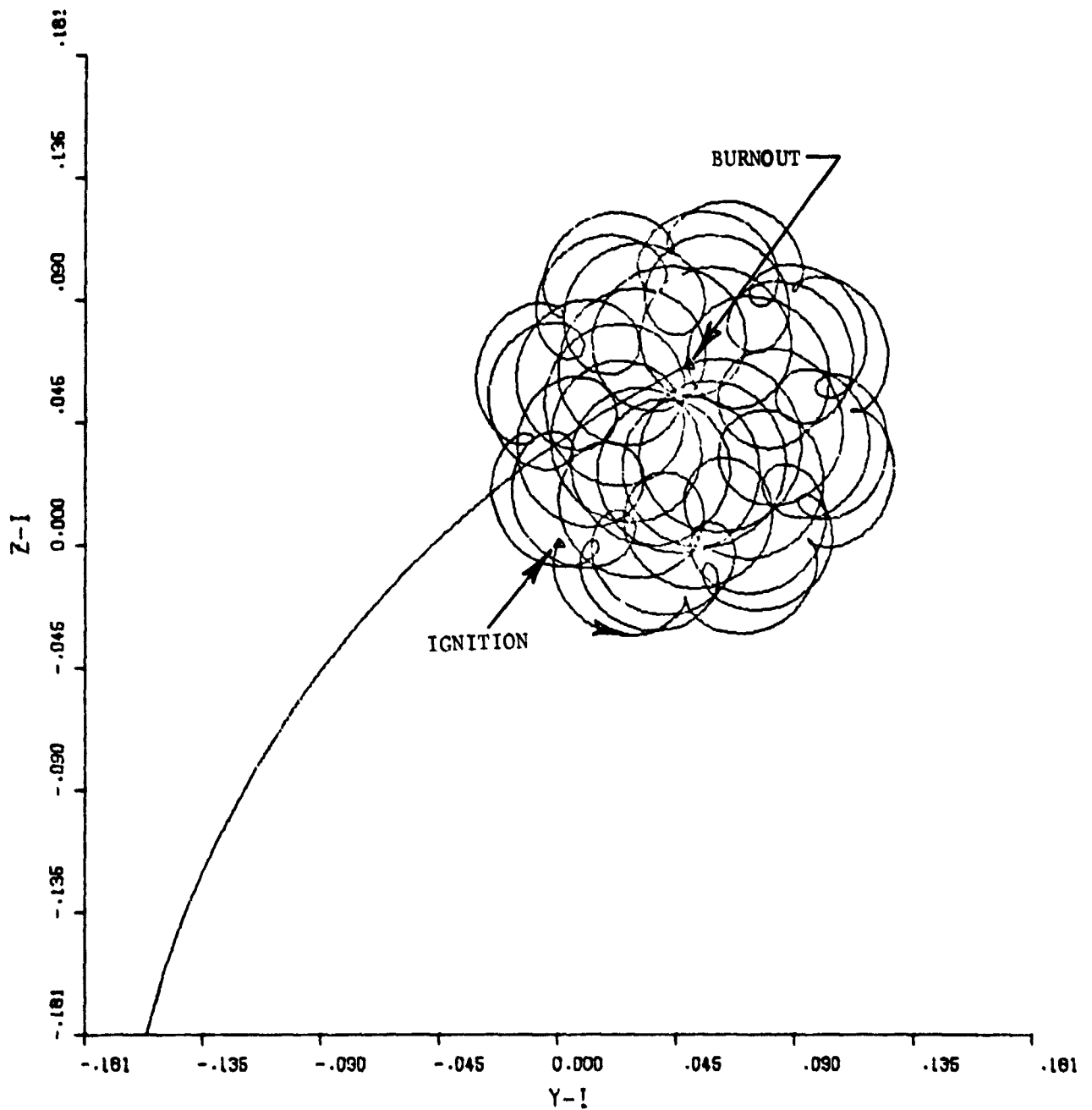


FIGURE 12. EXAMPLE OF GRAPHIC OUTPUT ILLUSTRATING BURNOUT ANOMALY

### Error Sources Considered

Several error sources were simulated in order to determine their effect on dynamic behavior of the Red shift payload. These sources were

- (1) Ammonia venting from the payload
- (2) Scout fourth-stage tipoff
- (3) Fourth-stage thrust misalignment
- (4) Fourth-stage burnout unbalance
- (5) Payload static and dynamic unbalances.

Ammonia Venting. The payload includes a supply of liquid ammonia for use in cooling the maser cavity. After the ammonia changes to gas during the cooling process it is vented overboard, normal to the roll axis, at Scout Station No. 29.97. Gaseous ammonia is vented at a rate of 0.28 pound-per-hour with a resultant force of 0.0034 pound (Reference 30). Figure 13 shows the results of the ammonia venting for the first 100 seconds of operation following fourth-stage ignition. It is seen that the original disturbance which results in a half-cone angle of about  $0.6 \times 10^{-3}$  degree, decays by the end of fourth-stage thrusting to about  $0.2 \times 10^{-3}$  degree. During the coast, this angle is maintained, although modulated by the normal force due to the ammonia venting.

Fourth-Stage Tipoff. Figure 14 shows the effect of fourth-stage tipoff. The initial response is a half-cone angle of about 5 degrees, which is damped to about 1.1 degrees by the time of burnout. This corresponds quite well with the values of 5.22 degrees at ignition, given in Reference 31, and 1.11 degrees at burnout, given in Reference 29.

Thrust Misalignment. The effective 3- $\sigma$  thrust misalignment for the FW-4 engine is given as 0.3 degree in Reference 29. When this value is included in the simulation, the plot of Figure 15 results. The initial half-cone angle of about 4.6 degrees decays to about 1.8 degrees at engine burnout. The "stem" going to the lower left-hand corner of the plot is a result of simulating the engine burn as a single, rectangular burn. A more detailed simulation would show the 1.8 degree half-cone angle continuing during coast.

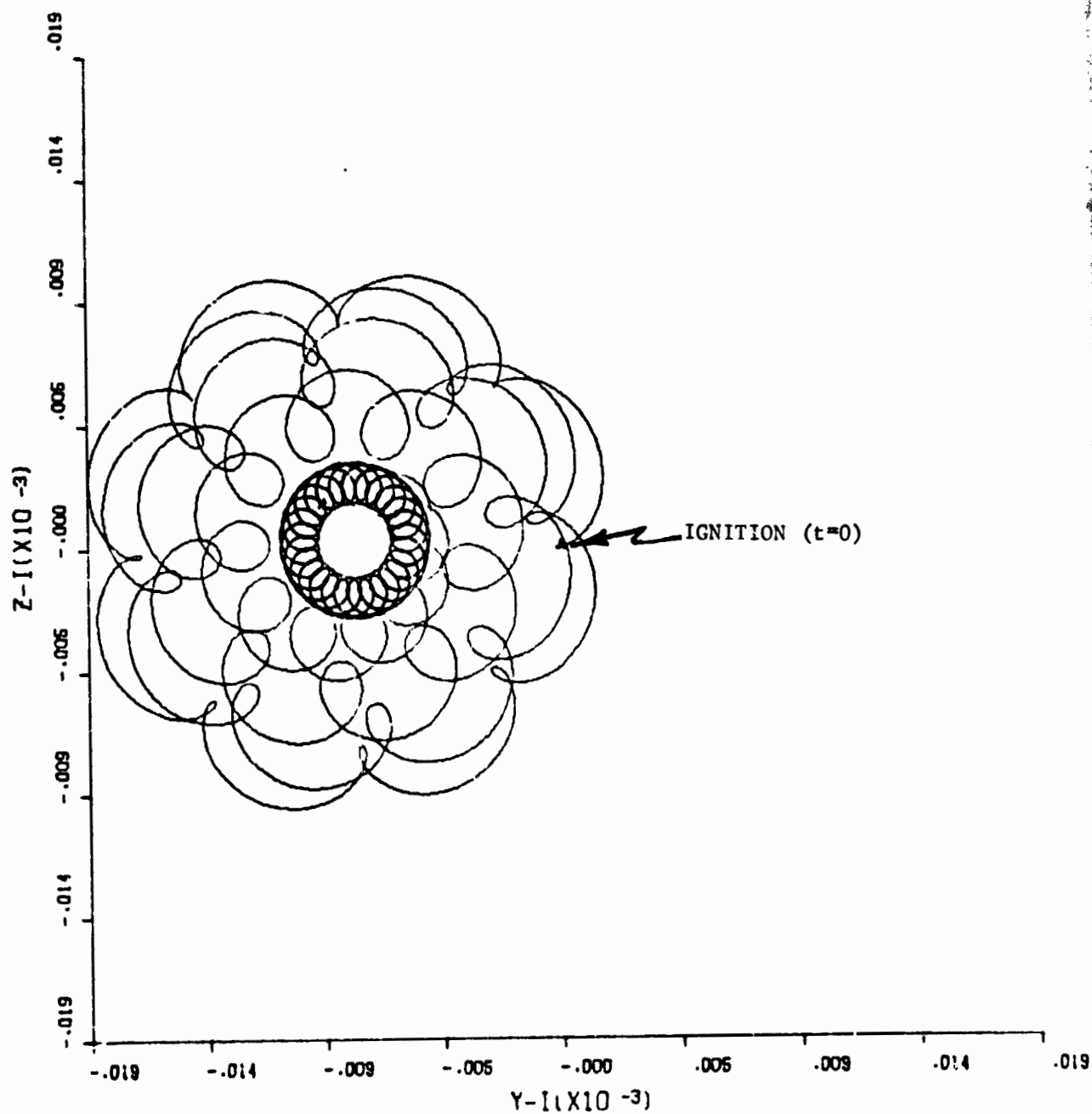


FIGURE 13. EFFECT OF AMMONIA VENTING FOR FIRST 100 SECONDS AFTER FOURTH-STAGE IGNITION

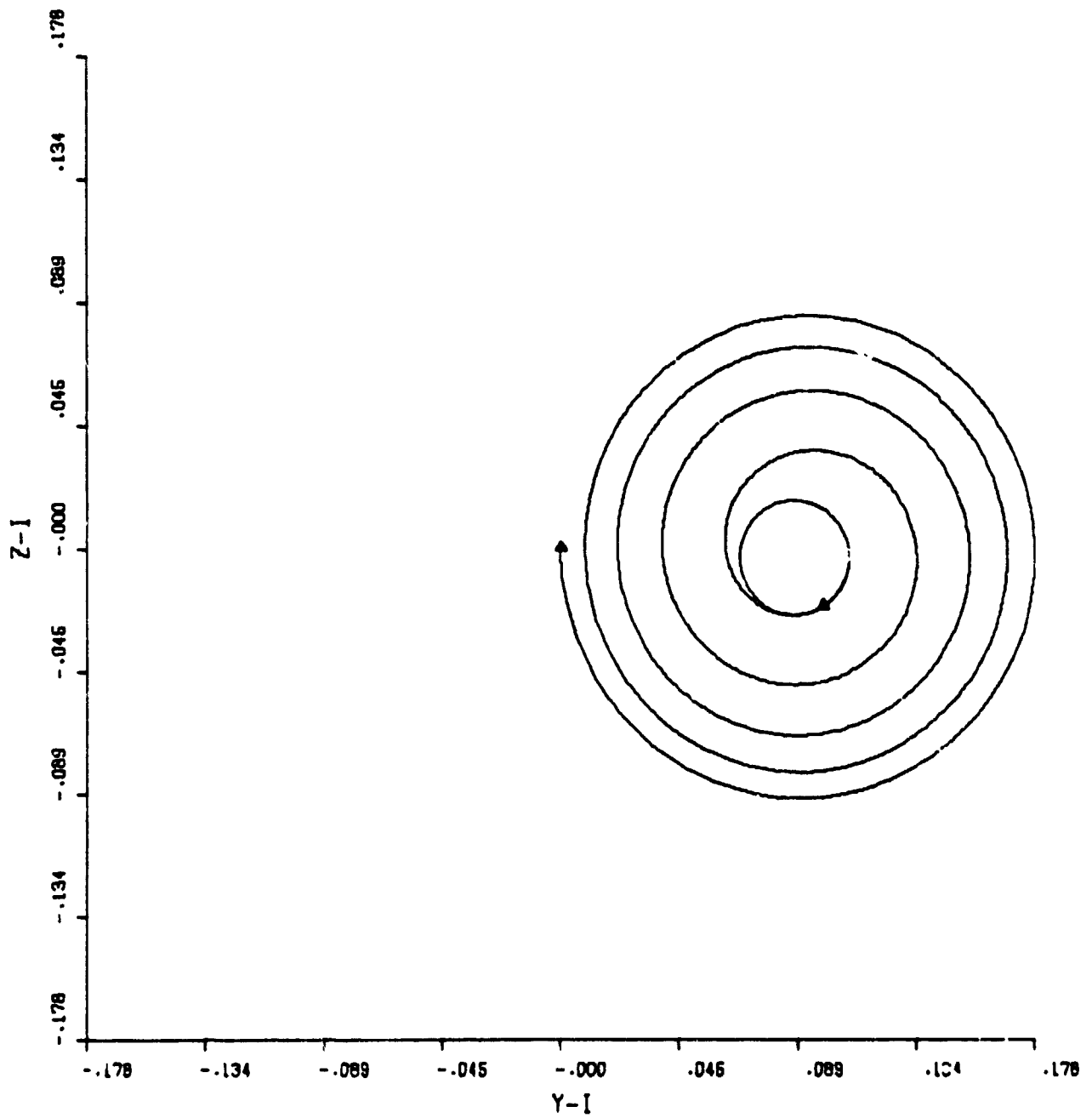


FIGURE 14. EFFECT OF TIPOFF ( $t=0-40$  sec)

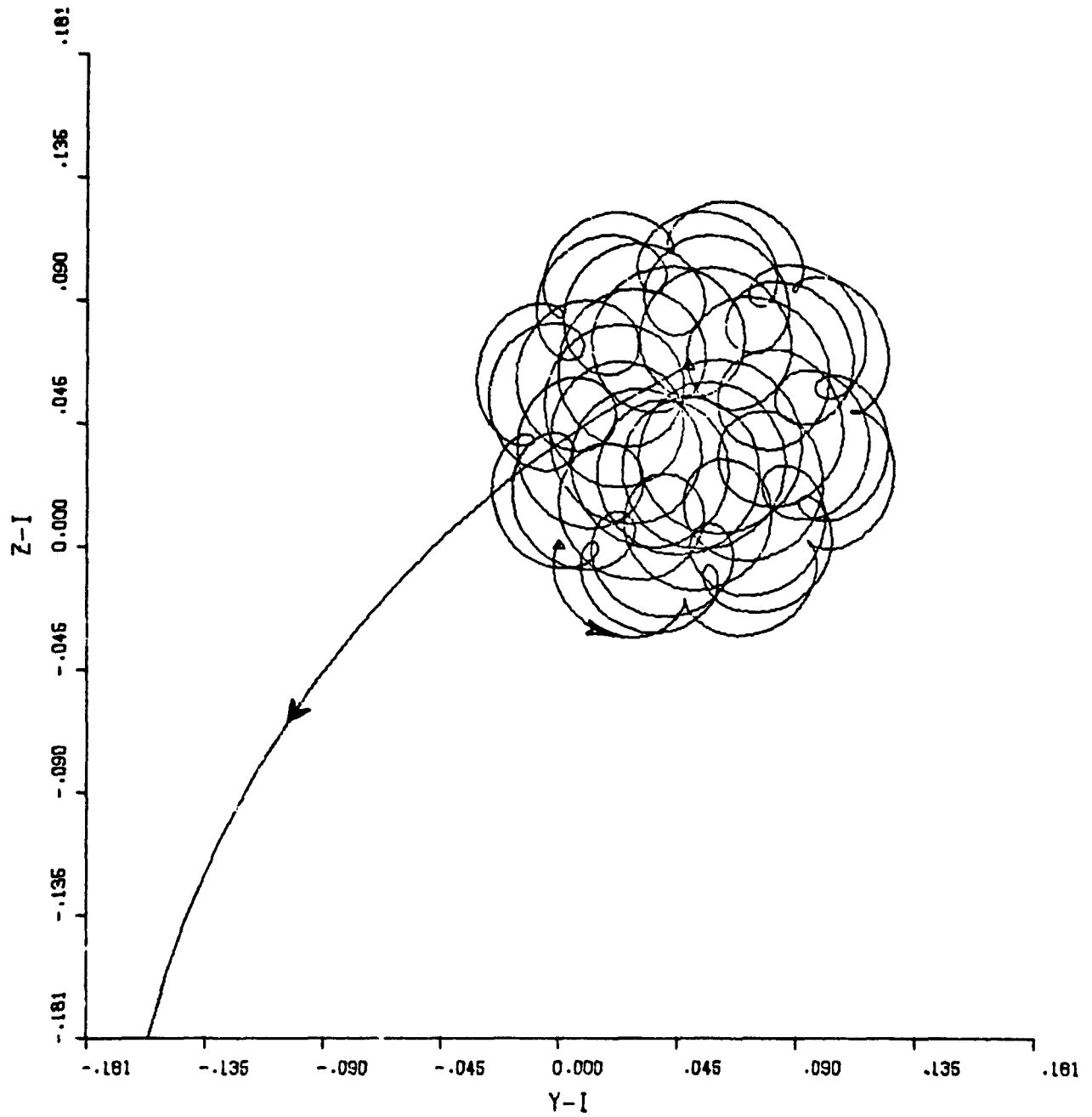


FIGURE 15. EFFECT OF THRUST MISALIGNMENT ( $t=0-30$  sec)



Fourth-Stage Burnout Unbalance. This error source is attributed to blistering of the case insulation (Reference 29). Although a small amount of flight data has resulted in a 3- $\sigma$  dynamic unbalance value of 2400 oz-in<sup>2</sup> for this source, the LTV design criterion calls for an upper limit of 8000 oz-in<sup>2</sup>. This latter value was used in the simulation. The effect of this error source was found to be insignificant and no plot is included in this report.

Payload Unbalances. Reference 20 gives 12 oz-in and 200 oz-in<sup>2</sup> for maximum values of static and dynamic unbalances, respectively. When these terms were added to the simulation, no significant error was found to result. Therefore, no plot is included of the effect of these error sources.

Thrust Misalignment and Tipoff. Since fourth-stage thrust misalignment and tipoff were the major error contributions, runs were made with both of these error sources combined in such a way as to produce maximum error. During these runs it was found that the initial half-cone angle was about 8.5 degrees as can be seen from Figure 16.

During this series of runs, it was decided to investigate the cause of the "tail" following engine cutoff. Three-segment and eight-segment models of the thrust and flow rate for the engine were incorporated into the simulation (See Figure 17). Results for one-, three-, and eight-segment models during the last portion of powered flight and the first few seconds afterward are shown in Figure 18-20, respectively. For the original, one-segment model (Figure 18), a half-cone angle of 20 degrees results. Figure 19 shows a half-cone angle of about 9.5 degrees for the three-segment model. When the 8-segment model is used (Figure 20), the half-cone angle is about 2 degrees. This is the same value that would be predicted by examining the trace of Figure 16 just before burnout. Thus, it is concluded that the anomalous behavior in many of the plots after burnout can be ignored.

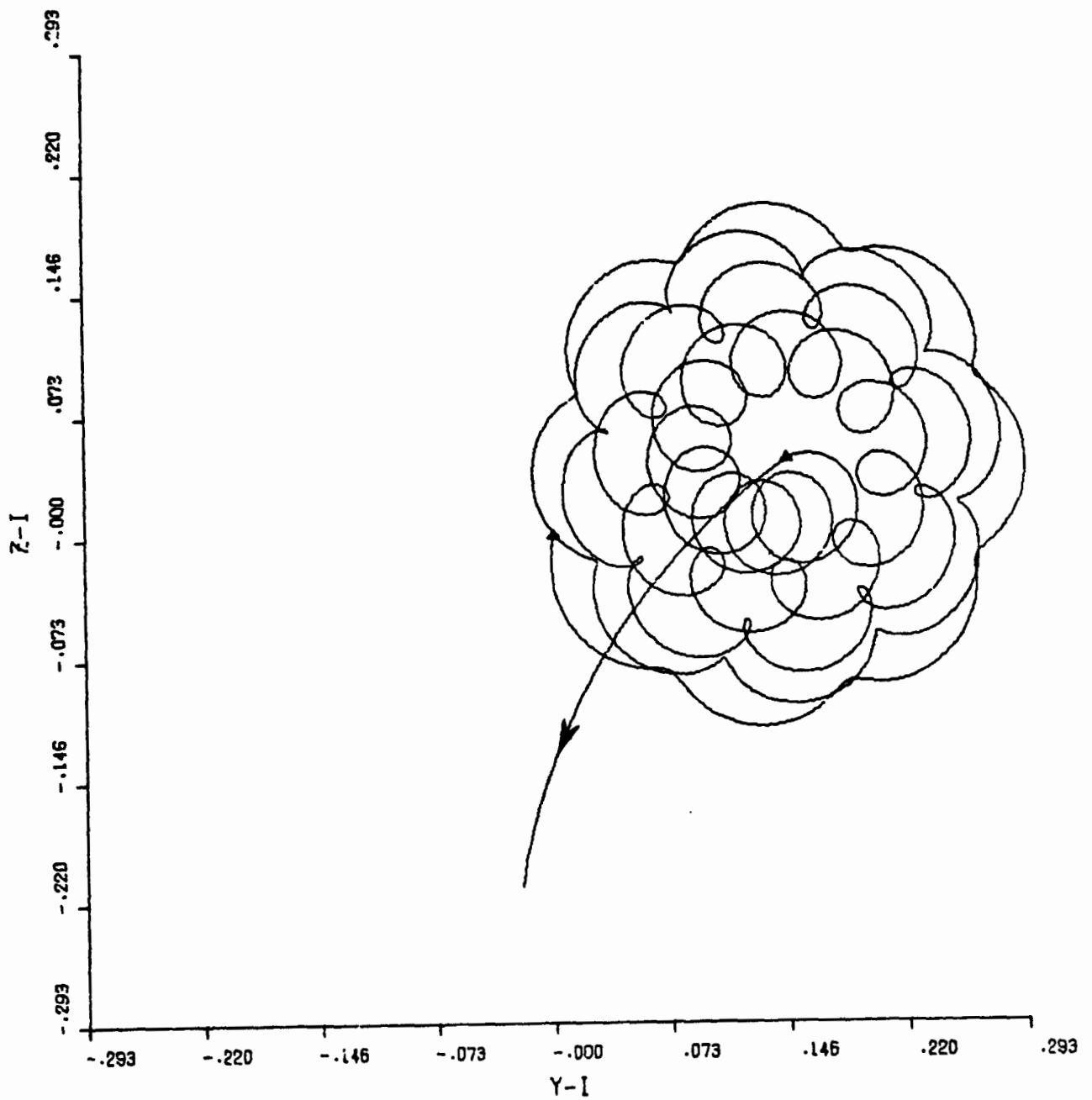


FIGURE 16. EFFECT OF WORST-CASE COMBINATION OF THRUST MISALIGNMENT AND TIPOFF ( $t=0-30$  sec)

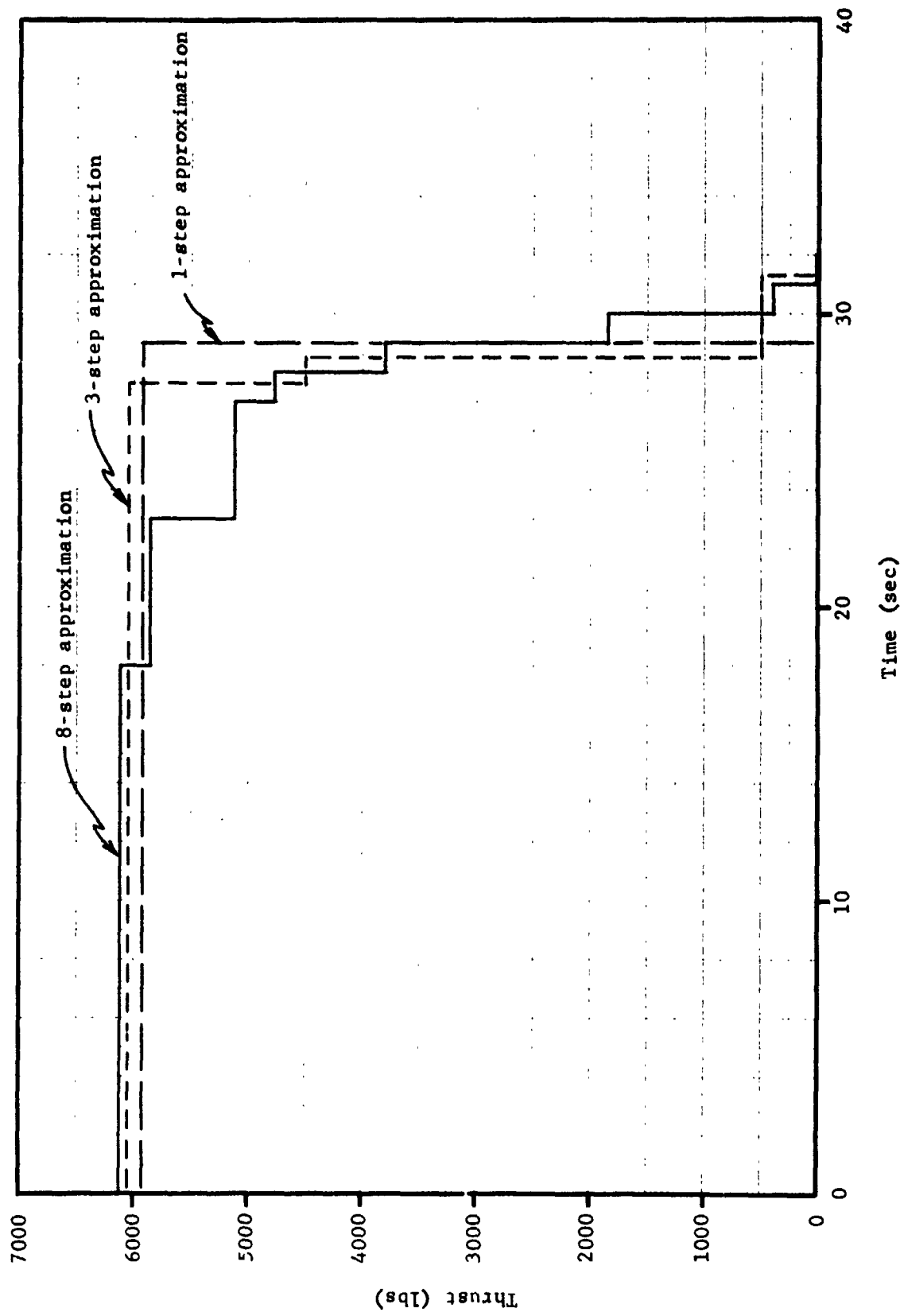


FIGURE 17. THRUST MODELS USED

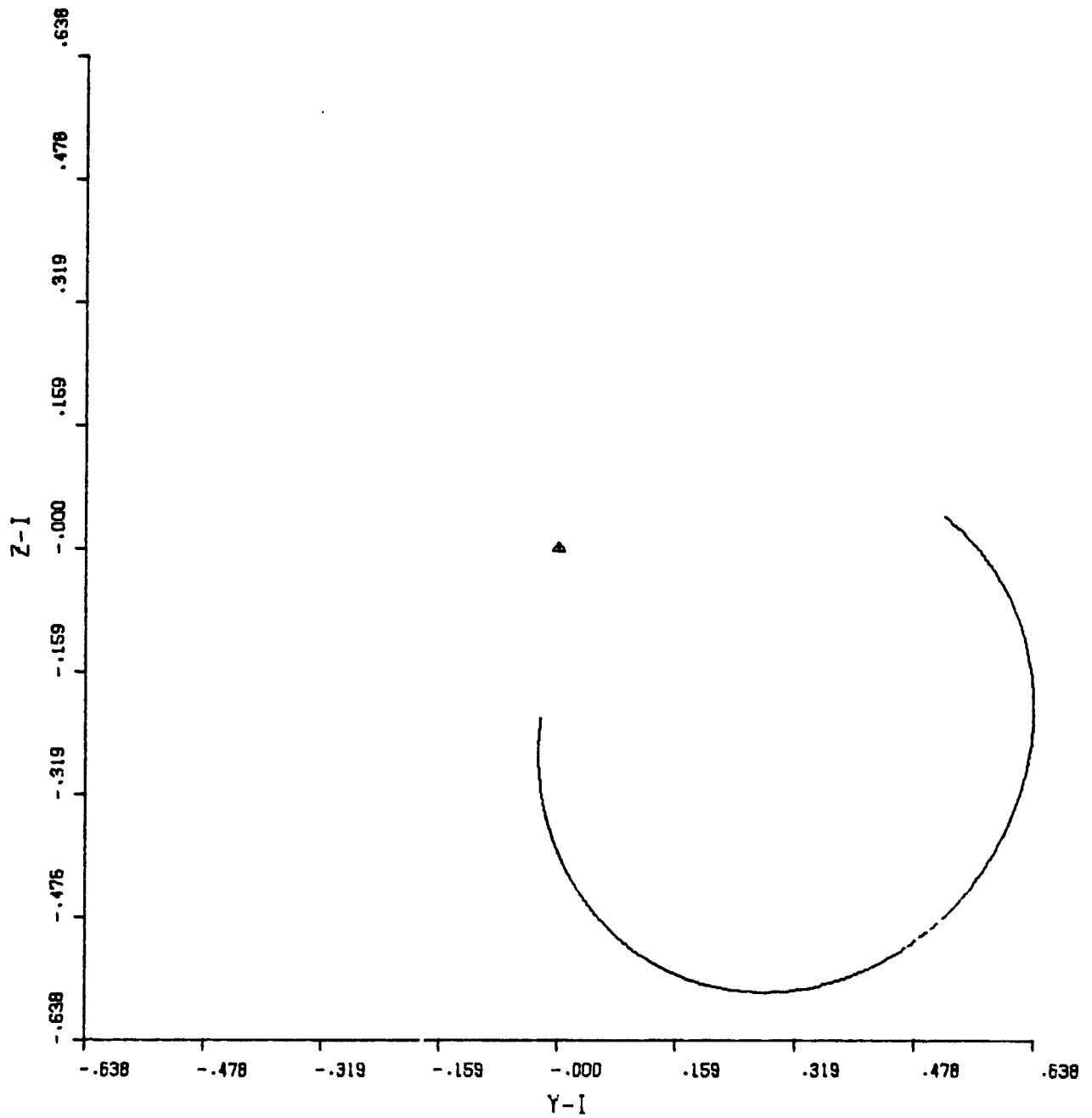


FIGURE 18. FINAL CONING WITH SINGLE-SEGMENT FUEL MODEL

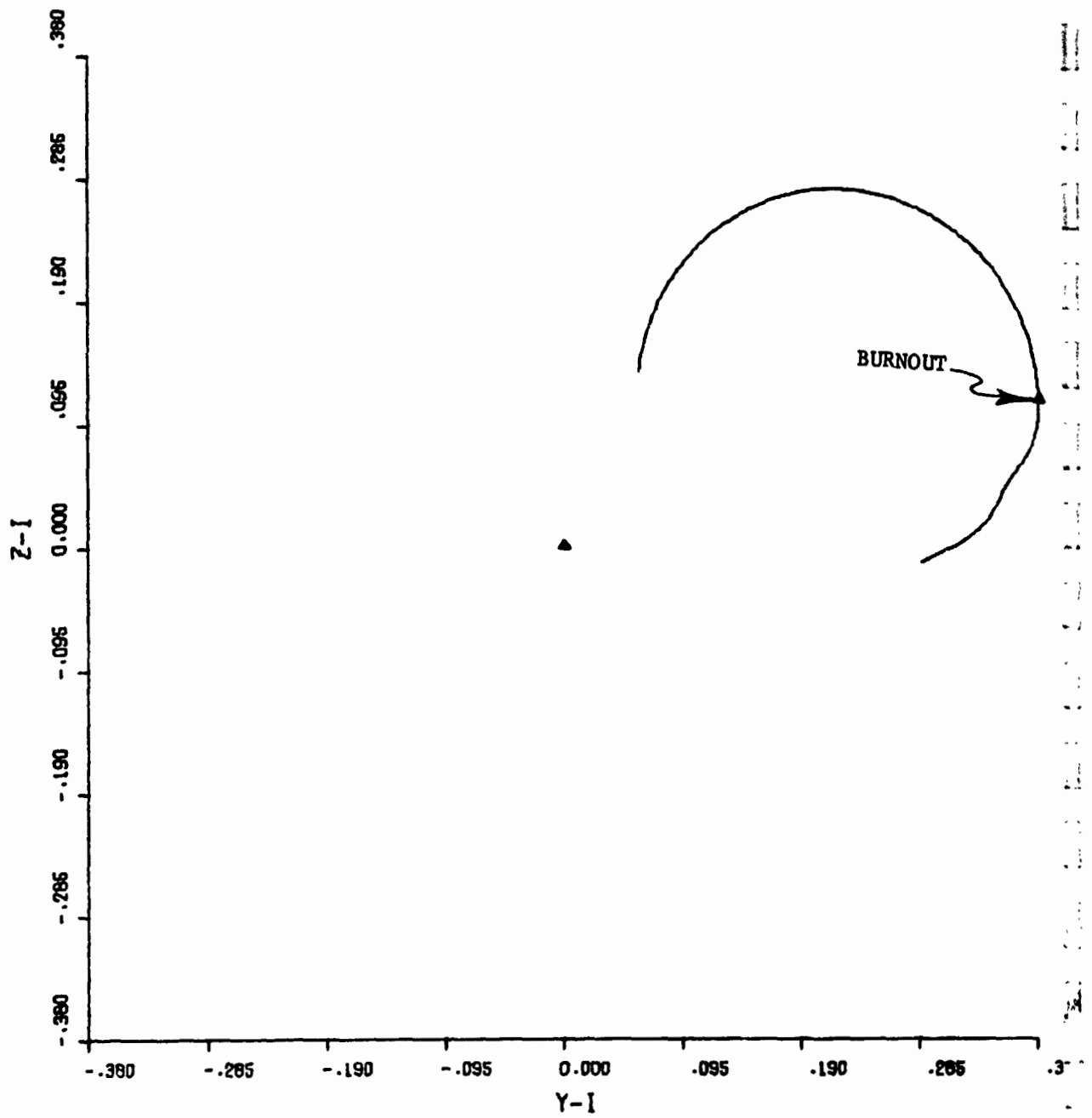


FIGURE 19. FINAL CONING WITH THREE-SEGMENT FUEL MODEL

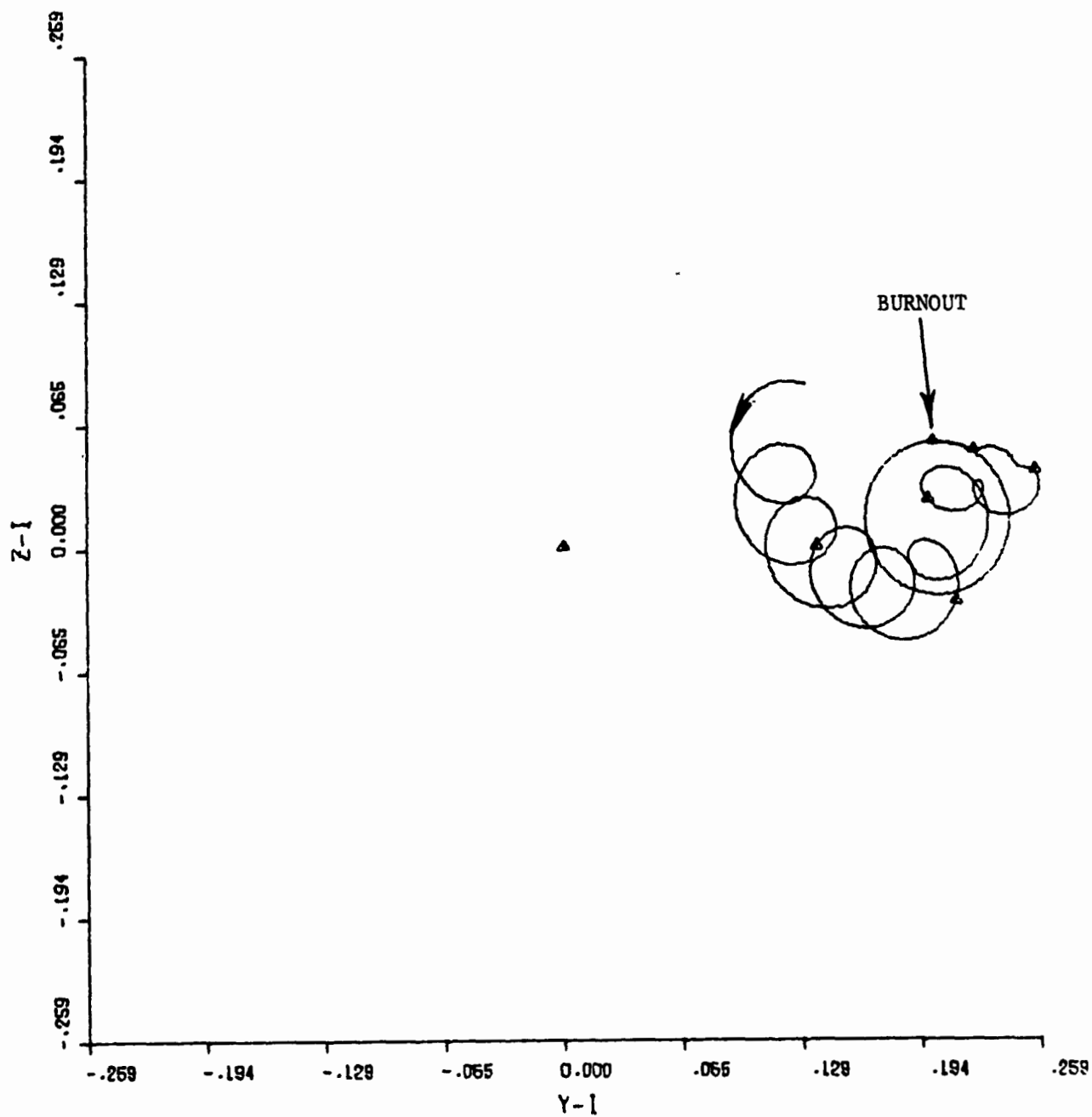


FIGURE 20. FINAL CONING WITH EIGHT-SEGMENT FUEL MODEL

Concluding Remarks

From the results of the investigations, it appears that the error sources considered are not likely to cause significant problems in conducting the Redshift mission. It must be realized, however, that the simulation used for most of these studies does not use detailed models of the vehicle and payload and, thus, subtle effects could remain undiscovered.

#### Task 4 Perform Mission Requirements Assessments

Studies conducted under this contract have been concerned with the assessment of conventional launch vehicle astrionics capabilities and their adequacy for projected mission requirements. Injection accuracy has been a primary concern. Navigation accuracy analysis techniques for both open loop (Scout, Titan IIID), and closed loop (Delta, Atlas/Centaur, Titan/Centaur, etc.) were developed. (References 1-3)

These techniques permit evaluation of current (or proposed improvements to) injection accuracy. To objectively apply these techniques, a concise set of allowable injection conditions must be known. Investigations of missions frequently indicate arbitrary or vague specification of allowable deviation from the desired aim point. For example, one payload was placed in an orbit well outside the specified "window" but was found to provide experimenters with more data than would have been obtained had the nominal orbit been achieved. Considerations such as these led to the investigation of the relationship of experiment oriented parameters such as orbit/earth and orbit/sun precession rates to satellite injection conditions.

Concurrently, Battelle personnel were involved to varying degrees in the initial planning phases of future missions (HEAO, SEASAT and LAGEOS). In each of these cases, potential experimenters needed answers to questions requiring analyses outside their individual technical disciplines. Thus, NASA launch vehicle offices and vehicle prime contractors were called upon to provide analytical support well in advanced of the approval of experiments and missions. Conducting effective tradeoff analyses of even a few alternative orbits can require significant manpower and computer time if traditional detailed analytical techniques are used.

To meet both the needs of the astrionic evaluation function and the mission planning function, the Interactive Graphics Orbit Selection (IGOS) program was written.

Experience has shown the value of presenting a synopsis of system propulsion capabilities and limitations to potential space transportation system users. This was accomplished by periodic publication of, Reference 34, the Launch Vehicle Estimating Factor Book (EFB) by the OSS Launch Vehicles and Propulsion Programs Division, Code SV [now Expendable Vehicle Programs (Code MV) in the Office of Space Flight (OSF)]. This planning handbook (EFB) contains data, usually in graphical form, for:



- (1) Launch Vehicle payload capabilities versus characteristic velocity,  $V_c$
- (2) Earth orbit and planetary mission  $V_c$  requirements
- (3) Determining Launch Vehicle payload capability versus Earth orbit parameters (perigee, apogee, and inclination) for specific vehicles
- (4) Mission restrictions (orbit life time, range safety, etc.).

These data are presented in a form suitable for interpretation by a payload planner. While this necessitates reasonable engineering approximations, the data are sufficiently accurate for trades between the users desires and the transportation system capabilities. Developing mission specifications using this handbook provided an opportunity for the payload planner to consider a wider range of alternatives than would be possible using detailed analysis techniques. Detailed analysis could be performed later in the planning cycle and be based on a feasible set of mission specifications.

The availability of interactive graphics terminals and central computer software has permitted developing various planning tools including one for preliminary mission planning which is far more effective than the traditional handbook format. Several years of successful operation of the NASA Interactive Planning System (NIPS) by both OSS and OA had previously demonstrated the feasibility and reliability of financial analyses performed using interactive graphics terminals for decision making, report generation, and data file maintenance. The interactive graphics tools have now been extended to permit preliminary mission planning by this program is far more versatile and effective for Earth orbital mission planning than the traditional handbook format.

A detailed users manual and sample work session are included in Appendices A and B. The following paragraphs summarize the operation of IGOS.

### IGOS Program Description

The IGOS program facilitates quick-response assessment of Earth-orbit mission requirements and their trade-offs with launch-vehicle capabilities. By using an interactive graphics computer terminal, a quick-response low-cost analysis can be initiated early in the mission planning cycle. Application of this program in no way eliminates the need for the traditional detailed mission analyses during later phases of mission planning. It does, however, reduce the need for major iterations in the planning cycle due to unacceptable orbit characteristics.

IGOS utilizes the capabilities of interactive graphics terminals, so experimenters and mission planners can clearly visualize the many possible orbit alternatives that can satisfy their mission requirements. The operating environment for the IGOS system is illustrated in Figure 21. The user enters a set of mission requirements at a remote graphics terminal and receives appropriate graphical and textual displays. The information displayed enables the user to select acceptable alternative Earth orbits.

Graphical output is in a two-dimensional design space - altitude and inclination for the vertical and horizontal axes. Thus, a point in the plot represents a circular orbit. Regions representing unacceptable orbits are shaded, as shown in Figure 22. The shaded areas result from the constraints imposed by the following requirements and phenomena:

- (1) Earth-observation coverage
- (2) Radiation environment
- (3) Sun-orbit precession
- (4) Orbit decay

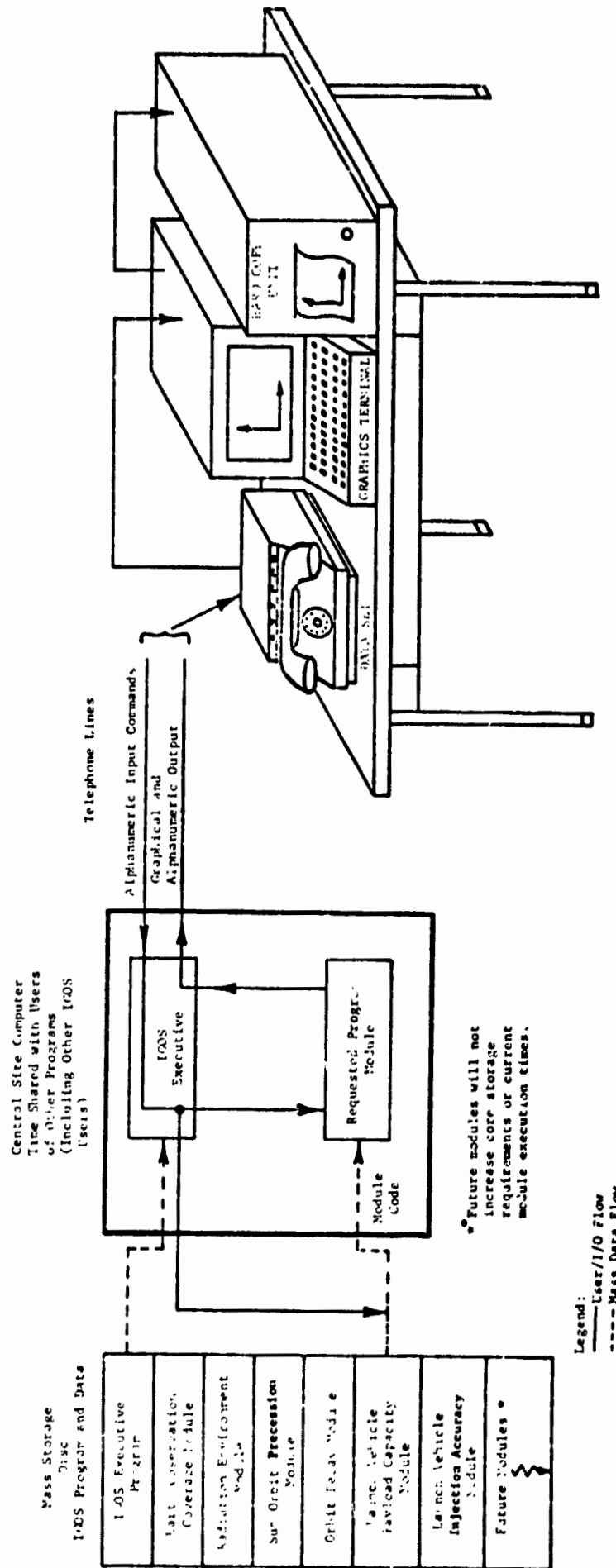


FIGURE 21. ICOS OPERATION

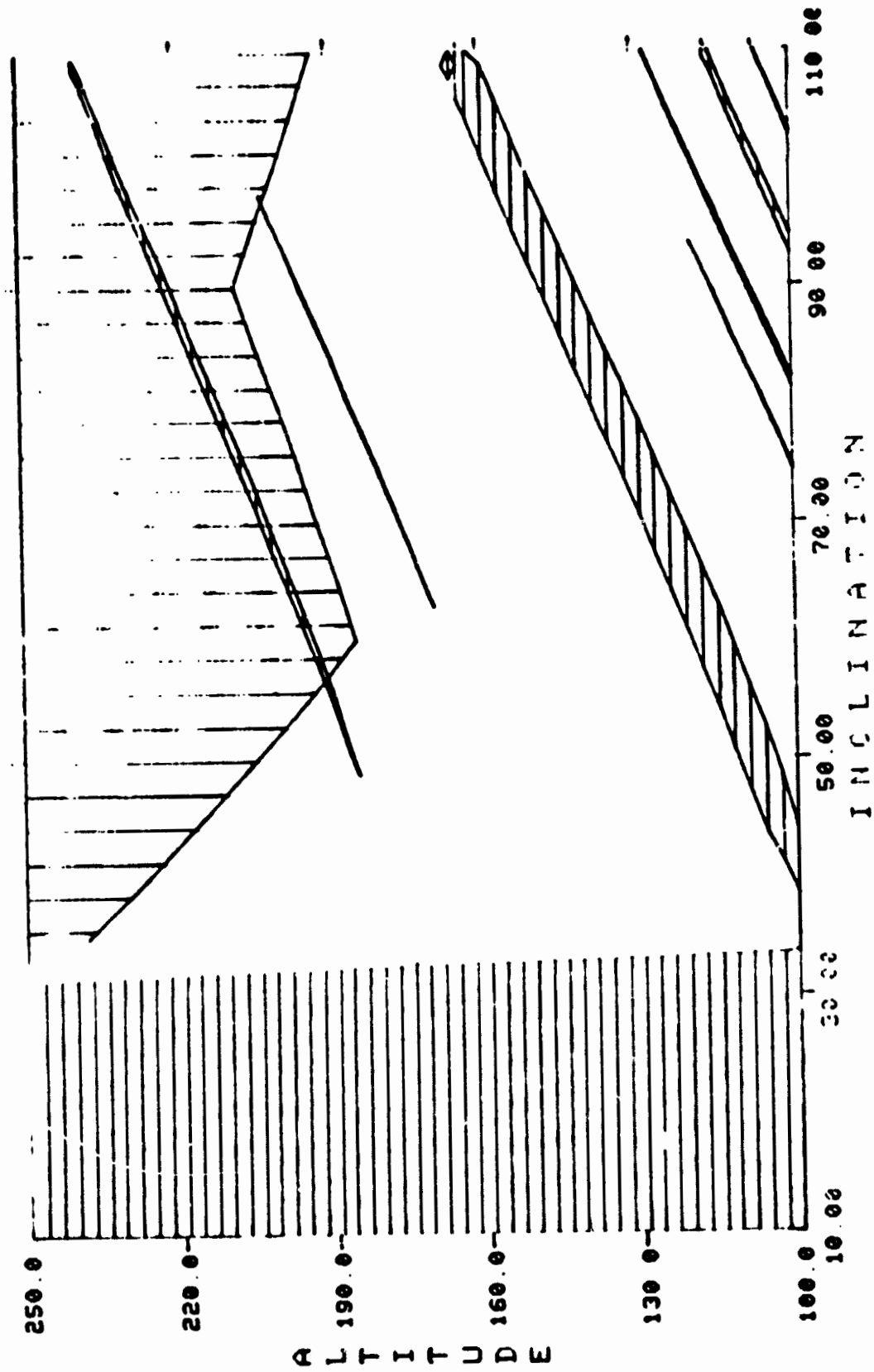


FIGURE 22. TYPICAL IGOS GRAPHICAL OUTPUT

- (5) Launch-vehicle injection accuracy
- (6) Launch-vehicle payload capabilities.

Each of these is described in the following paragraphs. The user-supplied data are listed and a sample plot is shown. This is followed by a hypothetical exercise using all of the features.

#### Earth-Observation Coverage

##### Input Data:

- Latitude range of interest,
- Days allowed for viewing all longitudes within the latitude range, and
- Sensor data (maximum slant range, minimum elevation above the horizon, field of view, and resolution).

In the resulting display, the shaded areas indicate all orbits which do not view every longitude in the latitude range of interest in the allowed time.

#### Radiation Environment

##### Input Data:

- Aluminum shielding density,
- Allowable fluence (flux-time integral) accumulated inside the shielding, and
- Mission duration for accumulating the fluence.

Orbits which experience excessive fluence are indicated by vertical hatching in Figure 22.

### Orbit to Sun Precession

#### Input Data:

- Allowable precession rate.

The acceptable region is shown by dashed vertical lines, as shown in Figure 23. The center line denotes the locus of zero precession (sun synchronous orbits), and the other two lines indicate the allowable limits for an acceptable precession rate.

### Orbit Decay and Launch-Vehicle Injection Accuracy

These separate phenomena are both related to a specific nominal injection condition, and their effects are displayed together.

#### Input Data:

- Injection altitude,
- Injection inclination,
- Spacecraft ballistic coefficient,
- Launch date, and
- Mission duration.

A vertical line is then displayed at the specified inclination, as shown in Figure 24. "Tick" marks indicate the nominal, plus and minus, one-sigma and three-sigma altitudes. Ticks on the left represent the dispersion of initial orbits; ticks on the right represent the corresponding altitudes after the specified decay time. Ticks occurring above the top of the plot are indicated by displaying their altitude; those below the bottom are annotated with the date they would pass the minimum altitude.

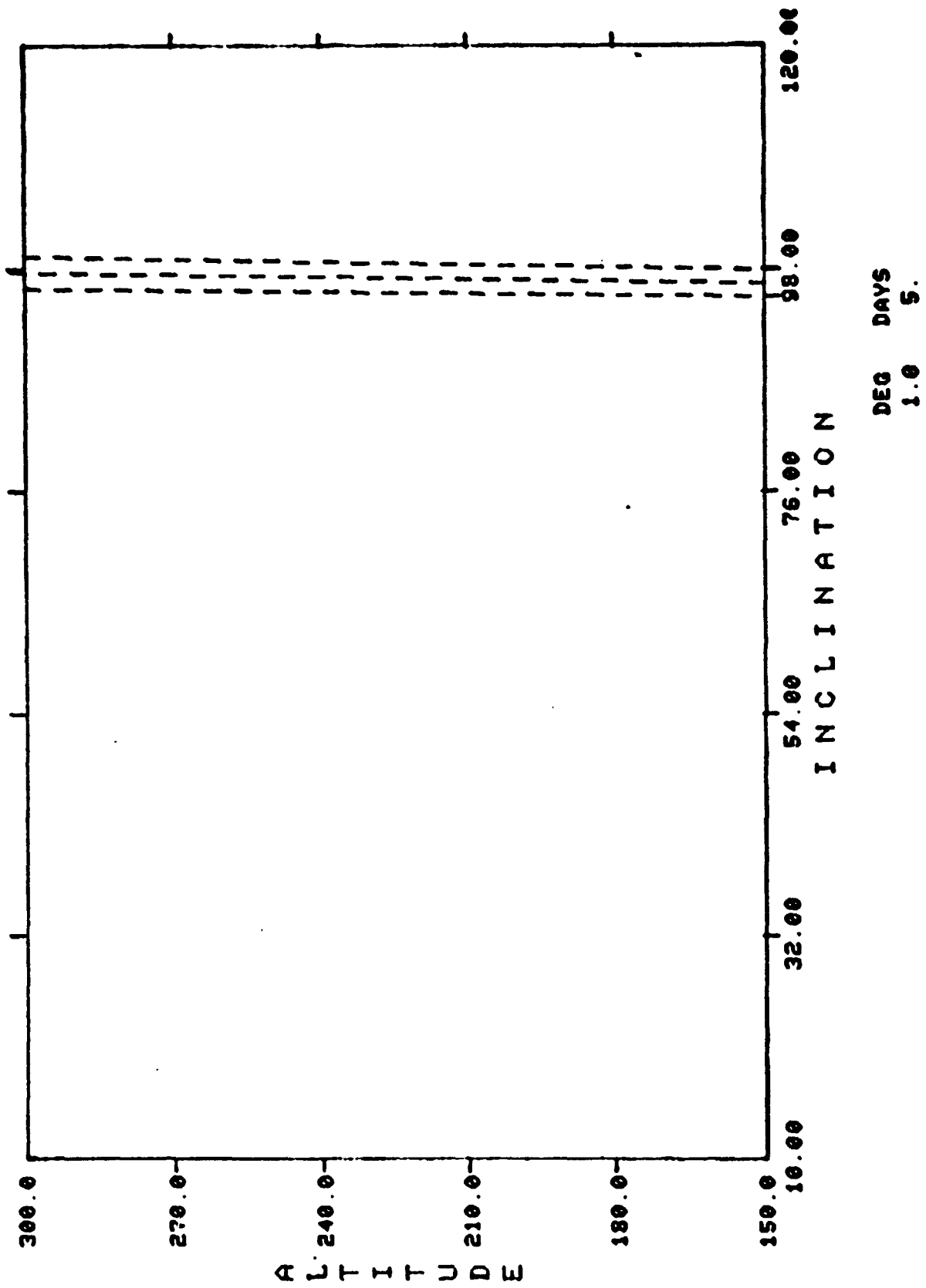


FIGURE 23. SUN-ORBIT PRECESSION LIMIT

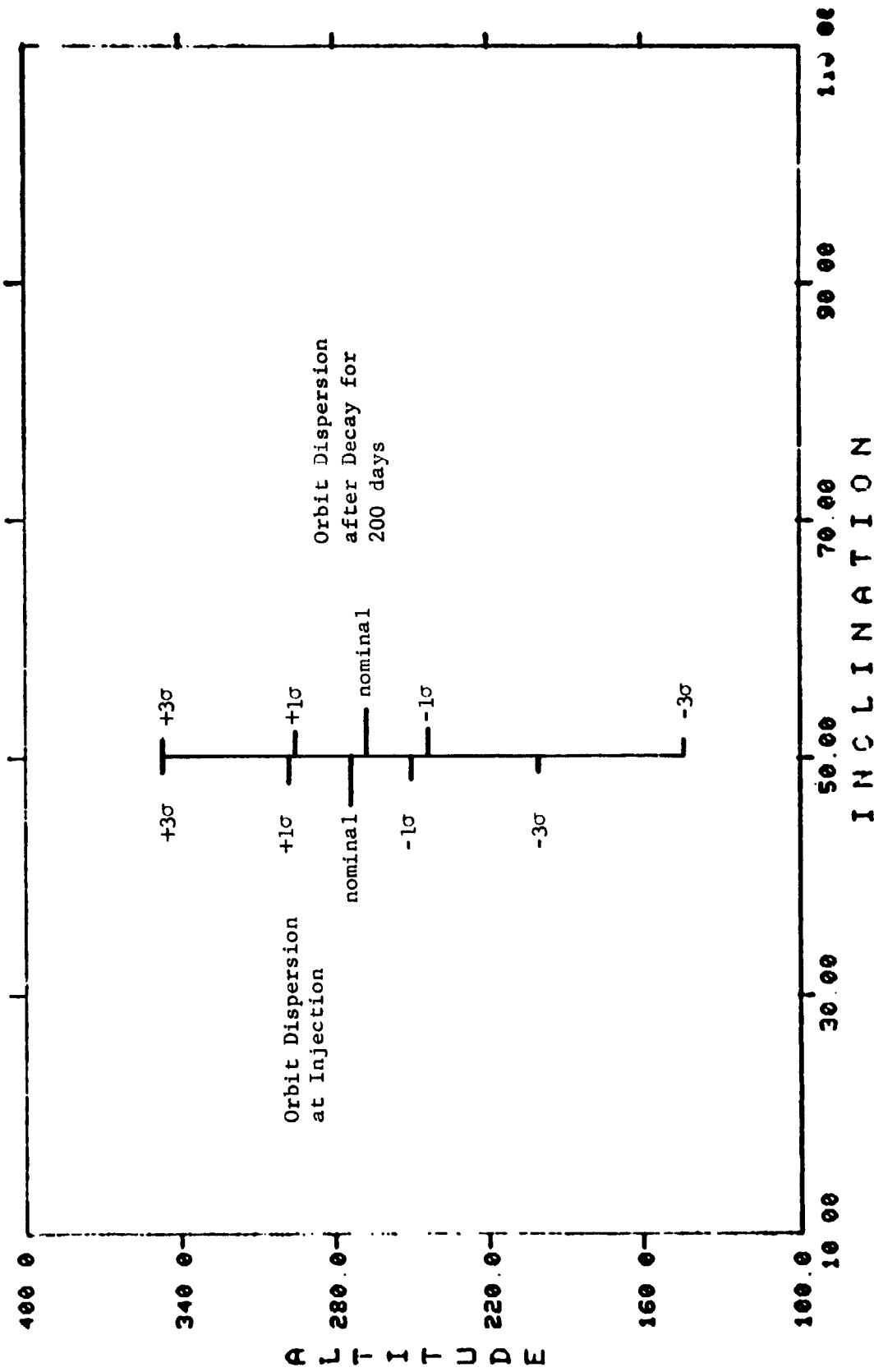


FIGURE 24. ORBIT DECAY AND LAUNCH-VEHICLE INJECTION ACCURACY



### Launch-Vehicle Payload Capabilities

#### Input Data:

- Launch vehicle and
- Payload weights of interest.

All launch-vehicle and launch-site data are stored with the program. When a launch vehicle is selected, equipayload weight contours are plotted, as shown in Figure 25. The contours are the altitude at which the vehicle can inject the payload into a circular orbit, as a function of inclination. For each inclination, all of the possible launch sites for the selected vehicle are considered, and the site yielding the highest altitude is chosen. Launch azimuth constraints and plane change losses are included in the performance calculations.

Although Figures 22 through 25 show separately the important features of IGOS, the full benefit of the program is apparent when these plots are superimposed and modified interactively. Consider the following problem.

It is desired to view all the Earth's surface between  $20^{\circ}$  and  $60^{\circ}$ N latitude at least once every 30 days for a 200-day mission. Assume a sensor with the following characteristics:

- Maximum slant range 1200 n.mi.
- Minimum elevation  $40^{\circ}$
- Field of view  $40^{\circ}$
- Resolution of 10 n.mi. on the Earth  $\approx 0.1^{\circ}$  at the sensor.

The orbit should precess relative to the sun less than  $30^{\circ}$  during the 200-day mission.

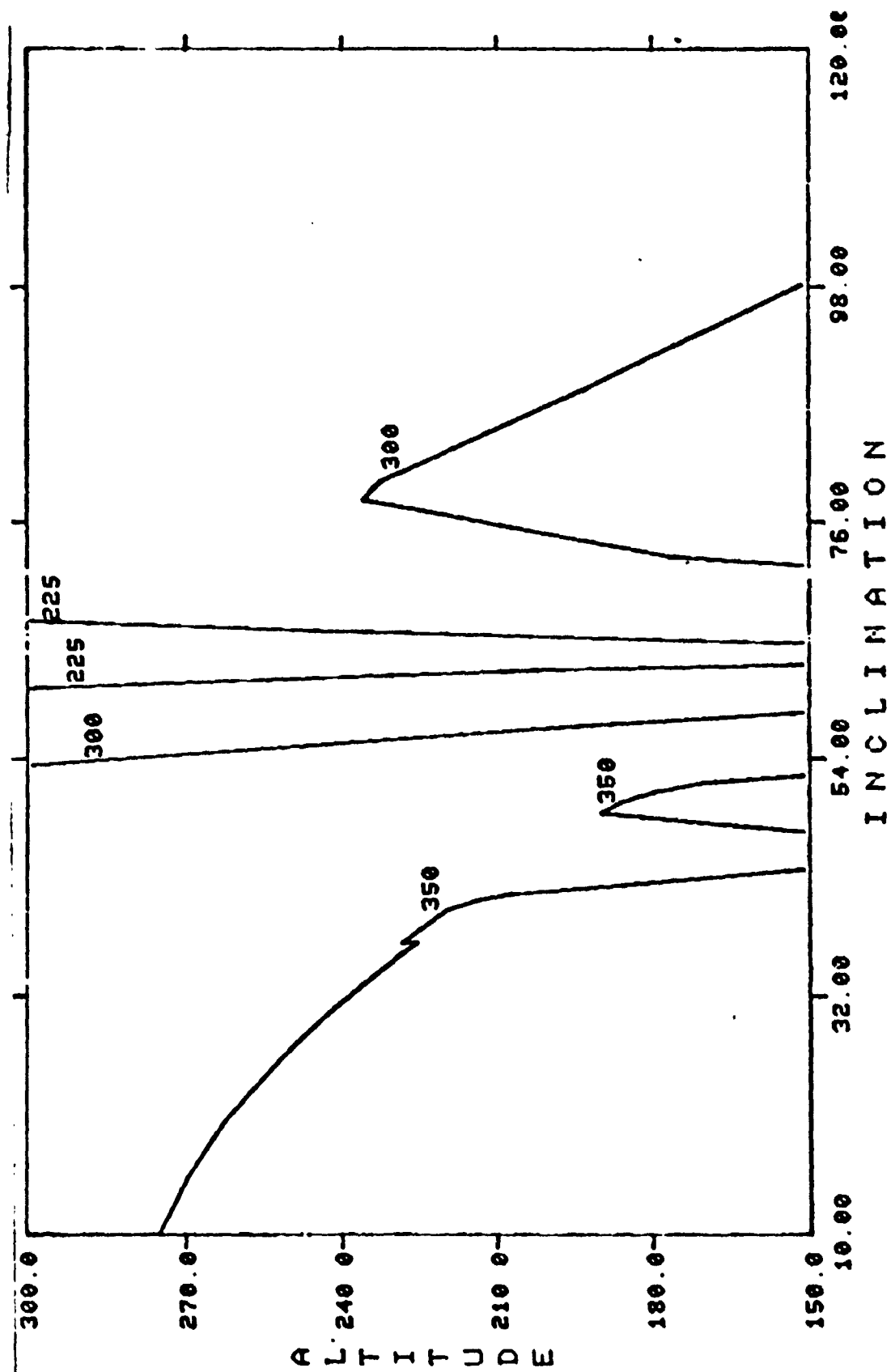


FIGURE 25. LAUNCH VEHICLE PAYLOAD WEIGHT CONTOURS

It is feasible to carry  $0.15 \text{ g/cm}^2$  of shielding to protect critical subsystems, and it is desired to keep the fluence below  $1.24 \times 10^{12}$  1-Mev equivalent electrons per  $\text{cm}^2$  over the 200-day period.

A first look at these requirements results in the plot shown Figure 26. Study of the display indicates that orbits of interest are near  $90^\circ$  inclination. Figure 27 was created to "zoom in" on those inclinations.

A trial nominal orbit of 185 n.mi. altitude,  $96^\circ$  inclination, and a tentative launch vehicle (hypothetical data are shown) are selected, which result in the solid vertical line showing injection dispersions and orbit decay being added to the display (Figure 27). That line shows that the expected injection dispersions lie across two unacceptable regions (insufficient coverage). Also, there is noticeable decay in 200-days, especially for a  $-3\sigma$  injection. Using the indicated decay as an estimate of decay rate, an injection near  $+2\sigma$  would pass through the narrow unacceptable region. Likewise, injection near  $-3\sigma$  would pass through the larger unacceptable region. While this region is wider, the decay rate at the lower altitude is faster. More detailed evaluation of this problem would be possible by plotting the decay for shorter mission times to establish the time spent in the unacceptable regions. Likewise, other coverage requirements could be analyzed to establish what coverage is achieved in the unacceptable regions.

This example demonstrates the capability of IGOS to serve as an automated sketch pad for rapid assessment of alternative orbits. The availability of such a tool offers several benefits. First, the quick-response analysis will ensure that a wider range of alternatives is considered early in the planning cycle, thus the orbit finally selected will be more likely to be a best match to the all of the objectives of the experimenters. Second, the improved preliminary planning cycle will reduce costly iterations during the later detailed analysis phases of mission planning.

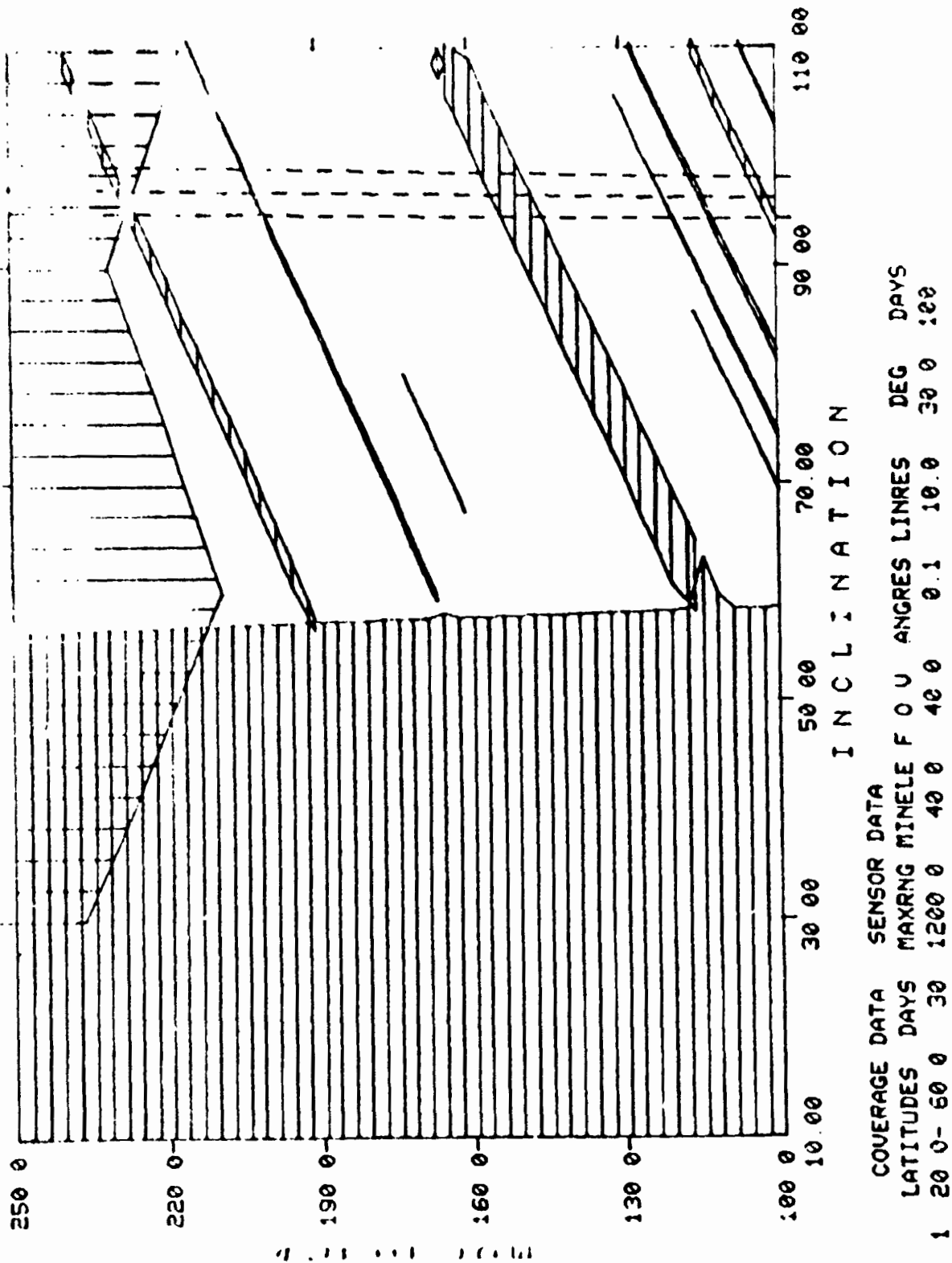


FIGURE 26. SAMPLE PROBLEM COVERAGE, RADIATION, AND SUN-ORBIT PRECESSION REQUIREMENTS

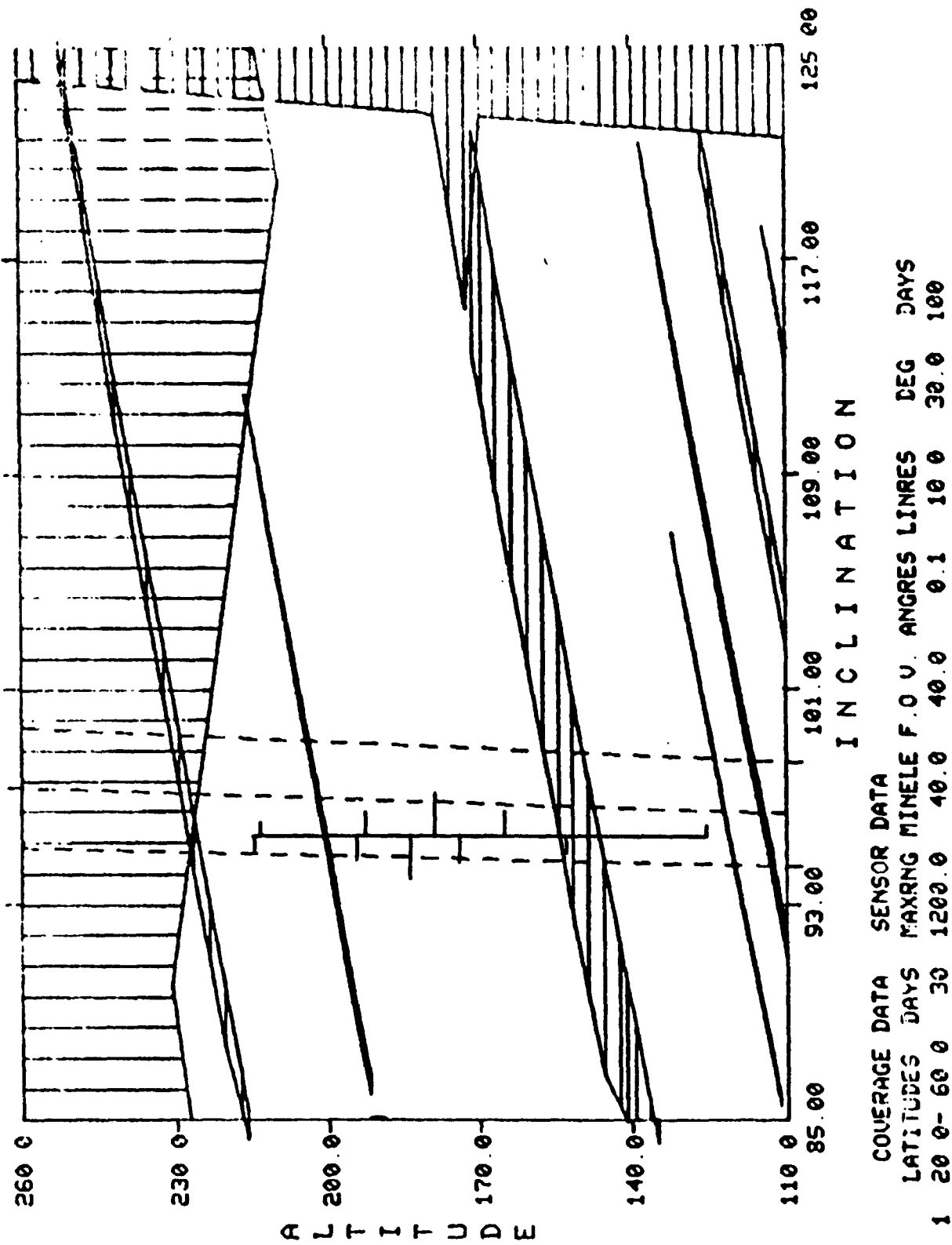


FIGURE 27. SAMPLE PROBLEM WITH TRIAL ORBIT AND LAUNCH VEHICLE

This program displays a concise set of mission requirements in terms of allowable injection dispersions. This format provides the mission specifications necessary to assess the suitability of booster guidance accuracy for both current systems and proposed modifications. The program is currently operational on the Battelle-Columbus computers with terminals in Columbus and at NASA Headquarters and is on computers at the Marshall Space Flight Center.

#### IGOS Mathematical Models

IGOS uses a set of separate mathematical models, each with its own input parameters and each computing data for plotting on a common set of scales. The program is organized into groups of subroutines, each associated with a separate mission analysis phenomena. These groups of routines can be thought of as separate analysis programs. Each generates data for plotting in the following two-dimensional design space:

Altitude  $h$ ,  $h_{\min} - h \leq h_{\max}$ , and

Inclination,  $i$ ,  $i_{\min} - i - i_{\max}$ .

The following discussion describes each of the separate models.

#### Earth Coverage Model

The object of the Earth coverage model is to shade those portions of the design space ( $i$  and  $h$ ) which do not satisfy the requirement to view all points on the Earth's surface between latitudes  $\theta_1$  and  $\theta_2$  at least once in any time period,  $T_c$ .

The analysis considers a sensor model which computes the radius of the circular area on the Earth's surface viewed at any instant in time. This radius is expressed in terms of the angle,  $\psi$ , of a cone from the Earth's center and is a function of the orbit altitude and the sensor characteristics as discussed in the Sensor Model section later in this report.

When a single latitude is considered, the swath viewed by a sensor intersects the latitude in one or two bands of longitude with width  $V$ .  $V$  is a function of the angle,  $\psi$ , the latitude  $\theta$ , and the orbit altitude and inclination.

The ground track of the orbit shifts during each orbital pass due to the Earth's rotational rate,  $\omega_e$ , and the orbit's precession rate,  $\omega_p$ . Each pass is shifted in longitude by an angle,  $S$ . After many orbital passes, a distribution of ground track/latitude intersections results. The spacing between these intersections are referred to as gaps,  $G$ . If the largest gap is less than the longitude viewed, total coverage is achieved. That is, when

$$G_M(T_c, h, I) \leq V[\psi(h), \theta, h, I] \quad (20)$$

is satisfied, adequate coverage is achieved.

The following sections discuss the sensor model with viewing angle ( $\psi$ ), the longitude viewed ( $V$ ), the orbit shift ( $S$ ), and the maximum gap ( $G$ ) in that order.

Earth-Observation Sensor Model. IGOS includes a sensor model which is used to calculate the instantaneous area viewable as a function of satellite altitude. Among the parameters included are the following:

- (1)  $\theta_o$  = sensor field of view limit
- (2)  $a_o$  = sensor angular resolution
- (3)  $s_o$  = maximum sensor-to-target slant range  
(may be limited by uplink sensitivity or downlink power supply)
- (4)  $\gamma$  = minimum elevation angle (must be set to meet minimum lighting constraints, to avoid excess refraction of light signal, and to clear ground obstructions).

Items 1 and 2 are sensor parameters. Items 3 and 4 may be either sensor parameters or mission design factors.

Other variables and parameters used in the model include the following:

- (5)  $s$  = slant range
- (6)  $h$  = altitude
- (7)  $\psi$  = viewed area half-angle
- (8)  $\gamma$  = elevation
- (9)  $\theta = \pi - 2(\psi + \gamma)$
- (10)  $X_C$  = linear resolution at target center
- (11)  $X_r$  = linear resolution at target perimeter
- (12)  $R_E$  = earth radius
- (13)  $L_s, L_\gamma, L_\theta$  = flags which indicate which parameter limits the radius of the viewed area.

Figure 28 depicts some of the relationships among these variables.

The constraints to be satisfied are:

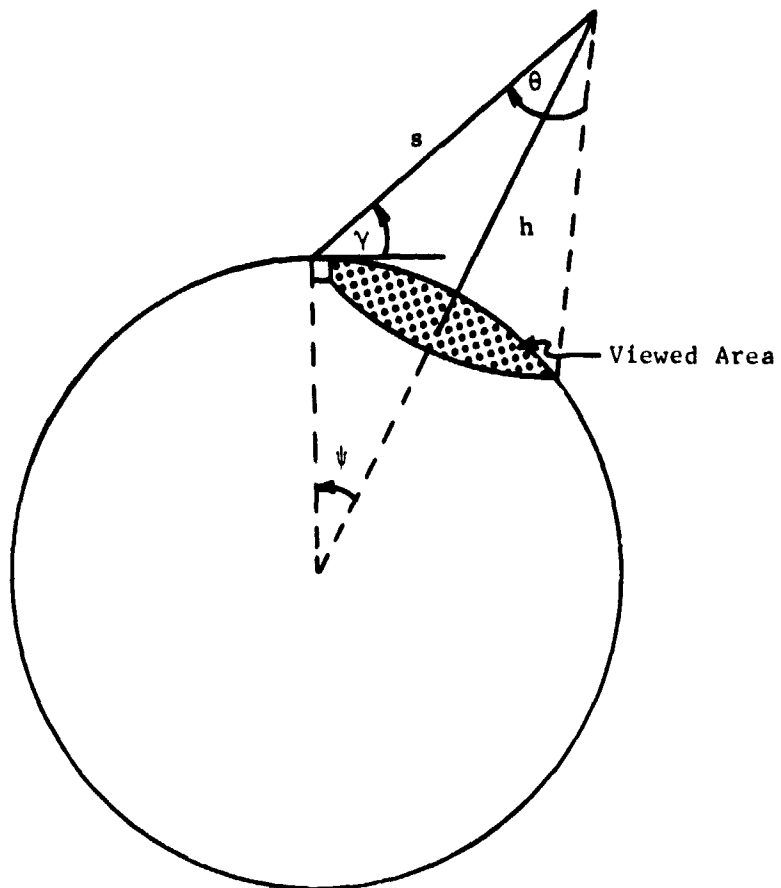
- (14)  $s \leq s_o$
- (15)  $\theta \leq \theta_o$
- (16)  $\gamma \geq \gamma_o$
- (17)  $X_L \leq s A_o / \sin \gamma$

As defined here, a smaller value for resolution indicates "better" resolution. Generally, each restricted parameter defines  $\psi$  as a function of altitude. The composite graph of  $\psi$  as a function of  $h$  is the piecewise-smooth curve representing, at each altitude, the most restrictive parameters. Figure 29 shows the flow of the calculation and illustrates the equations used. The limiter flags are initialized to zero. If the altitude is greater than the maximum sensor-to-target slant range, the viewed-area half-angle is zero. Otherwise, it is assumed that the limiting parameter is the elevation restriction and theta is calculated. If the sensor field of view limit is exceeded, theta is set equal to it and the elevation angle is recalculated. In either case, if the resulting slant range is too great both theta and the elevation angle are recalculated after setting the slant-range-to-target-perimeter equal to its limiting value.



To illustrate the utility of the model, an example is presented. The sensor is assumed to have a field of view  $\psi = 40$  degrees and an angular resolution of 0.01 degree. The desired lineal resolution is 1 nautical mile. The minimum elevation angle is 40 degrees and the range limit is 1200 nautical miles.

In Figure 30, the solid curves show  $\psi$  as a function of  $h$  considering each limit as if it were the only constraint. The cross-hatched segmented line is the piecewise-smooth curve representing  $\psi$  as a function of  $h$ . In this case, the resolution constraint is never a limiting factor for altitudes ranging up to 1000 nautical miles. The sensor field-of-view is limiting for the lower altitudes. At 660 nautical miles the elevation angle is the most restrictive. At 870 nautical miles, the range restriction is dominant. The maximum value of  $\psi$  (approximately 12 degrees at 870 nautical miles altitude) corresponds to a great circle distance of about 720 nautical miles on the viewed area.



- $s$  = Slant range  
 $h$  = Altitude  
 $\gamma$  = Elevation  
 $\psi$  = Viewed area half-angle  
 $\theta = \pi - 2(\psi + \gamma)$

FIGURE 28. MODEL PARAMETERS

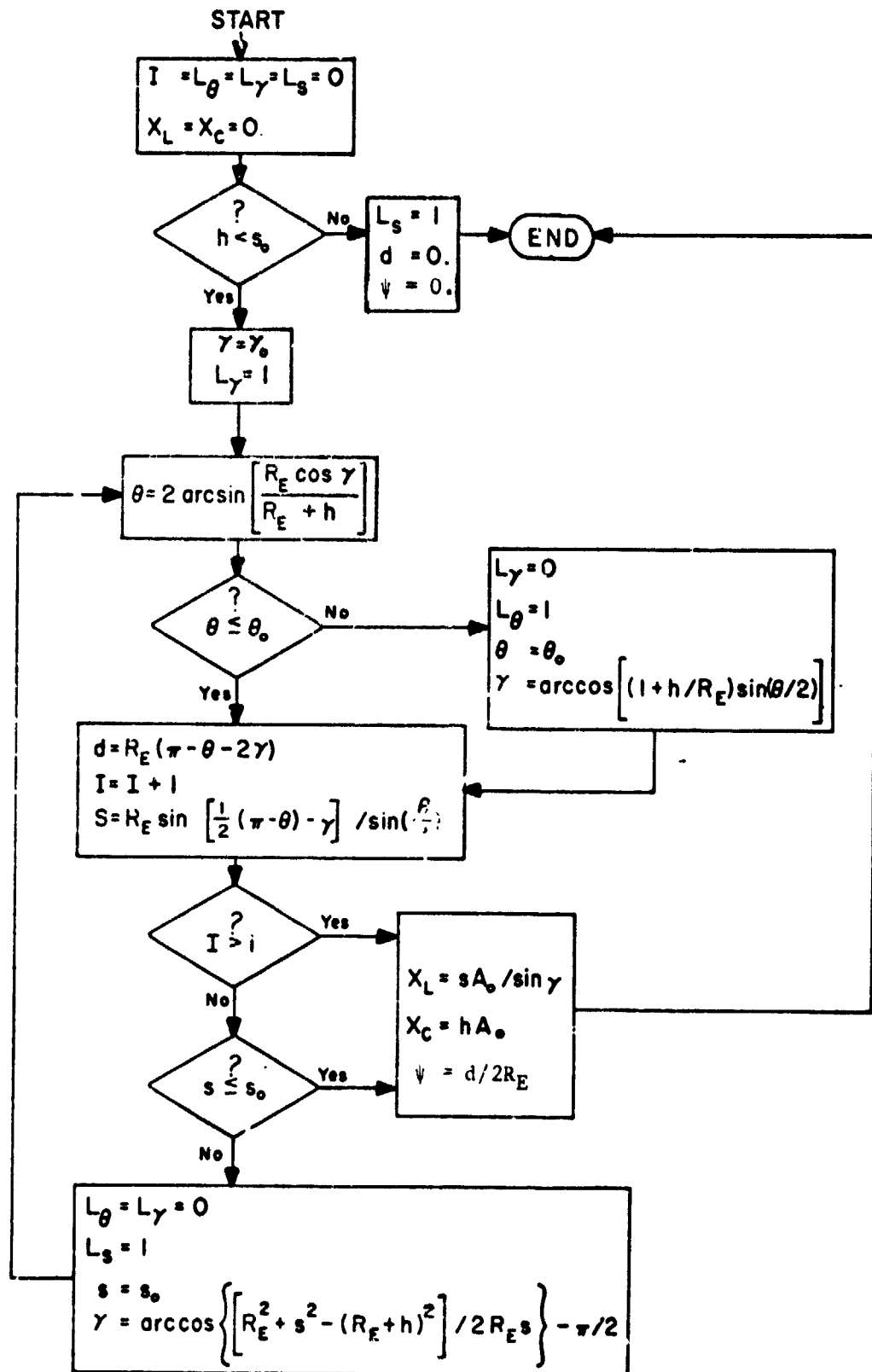


FIGURE 29. FLOW DIAGRAM FOR SENSOR MODEL

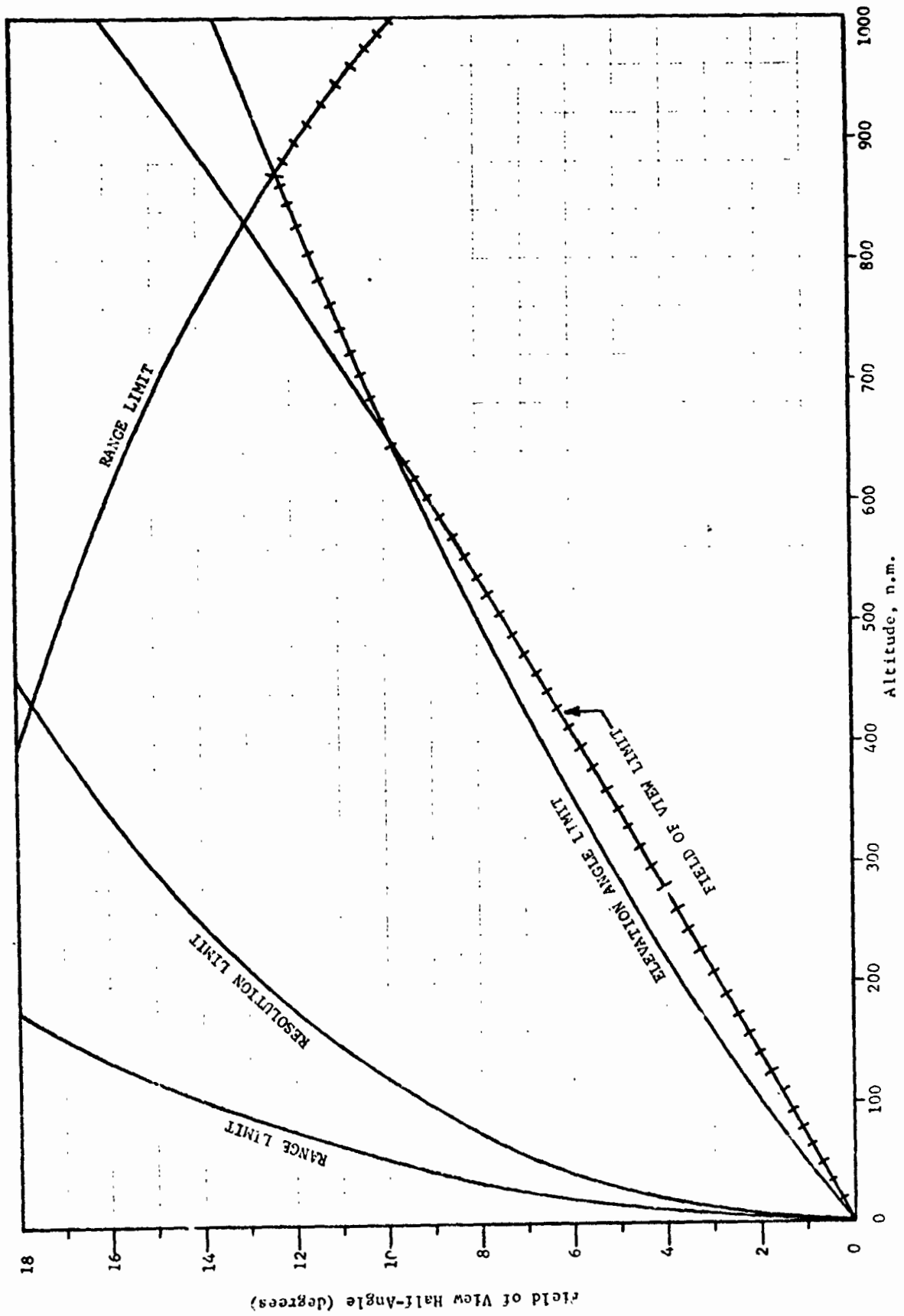


FIGURE 30. FIELD-OF-VIEW HALF-ANGLE AS A FUNCTION OF ALTITUDE

Longitude Viewed. A single orbit pass covers the surface of the Earth with a swath as shown in Figure 31. The band of longitudes viewed,  $V$ , is shown for a particular latitude,  $\theta$ . Note that for a larger inclination the longitude viewed would be two smaller bands, while for a smaller inclination no longitude would be viewed.

To compute the portion of any latitude viewed in a single satellite pass, it will be convenient to develop the orthogonal transformation from a set of orbit related coordinates,  $r_o$ , to Earth coordinates,  $r_e$ . This transformation is

$$\begin{bmatrix} c_\phi & -s_\phi & 0 \\ s_\phi & c_\phi & 0 \\ 0 & 0 & 1 \end{bmatrix} \begin{bmatrix} 1 & 0 & 0 \\ 0 & c_I & -s_I \\ 0 & s_I & c_I \end{bmatrix} = \begin{bmatrix} c_\phi & -s_\phi c_I & s_\phi s_I \\ s_\phi & c_\phi c_I & -c_\phi s_I \\ 0 & s_I & c_I \end{bmatrix} \quad (21)$$

where

$c_\phi$  and  $s_\phi$  = the cosine and sine of the precession of the orbit relative to the earth, i.e.:

$$\phi = (\omega_p - \omega_e)t_1$$

$c_I$  and  $s_I$  = the cosine and sine of the inclination, and the coordinates are:

$$r_e = \begin{bmatrix} x_e = \text{in the equatorial plane} \\ y_e = \text{in the equatorial plane, normal to } x_e, \\ z_e = \text{the polar axis} \end{bmatrix}$$

and

$$r_o = \begin{bmatrix} x_o = \text{the line of nodes,} \\ y_o = \text{in the orbital plane normal to } x_o, \\ z_o = \text{normal to the orbital plane} \end{bmatrix}$$

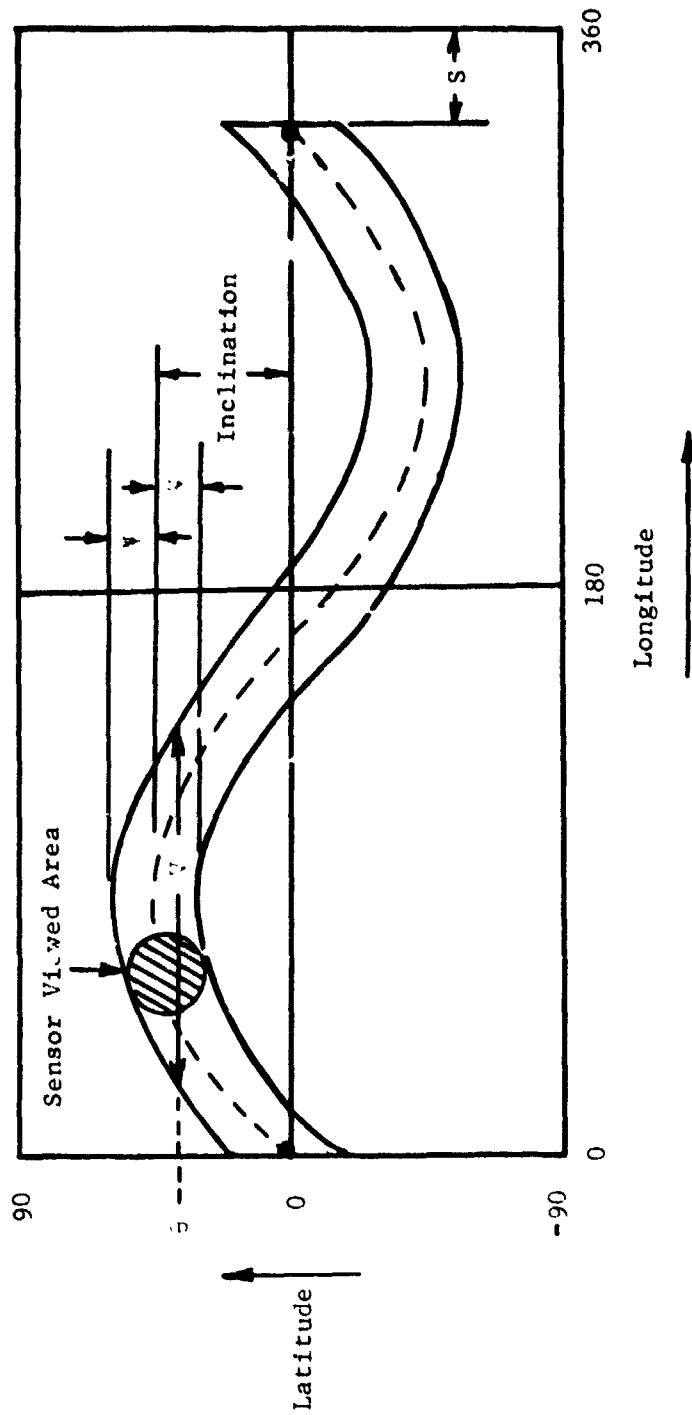


FIGURE 31. SINGLE PASS EARTH COVERAGE

Since all positions of interest are on the Earth's surface, which is assumed to be spherical, all position vectors are treated as unit vectors.

The upper and lower edges of the swath are expressed in orbital coordinates as

$$\underline{r}_o = \begin{bmatrix} c_\psi c_o \\ c_\psi s_o \\ \pm s_\psi \end{bmatrix} \quad (22)$$

where  $\psi$  is the sensor angle, and  $s_o$  and  $c_o$  are the sine and cosine of the orbit anomaly angle,  $\omega_o t$ .

The edges, in Earth coordinates, are found by applying the transformation of Equation 21 to Equation 22:

$$\begin{bmatrix} x_e \\ y_e \\ z_e \end{bmatrix} = \begin{bmatrix} c_\theta c_\psi c_o - s_\theta c_I c_\psi s_o \pm s_\theta s_I s_\psi \\ s_\theta c_\psi c_o + c_\theta c_I c_\psi s_o \pm c_\theta s_I s_\psi \\ s_I c_\psi s_o \pm c_I s_\psi \end{bmatrix} \quad (23)$$

The crossing of the latitude of interest is found by setting  $z_e$  equivalent to the sine of the latitude, then solving for the orbit angle

$$\omega_o t = \sin^{-1} \left[ (s_\theta \mp c_I s_\psi) / s_I c_\psi \right] \quad (24)$$

In the interval  $0 < \omega_o t < 2\pi$ , Equation 24 has four, two, or no solutions depending on the specific angles:

$$\begin{aligned} |I| &< (\theta - \psi) && \text{No solution} \\ (\theta - \psi) &< |I| &< (\theta + \psi) && \text{Two solutions, and} \\ (\theta + \psi) &< |I| && \text{Four solutions.} \end{aligned}$$

These cases correspond to no, one, or two bands of longitudes viewed at a specific latitude.

With sets of solutions for  $\omega_o t$  at the crossing of the latitude, the corresponding longitudes can be found from

$$\nabla = \tan^{-1} \left( y_e^+ / x_e^+ \right) - \tan^{-1} \left( y_e^- / x_e^- \right) + (\omega_p - \omega_e)(t^+ - t^-) \quad (25)$$

with  $x_e$  and  $y_e$  obtained from Equation 23. The band of longitudes viewed can be found by taking the appropriate differences of Equation 25 for the special cases of the solution to Equation 24. The resulting function is sketched for a single altitude in Figure 32. For use in IGOS, it is interesting to consider the value of  $\nabla$  as a function of both altitude and inclination (the design space) as shown in Figure 33.

Orbit Shift Parameter. To compute the distribution of gaps, it is necessary to know the amount of orbit shift per orbit period, shown as  $S$  in Figures 31 and 34. The shift is

$$S = \omega_{pe} t_o \quad (26)$$

where  $\omega_{pe}$  is the precession relative to the rotating Earth,

$$\omega_{pe} = \omega_p - \omega_e \quad (27)$$

and  $t_o$  is the orbit period,

$$t_o = 2\pi / \omega_o \quad (28)$$

Combining Equations 26, 27, and 28 gives

$$S = \frac{2\pi (\omega_p - \omega_e)}{\omega_o} \quad (29)$$



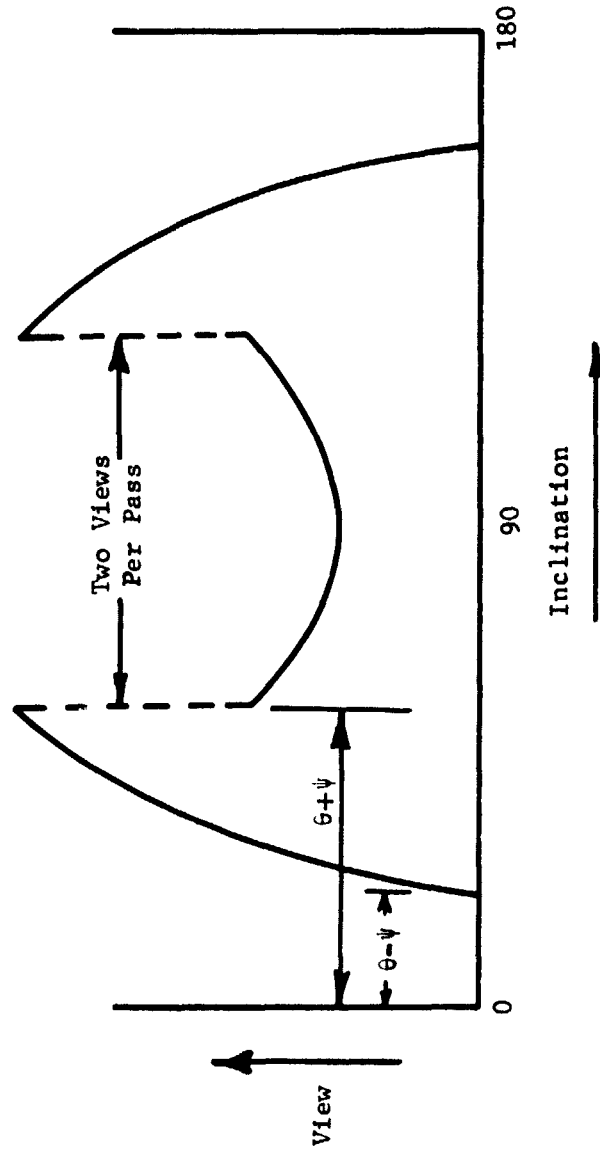


FIGURE 32. LONGITUDE VIEWED (V) VERSUS INCLINATION

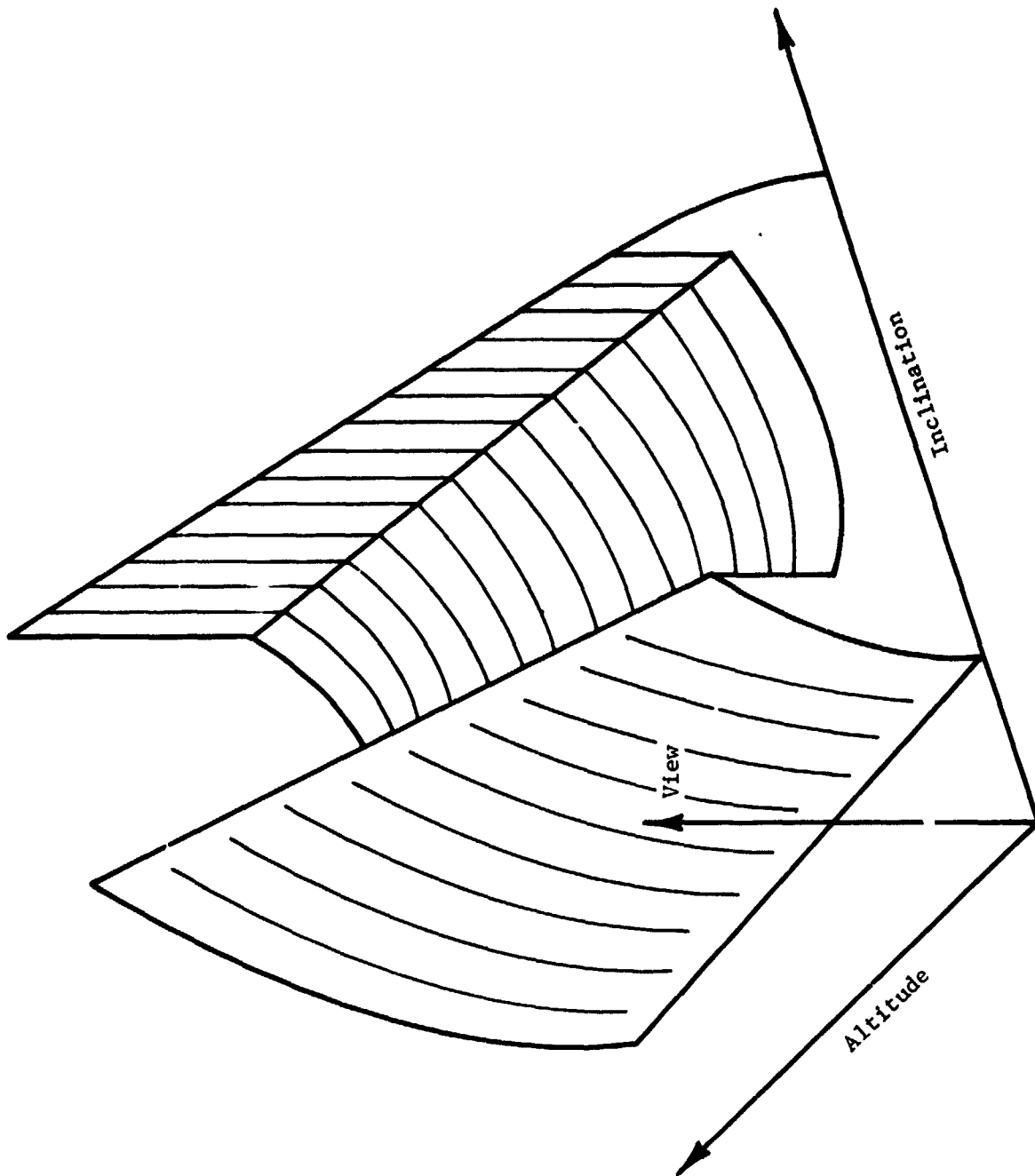


FIGURE 33. VIEW VERSUS INCLINATION AND ALTITUDE

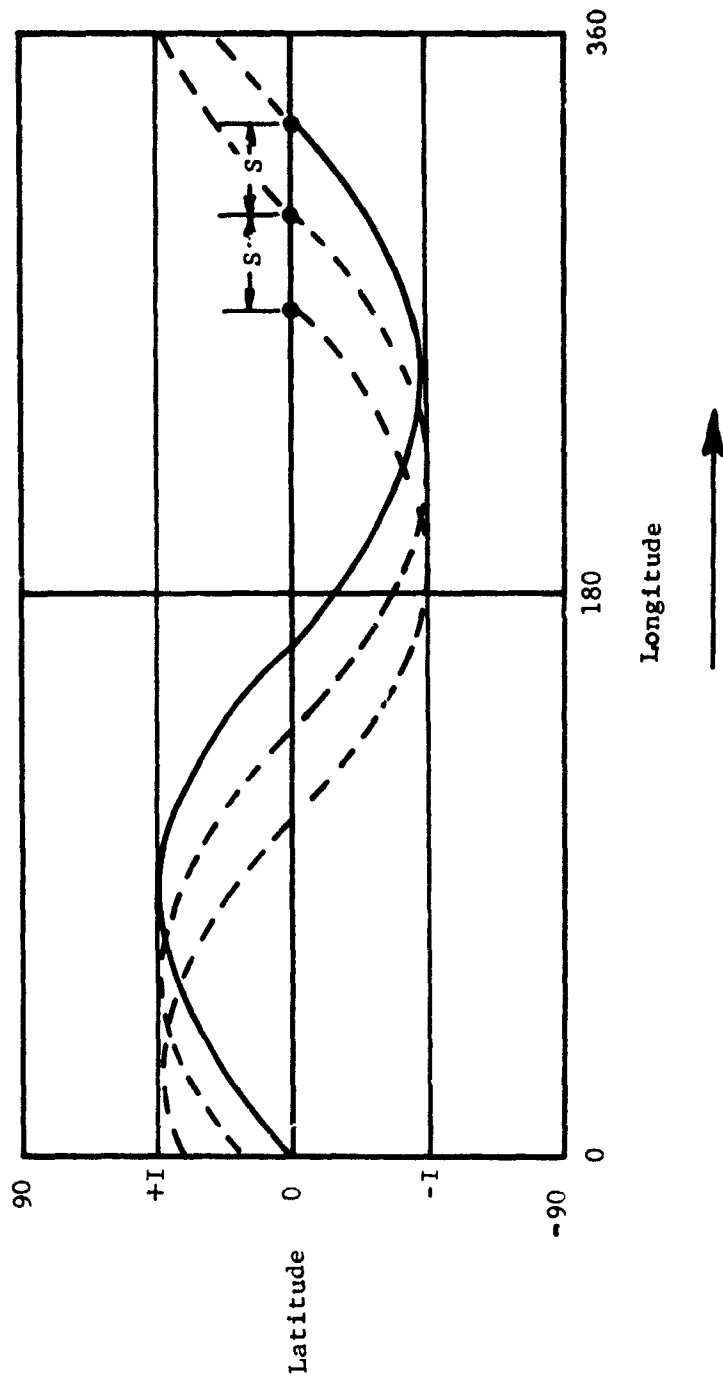


FIGURE 34. SUCCESSIVE GROUND TRACKS

The Earth's rate is a constant,  $\omega_e = 7.292 \times 10^{-5}$  rad/sec, while  $\omega_p$  and  $\omega_o$  are functions of the orbital altitude and inclination:

$$\omega_o = \mu^{1/2} / r^{3/2} \quad (30)$$

and from Reference 32

$$\omega_p = K_p (r_e / r)^{7/2} \cos I \quad (31)$$

where

$r$  = orbital radius ( $h + r_e$ ),

$r_e$  = Earth's equatorial radius (20902313 ft),

$\mu$  = Earth's gravitational constant ( $1.407528 \times 10^{16}$  ft<sup>3</sup>/s<sup>2</sup>), and

$K_p$  = -9.97 deg/day or  $-2.0149 \times 10^{-6}$  rad/s.

Substituting Equations 30 and 31 into Equation 29 gives

$$S = 2\pi \left[ \frac{K_p r_e^{7/2}}{\mu^{1/2} r^2} \cos I - \frac{\omega_e}{\mu^{1/2}} r^{3/2} \right] \quad (32)$$

It should be noted that, for constant altitude,  $S$  is linear on the cosine of inclination,

$$S = c_a(r) + c_b(r) \cos I \quad (33)$$

where

$$c_a = \frac{2\pi \omega_e r^{3/2}}{\mu^{1/2}}, \text{ and}$$

$$c_b = \frac{2\pi K_p r_e^{7/2}}{\mu^{1/2} r^2}$$

Thus, for a known altitude, it is a simple matter to convert between inclination and orbit shift. The relationship between shift and inclination is shown in Figure 35. The curvature of the loci of constant  $s$  result from the dependence on the cosine of inclination.

Distribution of Gaps. Figure 36 shows the subdivision of longitude by many orbital passes. Note that, for the first few passes, the gaps are:

- (1) 1 gap of  $(2\pi - NS)$ , and
- (2)  $N$  gaps of  $S$ .

However, after a specific number of passes, the original gaps are subdivided into even smaller intervals. In general, after any number of passes, three gap sizes exist such that:

$$G_1 N_1 + G_2 N_2 + G_3 N_3 = 2\pi, \text{ and}$$

$$N_1 + N_2 + N_3 = N + 1.$$

Now consider a fixed number of passes,  $N_p$ . For the IGOS coverage model

$$N_p = \frac{T \omega_c}{2\pi}$$

a constant for each altitude of interest. The coverage function requires calculation of the maximum gap width as a function of  $S$  [i.e.,  $G_M(S)$ ].

If many cases are evaluated, each with the same  $N_p$  and differing value of  $S$ , a plot such as Figure 37 will result. Note that, while there are generally three gap sizes, at specific values of  $S$  the smaller gap width goes to zero and the two larger sizes become equal. At any of these discrete values,  $S_i$ , there is only one gap size,  $G_i$ . These cases

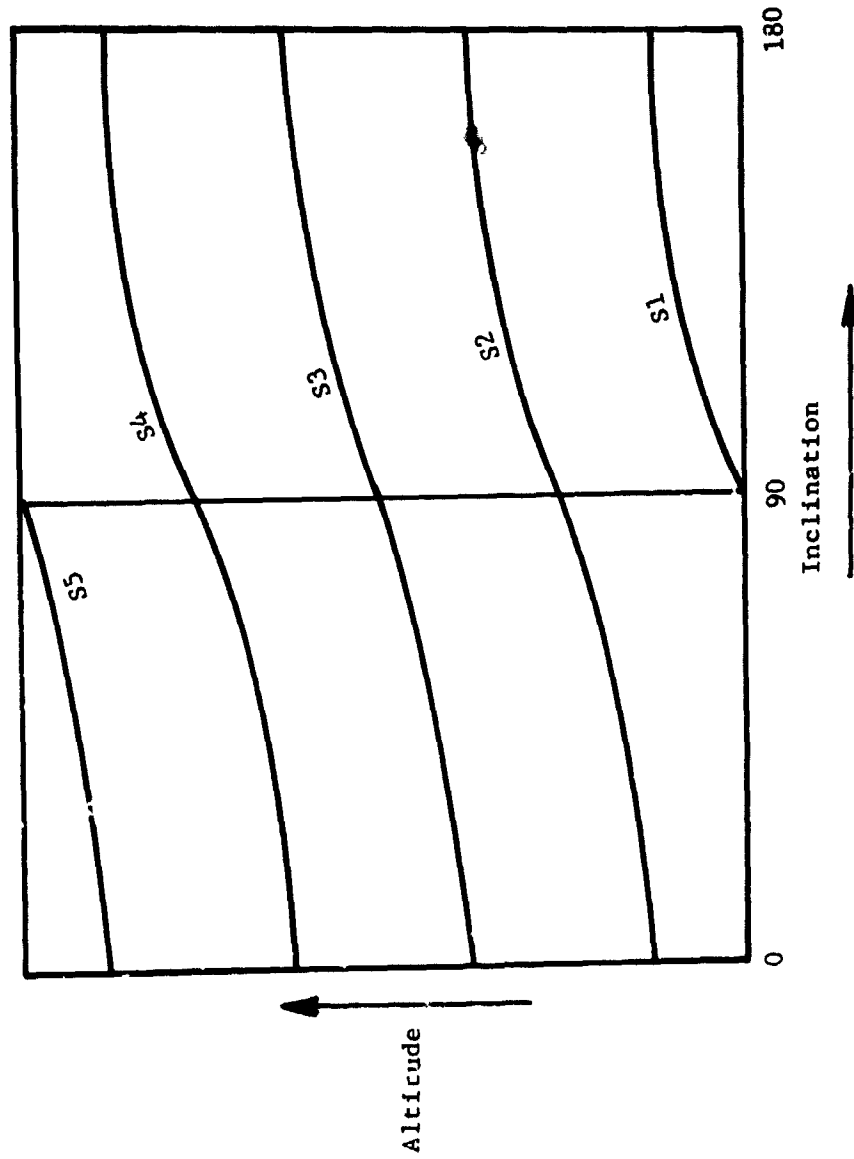


FIGURE 35. LOCUS OF CONSTANT SHIFT (S) VERSUS INCLINATION AND ALTITUDE

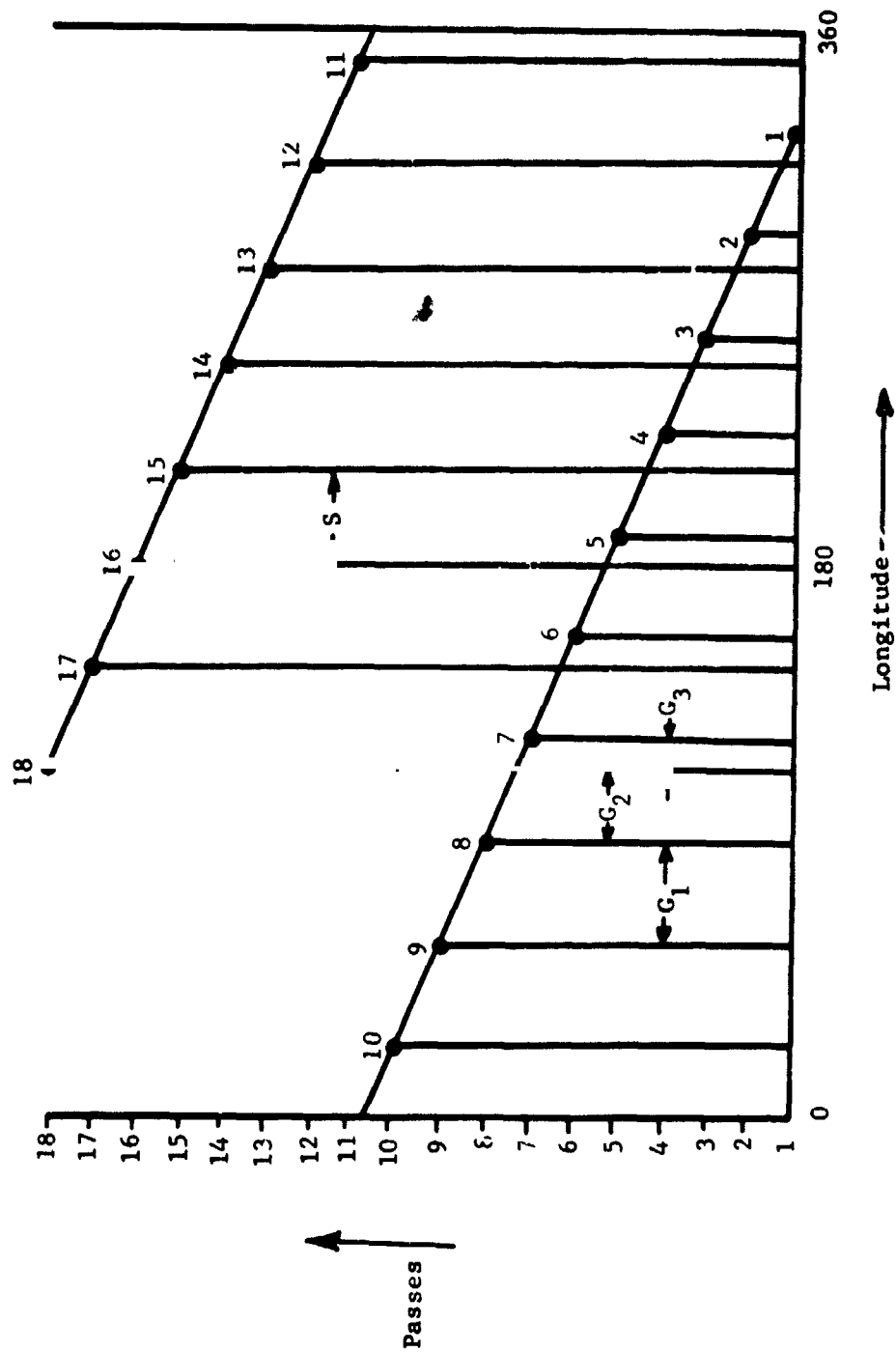


FIGURE 36. SUCCESSIVE NODES

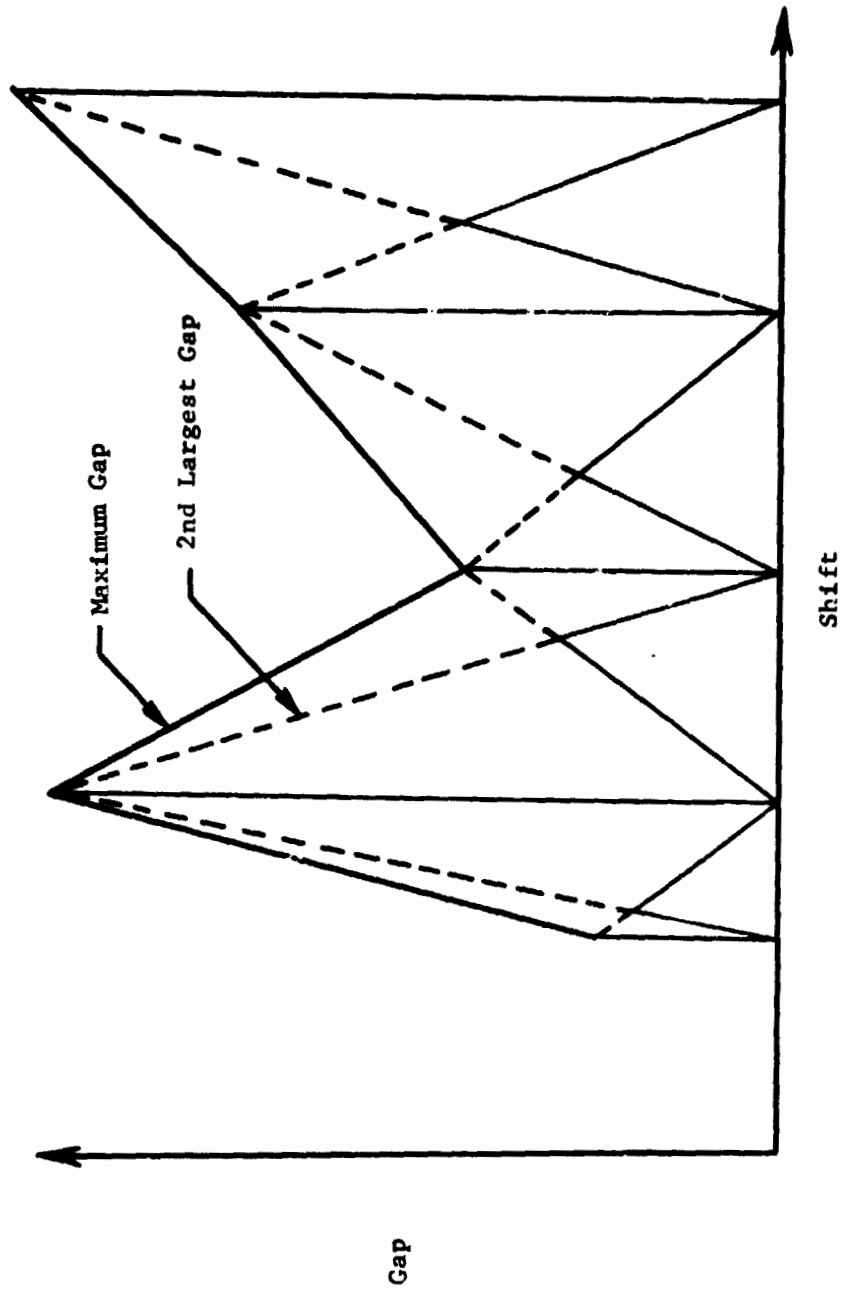


FIGURE 37. GAP SIZES VERSUS SHIFT



are the values of  $S$  which are an exact proper fraction of  $2\pi$ ,

$$S_i = \frac{M_i}{N_i} 2\pi \quad (34)$$

where the denominator  $N_i$  must be less than or equal to the number of passes.

The gap width is then

$$G_i = \frac{2\pi}{N_i}, \quad (35)$$

that is, with all gaps equal, the product of width and number must be  $2\pi$ . These values of  $S$  are often called resonant orbits.

With the discrete values known, the maximum gap varies linearly between successive points,  $S_i$  and  $G_i$ , as shown by the upper line of Figure 37. The fact that the maximum and all other gaps vary linearly with  $S$  can be shown by considering any pair of longitudes. After  $i$  passes, the longitude is

$$\phi_i = iS - 2\pi K_i$$

where  $K_i$  is the largest integer  $\leq iS/2\pi$ .  $K_i$  is needed to adjust  $\phi_i$  to be in the interval  $0, 2\pi$ . Thus, any longitude is piecewise linear on  $S$  and the gaps, which are merely differences  $\phi_i - \phi_j$  are also piecewise linear on  $S$ .

To compute the discrete values, we must find all values of  $S$  which are exact proper fractions of  $2\pi$  with denominators less than or equal to  $N_p$ . An example of a set of such points is shown in Figure 38. The points which represent proper fractions are shown solid. The improper fractions are shown as circles. The hyperbolae for constant  $M$  have been added to aid interpretation.

For a case with 10 passes, the maximum gap function is plotted in Figure 39. With 11 passes, the plot shown with a dashed line results. Note that one additional pass greatly changes the shape of the function.

When typical coverage times are considered,  $N_p$  can be quite large. For example, with near Earth orbits having periods on the order of 120 min (12 passes per day) and coverage times,  $T_c$ , of up to 30 days,  $N_p$  of up to 360 can be obtained. Plots such as Figure 38 and Figure 39 would have on the order of  $N_p^2$  points, a very large number. However, the function  $G_m(S)$  is needed only to establish when the gap width exceeds a known value  $G_o$ . To compute the  $S$  for which  $G_m(S) > G_o$ , only the point pairs with at least one point greater than  $G_o$  are needed. Thus, an algorithm for finding  $G_m(S)$  can be developed which does not require inspection of all possible points. The points will exceed  $G_o$  when

$$N_i < N_o = G_o / 2\pi \quad . \quad (36)$$

Thus, it is necessary to find each point (integer fraction),  $S_i, S_{i_m}$ , with a denominator less than  $G_o / 2\pi$ . Then, the nearest adjacent fractions ( $S_i^-$  and  $S_i^+$ ) with numerators less than  $N_p$  must be found. Using these points  $G_m(S)$  will result as shown in Figures 40 and 41. While the function is unknown for regions between points with  $G_i$  less than  $G_o$ , it is accurate for all segments above or crossing  $G_o$ . Thus, it is adequate for locating the values of  $S$  at any value  $G$  equal to or greater than  $G_o$ .

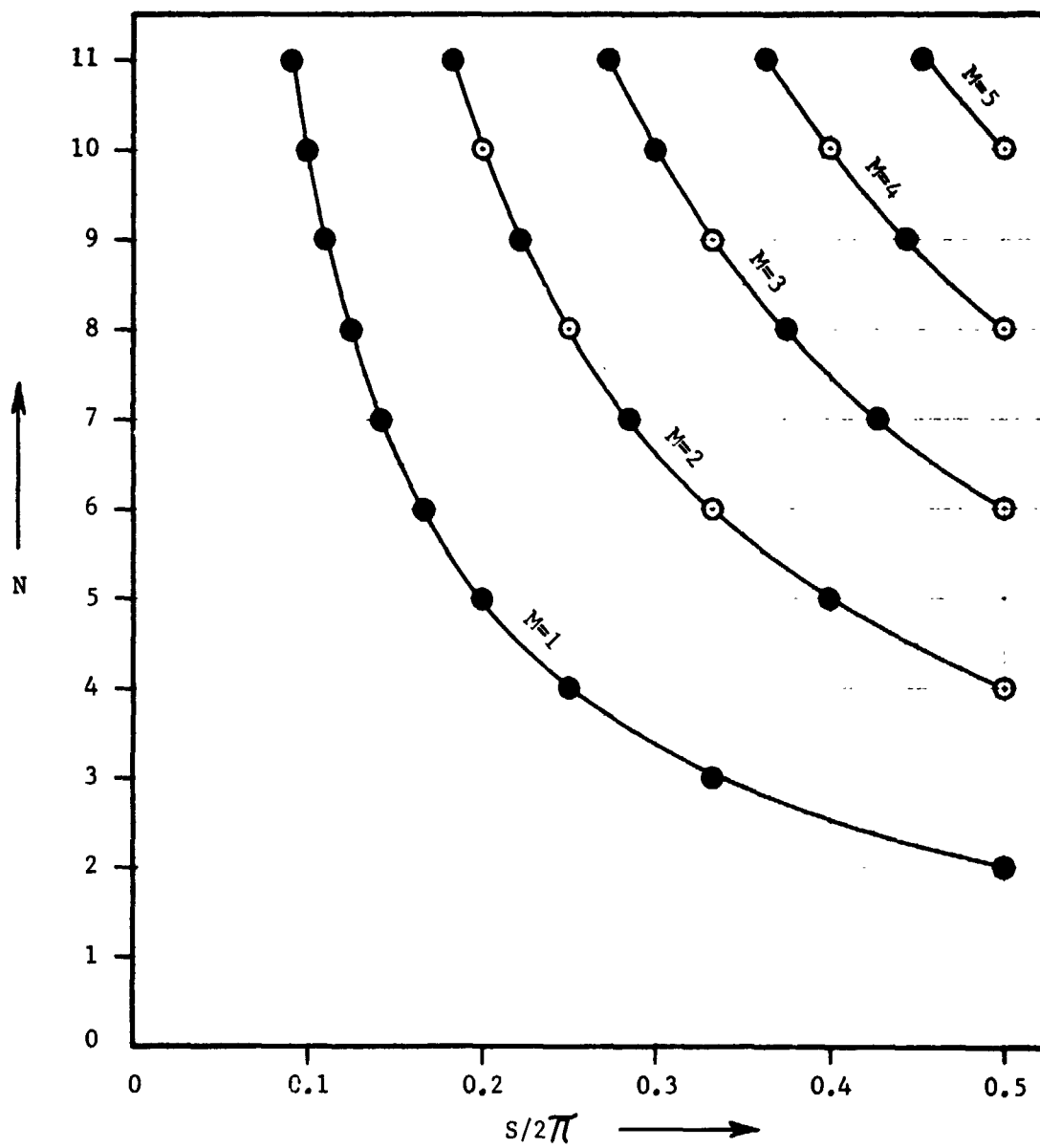


FIGURE 38. RESONANT POINTS VERSUS ORBIT SHIFT

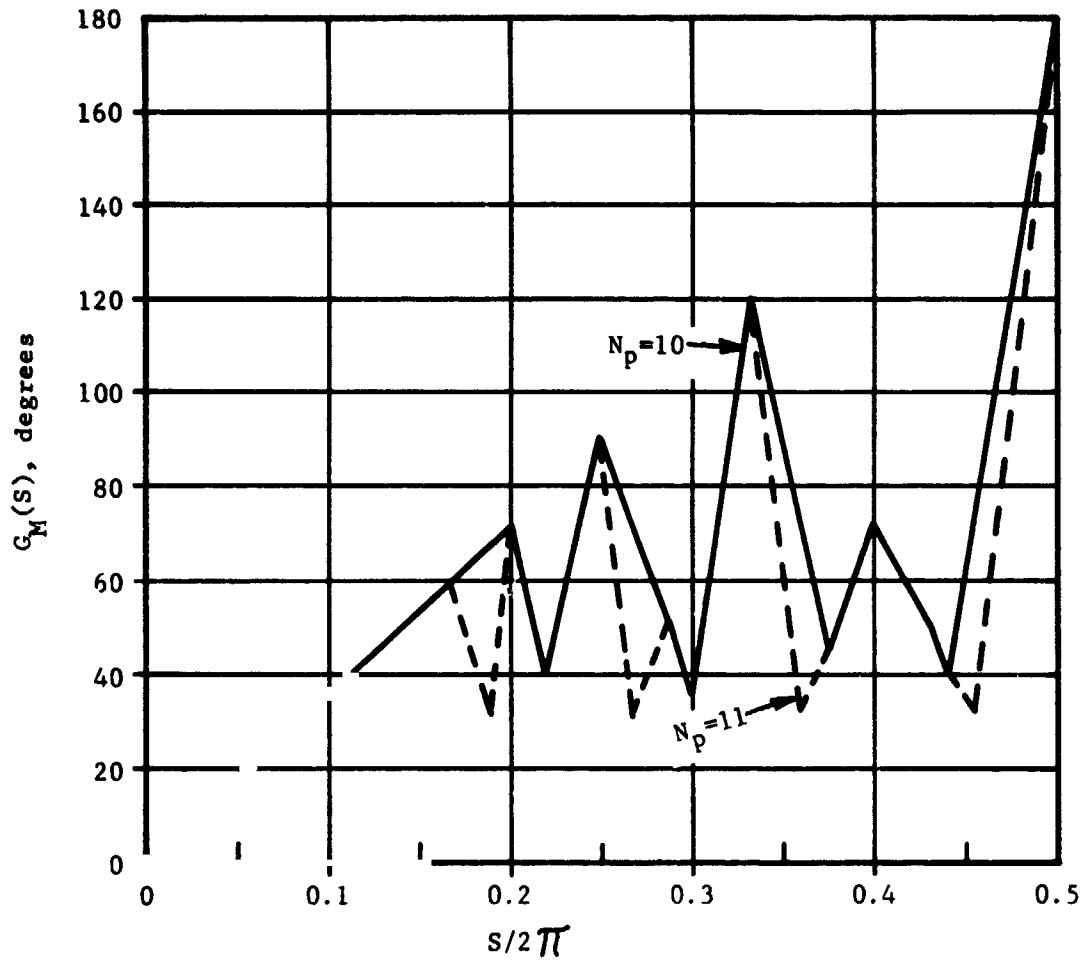


FIGURE 39. MAXIMUM GAP VERSUS ORBIT SHIFT

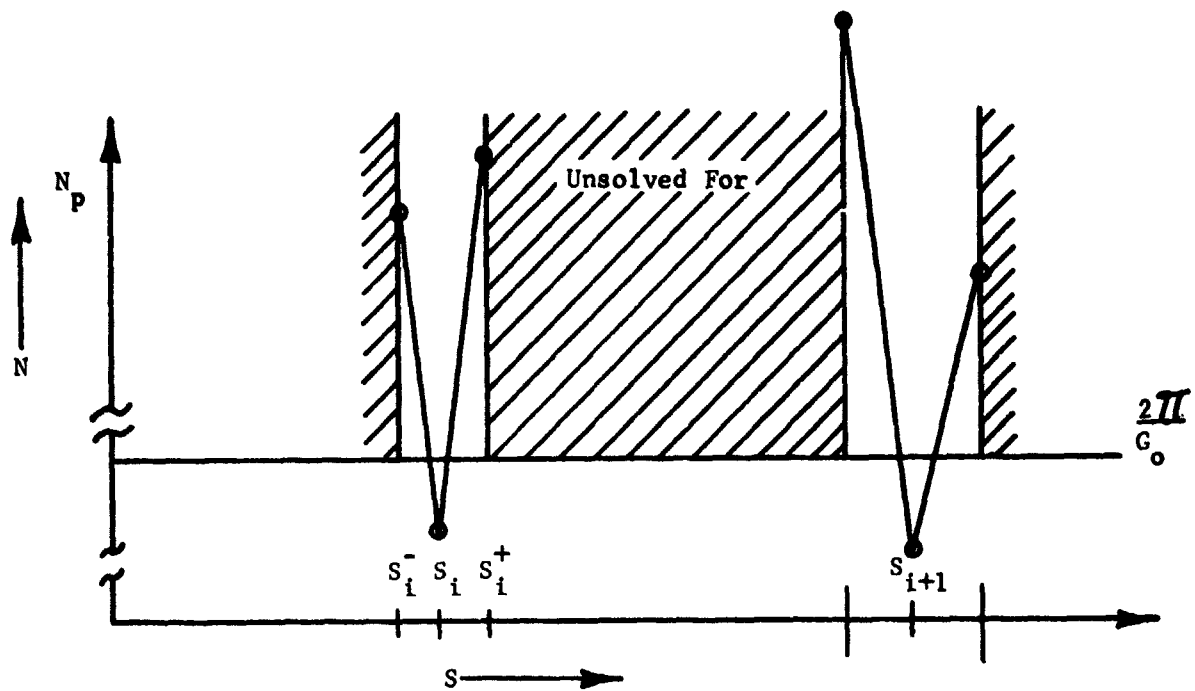


FIGURE 40. RESONANT POINTS VERSUS ORBIT SHIFT

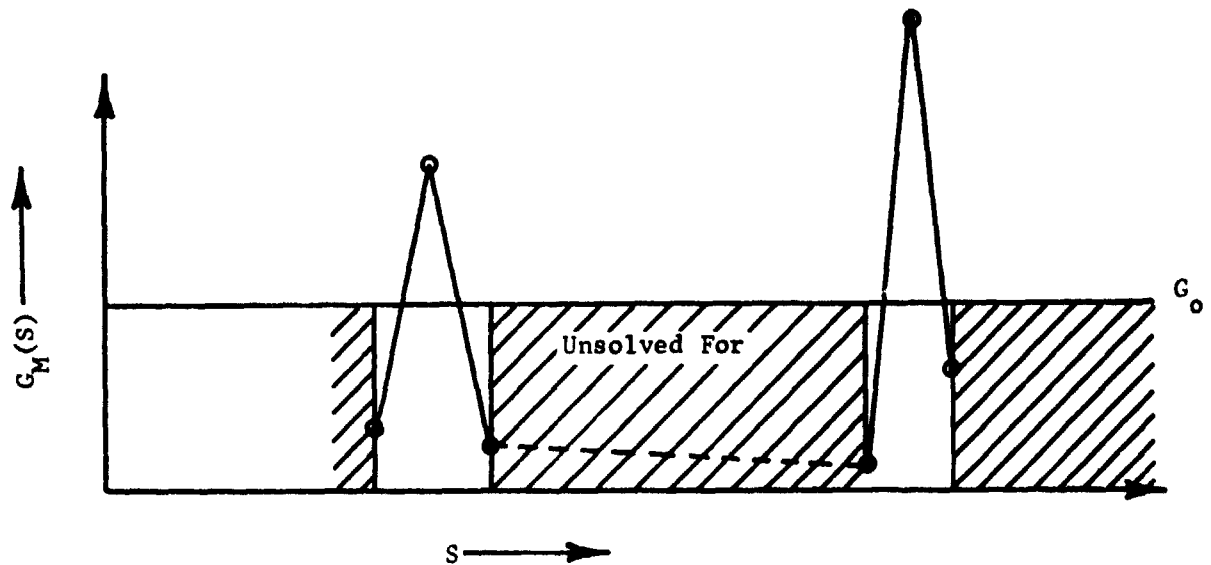


FIGURE 41. MAXIMUM GAPS VERSUS ORBIT SHIFT

A further reduction in the number of points to be calculated is possible because, for any one altitude, a limited range of inclinations and, thus, a limited range of  $S$  is of interest.

With the function  $G_m(S)$  known, and  $S$  determined from the altitude and inclination,  $G_m$  as a function of altitude and inclination are known. A sketch of this function is shown in Figure 42. The sketch has been simplified to ease interpretation. In general, the function is a series of ridges and valleys which are distributed along the locus of equal orbit shift as shown earlier in Figure 35.

Combined Coverage Model. The IGOS coverage model operates by combining the longitude viewed model (Figure 33) and the maximum gap distribution model (Figure 42) as shown in Figure 43. Adequate coverage is assured when  $V$  is greater than  $G$  giving a display such as that shown in Figure 44.

The plot is generated by solving for the gap distribution (Figure 37) for each of 51 discrete altitudes. The approximation of Figures 40 and 41 are used to reduce execution time and core storage. The minimum gap considered,  $G_0$ , is  $\psi/\cos \theta$  which is less than the smallest value of  $V$  versus inclination. When two latitudes ( $\theta_1$  and  $\theta_2$ ) are specified, the longitude viewed function  $V$  uses the minimum of that for the two extremes of latitude.

When the inclination is such that two bands of longitude will be viewed, the second largest gap distribution is used (shown by a dotted line in Figure 37). This accounts for subdivision of the largest gap by the second "view" of the desired latitude.

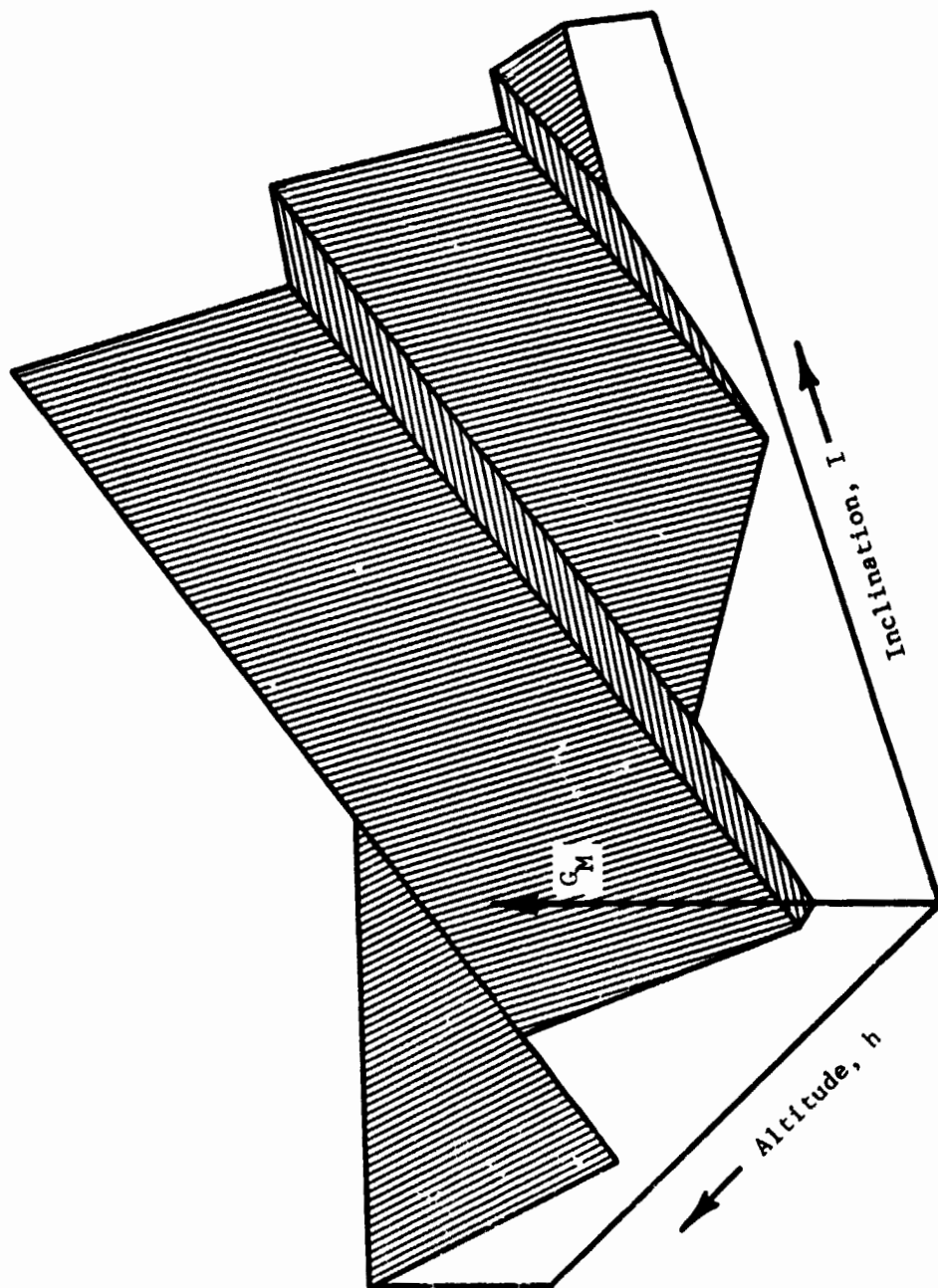


FIGURE 42. MAXIMUM GAP VERSUS ALTITUDE AND INCLINATION

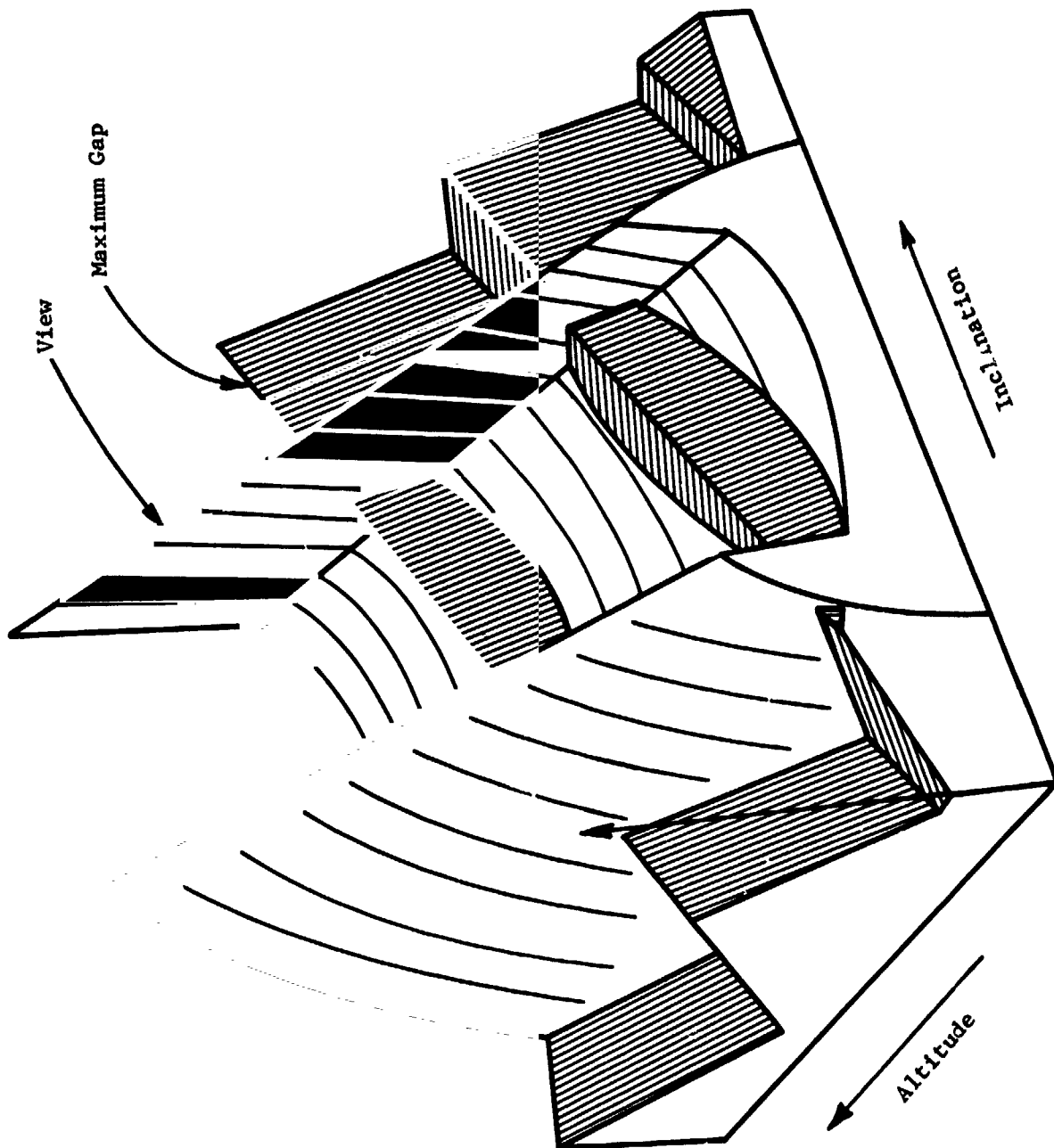


FIGURE 43. COMBINED VIEW AND MAXIMUM GAP VERSUS INCLINATION AND ALTITUDE



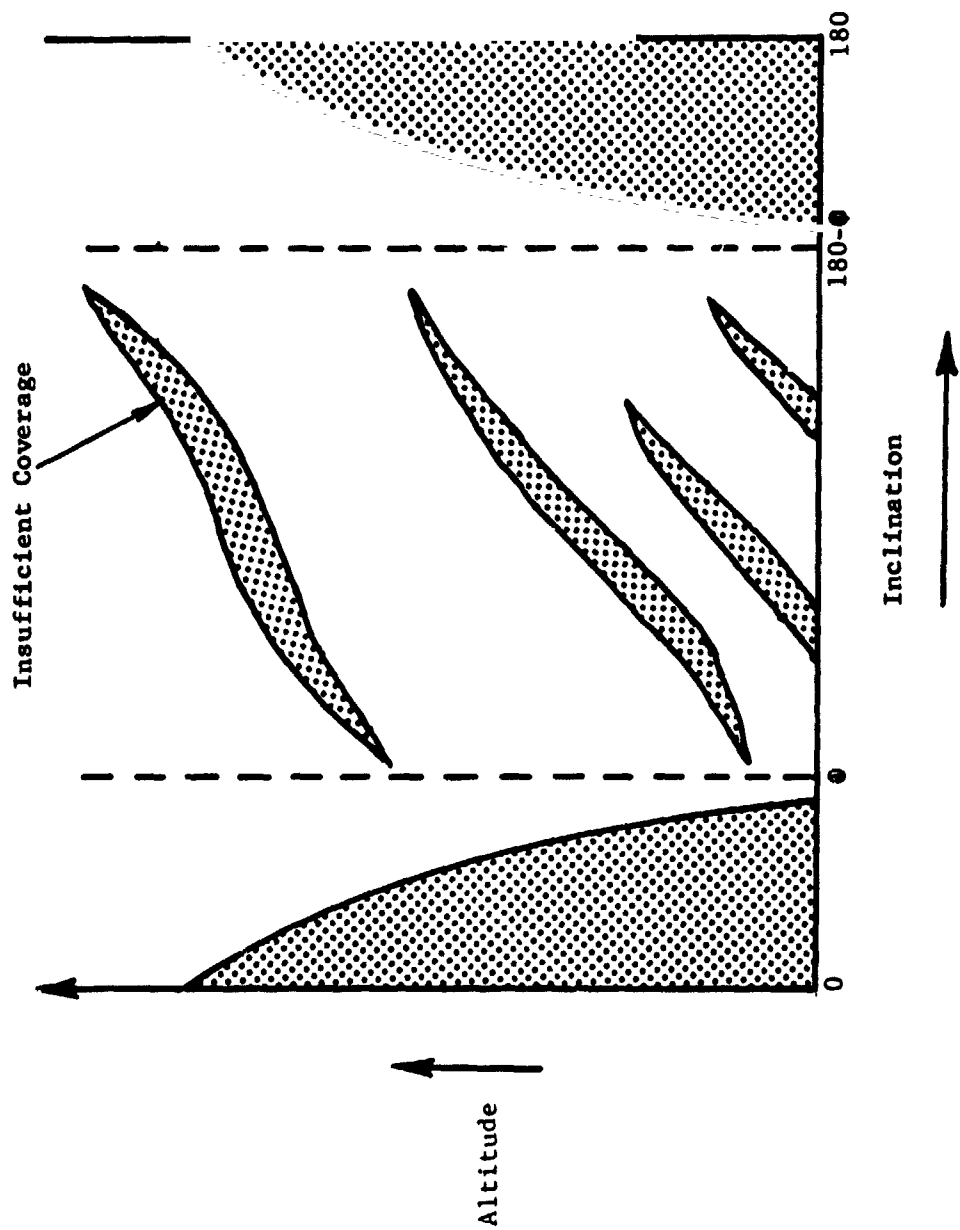


FIGURE 44. TYPICAL COVERAGE MODEL OUTPUT

When a large range of altitudes is considered, there is a risk that none of the 51 discrete altitudes considered will fall in a forbidden (inadequate coverage) region. The forbidden coverage (values of S) may fall between two discrete altitudes. This would result in a "clear" area on the screen with no warning to the user. If the space between the discrete altitudes is large enough for this to occur, evaluations are made for additional discrete altitudes between those 51 usually used. Any "forbidden" conditions encountered in the sub interval are plotted as if they occurred at the nearest usual discrete altitude.

This coverage model has been exercised on a large number of cases and has proven to be an excellent means of indicating which orbits have the desired Earth coverage patterns.

#### Radiation Environment

The IGOS radiation model involves a straight-forward use of data published in Reference 33. These data are log-log plots of equivalent 1 Mev electron fluence per day versus altitude for several shielding densities at inclinations of 0, 30, 60, and 70 degrees. IGOS computes the maximum altitude versus inclination display by linear interpolation of the log-log data.

#### Orbit-to-Sun Precession

The orbit-to-Sun precession lines are plotted by solving Equation 31 for the inclination as a function of altitude and the allowable precession rate

$$I = \cos^{-1} \left( \frac{\omega_p}{K_p} \left( \frac{r}{r_e} \right)^{7/2} \right) \quad (37)$$

where the allowable precession rate is computed from the allowable orbit/Sun precession angle,  $\phi_{so}$ , and time,  $T_{so}$ , (both user entered data), and the angular rate of the Earth's motion about the sun,  $\omega_{es}$ ,

$$\omega_p = \omega_{es} \pm \phi_{so} / T_{so} \quad (38)$$

Plotting Equations 37 and 38 results in two lines of altitude versus inclination, between which the orbit will process relative to the sun less than  $\phi_{so}$  in time,  $T_{so}$ .

#### Orbit Decay

The IGOS decay model operates by numerical (4th-order Runge-Kutta) integration of

$$\dot{h} = \frac{-1}{\left( dL / dh \right)} \quad (39)$$

where  $dL/dh$  is the derivative of orbit lifetime as computed in Reference 34. Using the technique of Reference 34, for circular orbits,

$$\frac{dL}{dh} = B_c \cdot f_s(t,h) \cdot \frac{dfe(h)}{dh} \cdot f_I(I) \quad (40)$$

where

- $B_c$  = the spacecraft ballistic coefficient,
- $f_s(t,h)$  = the solar activity factor,
- $f_I(h)$  = the normalized lifetime, and
- $f_I(I)$  = the inclination factor.

IGOS contains the data for  $f_1$  and  $f_1$ , as shown in Figures 45 and 46, which were taken directly from Reference 34.

The solar activity factors requires estimation of future solar activity. Predictions to 1988 were obtained from MSFC and supersede the values given in Reference 34. The solar activity factor is computed from

$$f_s(t,h) = f_t(t)^X \quad (41)$$

where the exponent X is

$$X = .89027 (3 + 3.5 \alpha - .5 \alpha^2) , \text{ and}$$

$$\alpha = (h - 360)/240$$

with h expressed in km. The time factor  $f_t(t)$  is plotted in Figure 47.

IGOS implements the functions shown in Figures 45, 46, and 47, by performing linear interpolation and the appropriate unit conversions.

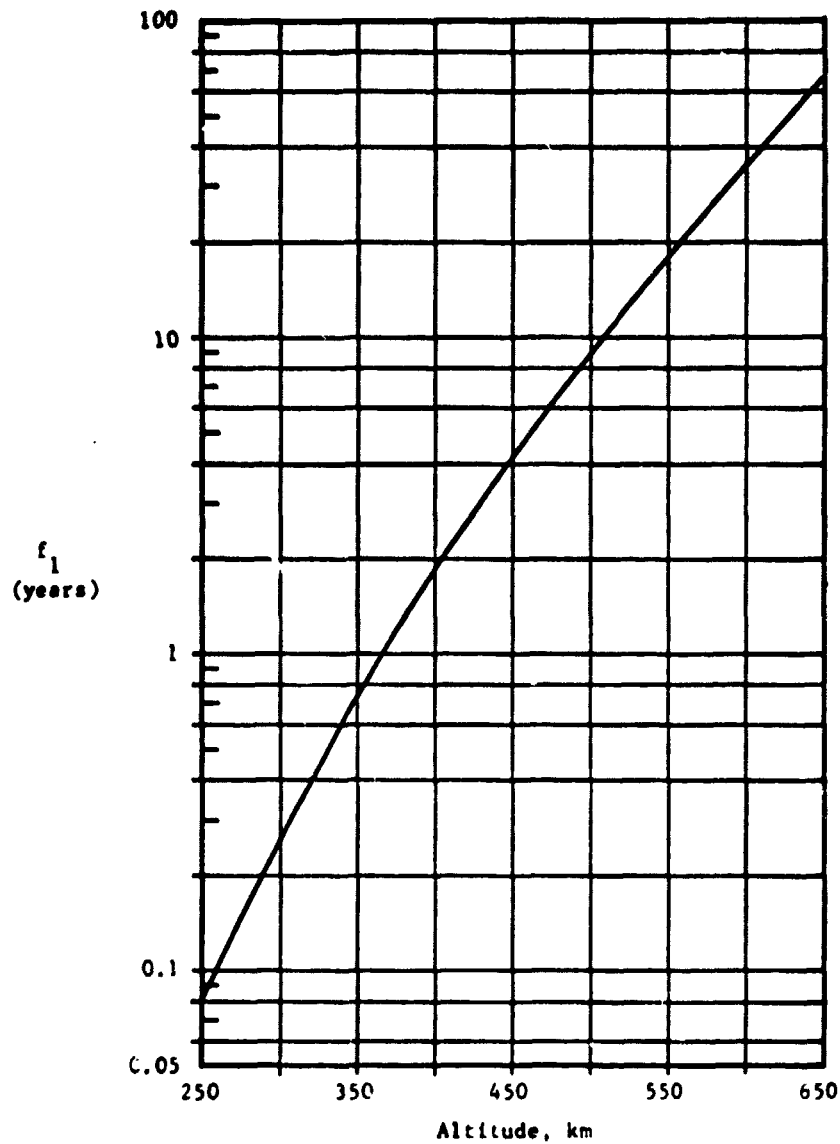
The differential equations, Equations 39 and 40, require the derivative of  $f_1(h)$ . This is computed numerically from

$$\frac{df_1(h)}{dh} = \frac{f_1(h + dh) - f_1(h - dh)}{2 dh} \quad (43)$$

with dh set to 0.5 n. mi. Integration steps are computed by

$$dt = \text{Min} \left\{ \begin{array}{l} dt_{\text{max}}, \\ \text{or} \\ -dh_{\text{max}} / h \end{array} \right\} . \quad (44)$$

With  $dt_{\text{max}} = 0.2$  years and  $dh_{\text{max}} = 0.1$  n. mi. Thus, no integration step exceeds either 0.2 years or 0.1 n. mi. Initial conditions are entered by the user and integration is stopped when time equals the specified mission duration, or altitude decays to the value represented by the bottom of the IGOS plot.

FIGURE 45.  $f_1$  (h), THE NORMALIZED LIFE TIMEFIGURE 46.  $f_I$  (I), THE INCLINATION FACTOR

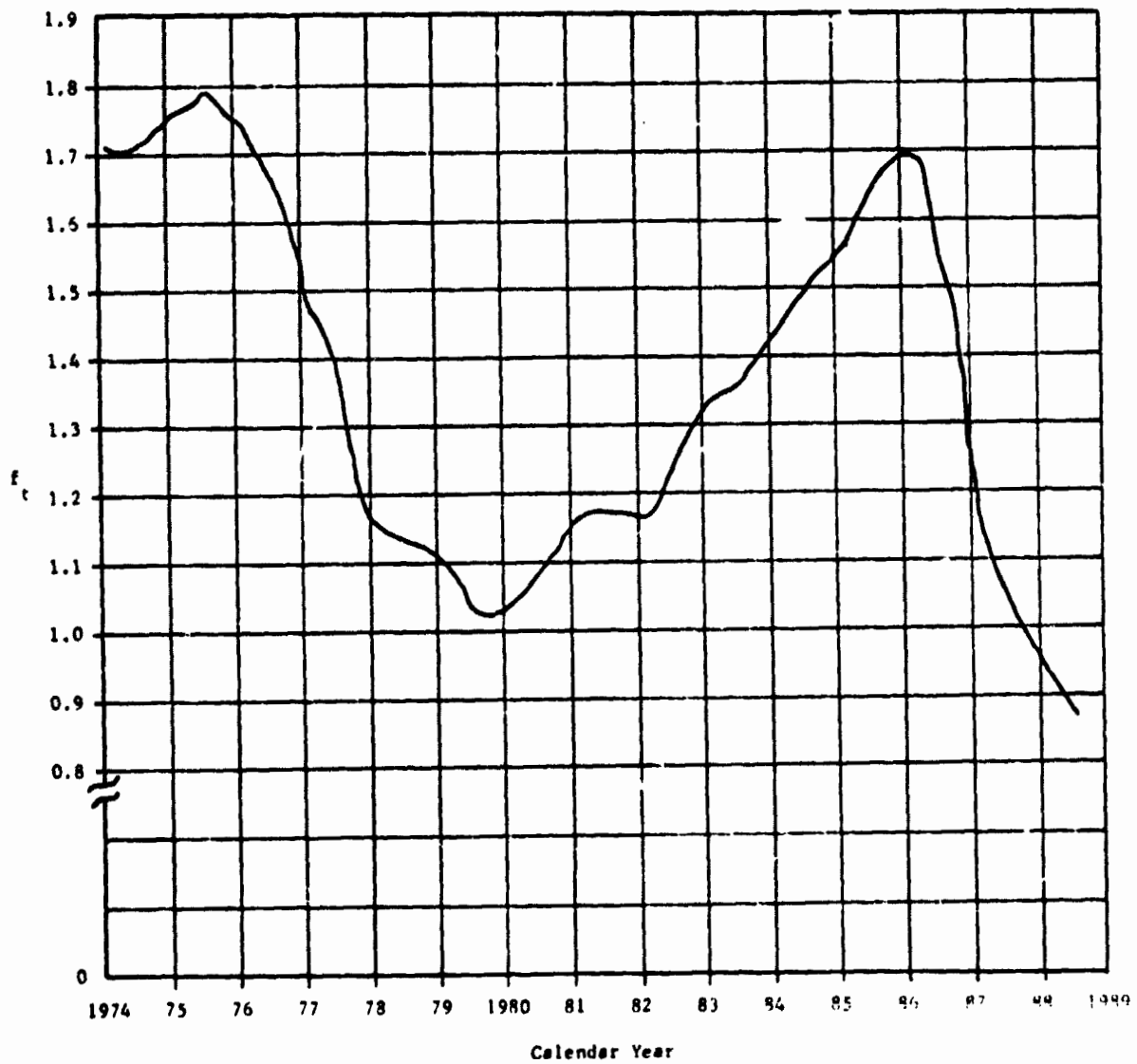


FIGURE 47. SOLAR ACTIVITY TIME FACTOR  $f_t(t)$

### Launch Vehicle Injection Error Model

IGOS requires data for the dispersions in injection altitude (semi-major axis) as a function of orbit altitude and inclination. For all current conventional launch vehicles, the inclination dispersions are negligible for ordinary purposes and are not considered by IGOS.

In its current version, IGOS contains only a Scout error model. The other vehicles utilize closed loop guidance and the resulting errors are small enough as to be, in general, negligible. If the injection errors of these vehicles are of interest for specific sensitive applications, they could be included by creating injection error tables similar to those included for the Scout. The data can be obtained from the launch vehicle project offices.

### Scout Error Model

The Scout Project Office and LTV suggested Reference 35 as the best source of Scout accuracy data. This report includes altitude, velocity magnitude, and flight path angle dispersions. These data were combined to obtain the equivalent circular orbit semimajor axis dispersions shown in Figure 48. IGOS performs linear interpolation on the data to obtain the one sigma altitude dispersions as a function of nominal orbit altitude.

### Launch Vehicle Performance Model

The IGOS launch vehicle performance model accesses a mass storage data file with a separate file record for each vehicle. To add a vehicle to the IGOS data file, the following data are required:

- (1)  $VR_{ij}$ , the horizontal inertial velocity capability of the booster vehicle for an east-launch from ETR with a given payload ( $P_i$ ) to a given altitude ( $A_j$ ). Up to 20 payloads and 5 altitudes may be used.
- (2)  $V4_i$ , the delta-velocity of the fourth stage (Scout vehicles only) carrying payload,  $P_i$ , and
- (3)  $ILS_K$ , the indices of the sites from which the vehicle may be launched.

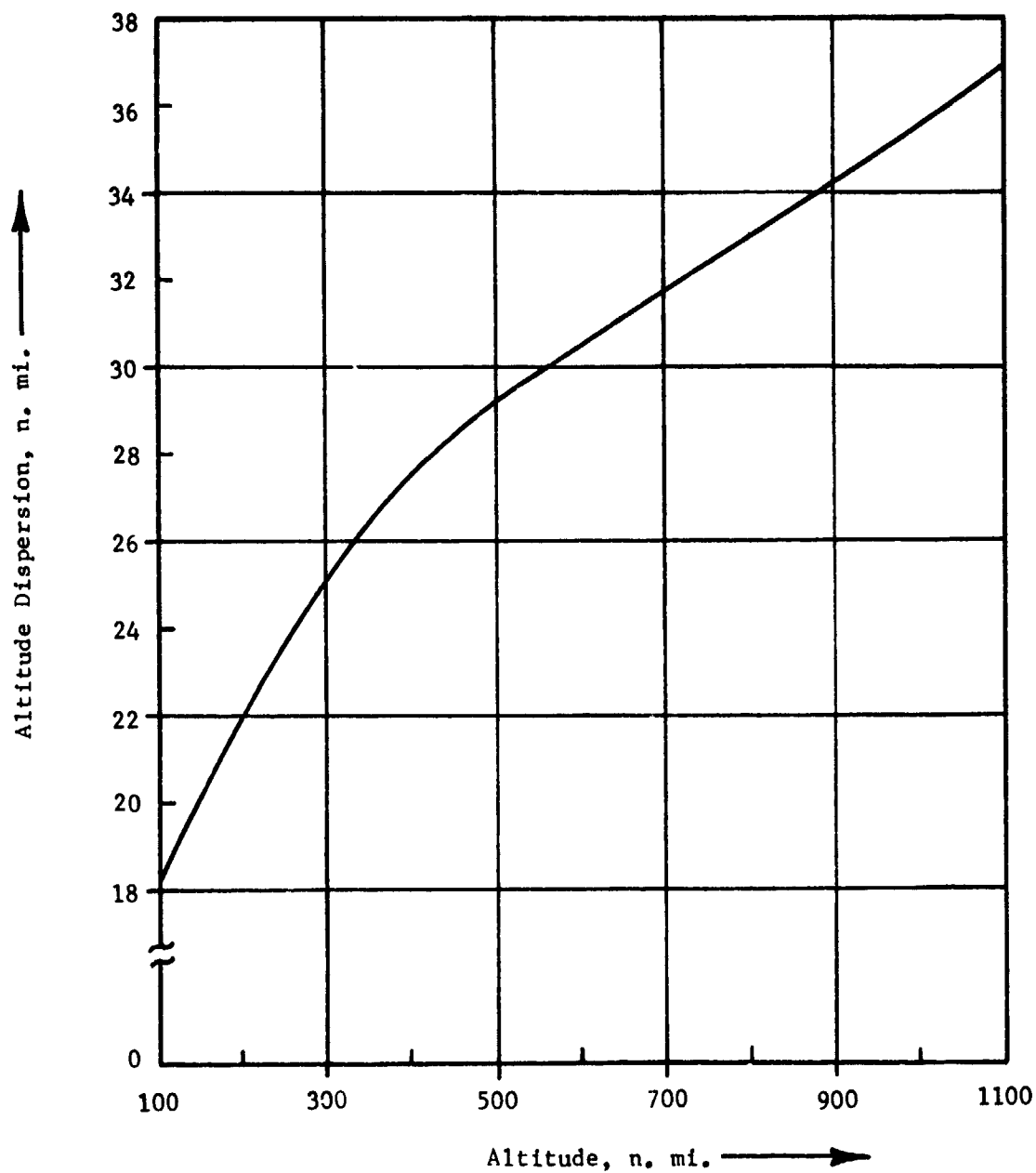


FIGURE 48. ONE SIGMA SCOUT ALTITUDE DISPERSIONS



These data may be obtained from published launch vehicle performance documents, or created using the NLVP-Performance program described in Reference 2 (or other similar programs).

When the IGOS user specifies a particular launch vehicle, a set of vehicle performance tables are created from the performance data file. At this time, the range of altitude and inclination of interest have been defined. These tables consist of:

- (1)  $PL_{ij}$ , the payload capability for a circular orbit at altitudes  $H_i$  and inclination,  $I_j$ ,
- (2)  $LS_{ij}$ , the launch site used in computing  $PL_{ij}$ , and
- (3)  $AZ_{ij}$ , the launch azimuth used in computing  $PL_{ij}$ .

The program computes 41 inclinations and 9 altitudes. The 9 altitudes are distributed evenly across the range of the IGOS plot. For the inclinations, a set of 25 predetermined inclinations, shown in Table 5, are examined and those that lie in the range of the IGOS plot are selected. The set of 41 inclinations is then filled by interleaving additional inclinations chosen evenly across the range of the IGOS plot. This technique is used to insure sufficient detail in the plots near the regions of plot discontinuities. Thus, the inclinations have been chosen near the launch site latitudes and near the inclinations for which the preferred launch site changes with inclination.

A set of launch site data is also stored. These data consist of launch site latitude and the launch azimuth constraints for each site.

The payload table,  $PL_{ij}$ , is computed by computing the payload capability from each launch site permissible for the vehicle. If more than one site is permissible, the site giving the greatest payload is used. The direct ascent launch azimuth is computed. If this azimuth exceeds the launch azimuth constraint for that site, the constraint value is used and a plane change penalty is computed.

With the payload table  $PL_{ij}$  computed, the user then enters a specific payload value (PD) of interest. An altitude versus inclination contour is then plotted by linear interpolation at each inclination to compute the altitude corresponding to PD.

TABLE 5. PRESTORED INCLINATIONS FOR IGOS PERFORMANCE TABLES

1	0	14	49.00
2	2.99	15	50.00
3	3.01	16	51.00
4	28.39	17	64.00
5	28.41	18	65.00
6	36.99	19	66.00
7	37.01	20	79.00
8	40.00	21	80.00
9	41.00	22	81.00
10	42.00	23	142.99
11	44.00	24	143.01
12	45.00	25	180.0
13	48.00		

## CONCLUSIONS AND RECOMMENDATIONS

The following summarizes Battelle's recommendations for further research based on the current status of the work for each task and the current trends of NASA advanced studies activities.

### Task 1

The computer codes, described in Table 2, have generally proven to be useful in the conduct of VSPRE studies. Several, however, have been widely used beyond the scope of VSPRE. Others could also, with further development, have similar continuing utility.

#### EOMP-I

In addition to EOMP use on VSPRE at Battelle, and by NASA at MSFC, it has frequently been used by Battelle on both the DIGS (Delta Inertial Guidance System) project and NLVP (NASA Launch Vehicle Project). Some of these users also made several useful modifications to it:

- (1) Impact point dispersions (MSFC)
- (2) Metric output (MSFC)
- (3) Orbital launches for Shuttle upper stages (BCL/NLVP).

It is recommended that EOMP-I be maintained and modified as necessary to maintain its applicability in satisfying NASA booster dispersion analysis needs.

#### IGOS

This program has been given wide visibility within NASA and has generated considerable interest.

The concept of IGOS, allowing quick response assessment of candidate orbits in defining mission requirements, is of interest to mission planners as well as launch vehicle and astronautics specialists. The display of domains of acceptable orbits actually identifies candidate orbits which minimize the impact of injection dispersions. For defining astronautics requirements in a mission planning (orbit selection), the current IGOS is only a preliminary operational program. Several additional features have already been identified for inclusion in IGOS. These are discussed in the following paragraphs.

Specific Site Coverage\*. The IGOS Earth observation model presumes that the experimenter seeks frequent coverage of all longitudes in a given latitude band. For some missions, particular geographic locations are of interest; or, even with full longitude coverage, specific communication sites must be contacted for data down-links. An alternative coverage model could indicate orbits which view a specific set of sites.

Side Looking and Multiple Sensors. Many sensors view a portion of the Earth along a path displaced from the sub-satellite ground track. Also, many missions carry multiple sensors, each with a different set of viewing requirements. SEASAT, for example, carries multiple sensors, some of which are side looking. Straight-forward coding modifications to IGOS could enable it to handle such satellite missions.

Elliptical Orbits\*. The present version of IGOS considers only circular orbits. While extension of the philosophy of the IGOS design volume to a three-dimensional space (apogee, perigee, and inclination) is straight forward, graphic presentation of three-dimensional spaces is difficult. Most likely, the best approach would be to continue to display a two-dimensional plot with the third-dimensional spaces is difficult. Two examples would be: apogee and perigee at a specified inclination, or eccentricity and inclination at a specified semi-major axis. If extensive application of IGOS is contemplated, such modifications should be considered.

Shuttle Performance Calculations\*. With the exception of the launch vehicle performance model, all IGOS features are applicable to the Shuttle as well as conventional launch vehicles. If it were assumed that the users mission would determine the orbital parameters for an entire Shuttle flight, the Shuttle (and its upper stages, if any) could be added to the vehicle data file. However, most missions will use only a portion of the Shuttle capability. Within this framework a number of types of contours could be drawn by IGOS to aid the user in selecting an orbit. For example:

---

\*These efforts have been included in a new study, at Battelle funded by MSFC.

- The Shuttle user charges to any orbit,
- The extra delta-V required to reach any orbit from the lowest cost or "nearest" currently scheduled Shuttle orbit placement,
- Regions of common acceptability for experiment pallet sharing with other payloads.

All of these require access by IGOS to data files which contain current Shuttle schedules and other Shuttle payload data. Many groups within NASA are considering particular aspects of the Shuttle scheduling and planning problem. Some of these are tending toward automated data management which will result in data files similar to those that would be needed for IGOS.

It is recommended that the concept of IGOS receive continued funding. This will insure that the capability will exist to provide a quick response user oriented tool for orbit selection. With this tool, communications between the needs of the experimenter community and those responsible for NASA's transportation system capability could be conducted in a manner compatible with the needs associated with achieving the most efficient mission designs.

#### Other Computer Codes

The following computer programs have been written to support various VSPRE investigations. The source deck cards remain in the Battelle and/or MSFC files. They require minor modifications due to recent computer center operating systems changes if they are to be used in the future.

EOMP-II. This program was developed in 1972 to the point that, if adequate mission requirements are specified, it would be extremely useful on an operational basis. Since that time, effort has centered on the specification of mission requirements, resulting in the development of IGOS. During this time, NASA's attention has concentrated on astrionics requirements for the Shuttle era. Application to Shuttle upper stage astrionics would require a major revision of EOMP-II. For this reason, it is recommended that no further support be given EOMP-II until interest justifies revisions to it.

Monte Carlo. This program has served as a useful statistical analysis tool on a number of studies at BCL and MSFC. It is simple to use

and requires no significant maintenance. It is recommended that the Monte Carlo code be maintained in its present form. This would require minimal effort.

ABBACUS. ABBACUS was developed to aid in the evaluation of computer technology studies at MSFC. The funding for these technology studies is being revised. Continuation of the development and maintenance of ABBACUS should be commensurate with NASA's overall high reliability computer technology efforts.

Spun Stage Simulation. This is a small program useful in the study of a number of problems related to spinning stages. In addition to Scout, for which it was developed, spun stages are used on Delta and Atlas/Centaur and are now under consideration for a number of Shuttle era vehicle configurations. It is recommended that the spun stage program be maintained. This would require minimal funding.

### Task 2

A number of astrionics requirements studies has been performed under Task 2. Most recently, these studies have been directed at the requirements for high reliability computers. As mentioned in the discussion on ABBACUS recommendations, this particular study has been given low priority during the restructuring of NASA's combined high reliability computer funding.

More generally, the evolution of the Shuttle upper stage program will create the need for astrionics-mission studies similar to those performed on VSPRE. It is recommended that the capability to perform these studies be maintained.

### Task 3

Task 3 was created when there was a high interest in the Advanced Small Launch Vehicle (ASLV), a major, evolutionary, upgrading of Scout. Since then interest in ASLV has diminished. Concurrently, a number of less expensive modifications to Scout guidance have been proposed, analyzed by VSPRE and LTV, and implemented. It is anticipated that future improvement to the Scout may be considered. However, these will be of limited scope and could be analyzed under an effort similar to the current VSPRE Task 2. It is recommended that Task 3, be eliminated.

Task 4

With the creation of IGOS, a tool now exists to establish the accuracy requirements for expendable launches. It is recommended that an exercise be conducted to use IGOS to evaluate a set of baseline missions which will utilize NASA vehicles (conventional and Shuttle with upper stages). The evaluation should begin by considering the fundamental mission objectives such as coverage requirements or orbit lifetime. Using IGOS the domains of acceptable orbits can be established. The size of the domain may then be used for comparison to a set of launch system accuracies to establish which systems would be likely candidates and which would benefit from modification. These modifications could involve either accuracy improvement or cost reductions through using less accurate systems. If any system seems likely to benefit from modification, a cost study should be conducted to establish the cost/benefit when the system modification costs are included with per launch system hardware cost changes.

REFERENCES

1. "First Interim Scientific Report on Vehicle Systems and Payload Requirements Evaluation", Contract NAS 8-26491, Battelle Memorial Institute, Columbus Laboratories, October 19, 1971.
2. "Second Interim Scientific Report on Vehicle Systems and Payload Requirements Evaluation", Contract NAS 8-26491, Battelle Memorial Institute, Columbus Laboratories, October 19, 1972.
3. "Interim Scientific Report on Vehicle Systems and Payload Requirements Evaluation", Contract NAS 8-26491, Battelle Memorial Institute, Columbus Laboratories, October 19, 1973.
4. Hitt, E. F., and Rea, F. G., "Development of an Evaluation Technique for Strapdown Guidance Systems", NASA CR-86086, Interim Scientific Report, Contract No. NAS 12-550, Battelle Memorial Institute, Columbus Laboratories, February 13, 1968.
5. Hitt, E. F., and Koenke, E. J., "Evaluation of Strapdown Guidance Systems on Interplanetary Missions", AIAA Guidance, Control, and Flight Mechanics Conf., Pasadena, California, August 12-14, 1968, AIAA Paper 68-828.
6. Hitt, E. F., and Koenke, E. J., "Evaluation of Strapdown Guidance Systems on Interplanetary Missions", Journal of Spacecraft and Rockets, Vol. 6, No. 5, May, 1969.
7. Hitt, E. F., Rea, F. G., and Blutreich, J. N., "Development of an Evaluation Technique for Strapdown Guidance Systems", NASA CR-86286, Second Interim Scientific Report, Contract NAS 12-550, Battelle Memorial Institute, Columbus Laboratories, February 28, 1969.
8. Hitt, E. F., and Rea, F. G., "Astrionics Selection and Operation on Interplanetary Missions", AIAA, Guidance, Control, and Flight Mechanics Conf., Princeton, N. J., August 18-20, 1969, AIAA Paper 68-882.
9. Hitt, E. F., and Rea, F. G., "Astrionics Selection and Operation on Interplanetary Missions", Journal of Spacecraft and Rockets, Vol. 7, No. 3, March, 1970.
10. Hitt, E. F., Rea, F. G., Scott, R. W., and Blutreich, J. N., "Development of an Evaluation Technique for Interplanetary Astrionics", Third Interim Scientific Report, Contract No. NAS 12-550, Battelle Memorial Institute, Columbus Laboratories, February 28, 1970.
11. "Simulation and Effectiveness Evaluation of Integrated Avionics for Military Aircraft", AFAL-TR-70-2, Vol. 1, Contract F33615-69-C-1402, Project 4167, Battelle Memorial Institute, Columbus Laboratories, December 15, 1969, AD 865801.



# REFERENCES

12. "Simulation and Effectiveness Evaluation of Integrated Avionics for Military Aircraft", R&D Technical Report (Interim), Contract F33615-69-C-1402, Project 4167, Battelle Memorial Institute, Columbus Laboratories, April 6, 1970.
13. Rea, F. G., and Fischer, N. H., "Generalized Navigation Error Analysis", AIAA, Guidance, Control, and Flight Mechanics Conference, Santa Barbara, California, August 17-19, 1970, AIAA Paper 70-1004.
14. Meeting Memorandum for ARMMS Phase III Design Review, December 4, 1973, MSFC, VSPRE-MM-73-6.
15. "Introduction to ARMMS Concepts", Internal Memorandum, December 14, 1973, VSPRE-IM-73-10.
16. "Design of a Modular Digital Computer System", DRL4 Phase I Report (U), Contract NAS8-27926, Hughes Aircraft Company, April 15, 1972.
17. Vessot, Dr. R., "Experiment Description", Smithsonian Astrophysical Observatory (SAO), August 28, 1973.
18. Freeman, George W., "Burner II Data Regarding Spin Stabilized Upper Stage Error Propagation", The Boeing Company, Aerospace Group, Seattle, Washington, March 21, 1969.
19. Hess, Wilmot N. and Mead, Gilbert D. (editors), Introduction to Space Science, Gordon and Breach, Science Publishers, New York, 1968.
20. "Scout Users Manual", Vought Missiles and Space Company, September, 1972.
21. "Scout Planning Guide", Vought Missiles and Space Company, May, 1971.
22. "Scout F (34/-25 H/S) GRE-P Mission High Launch Elevation Angle Trajectory for Range Safety Consideration", Vought Missiles and Space Company, June, 1973.
23. Thomson, W. T., Introduction to Space Dynamics, John Wiley and Sons, New York, 1963.
24. "Scout S-181C, Final Flight Report", Vought Systems Division, LTV Aerospace Corporation, Dallas, Texas, June 13, 1973.
25. MSFC Letter S&E-ASTN-ESW (73-4), "Estimated Mass Properties of the Smithsonian Astrophysical (SAO) Redshift Program", April 23, 1974.
26. MSFC Redshift Weight Statement, August 9, 1973.

REFERENCES

27. MSFC Redshift Payload Installation Drawing 10M23000, Revision A, 2 sheets; Parts List, 1 sheet.
28. MSFC Redshift Payload Assembly Drawing 10M23005, 2 sheets; Parts List, 2 sheets.
29. "GR-P Spacecraft", Vought Systems Division Letter 2-16000/3L-68, December 5, 1973.
30. MSFC Letter from Ernest Natham to Fred Rea of BCL, September 11, 1973.
31. "Summary of Observed Half Cone Angle at Fourth Stage Separation and Ignition", DIR No. 23-DIR-1303, LTV Aerospace Corporation, November 1, 1971.
32. Theory of Satellite Orbits in Atmosphere, King-Hele, Butterworths, London, 1964.
33. The Trapped Radiation Handbook, General Electric Company, Santa Barbara, California, January 1973, DNA2524H.
34. Launch Vehicle Estimating Factors for Advanced Mission Planning, NASA Headquarters, 1973, NHB7100.5B.
35. "Scout Trajectory Report, Revision C", Vought Systems Division, LTV Aerospace Corporation, Dallas, Texas, April 1974 (25.395).

APPENDIX A

IGOS USERS GUIDE

As implemented on the Battelle-Columbus Laboratories  
CDC 6400, February 3, 1975

## APPENDIX A

### IGOS PROGRAM ACCESS

To use the Interactive Graphics Orbit Selection program, it is first necessary to establish communications with the host computer. For the Battelle Computer System, communications can be obtained by dialing the Battelle data lines as follows:

- (1) (614) 421-7000
- (2) (614) 421-7100
- (3) (614) 421-7040

In the event difficulty is encountered, the status of the Battelle Computers may be checked by calling (614) 291-9766 for a recorded message.

Successful connection will be indicated by output of the date and time and a request to "Login". In response to the login request type:

LOGIN,VSPRE,ORBIT,SUP,N

The terminal will indicate successful login by the request "COMMAND-". The following underlined commands should then be entered:

COMMAND - ATTACH,PRG,COVER,ID=VSPRE  
COMMAND - EFL,50000  
COMMAND - ETL,100  
COMMAND - PRG

These commands connect the program file, extend the central memory field length to 50000<sub>8</sub>, extend the time limit to 100<sub>8</sub> seconds, and begin execution of the program.

Program execution begins with the display of a heading and an inquiry to determine if a graphics terminal is being used.

The analyst is then able to exercise the program at his discretion using the command repertoire described later in this Appendix.

When execution of IGOS is completed (either by the IGOS command END, or by encountering a fatal execution error) the response "COMMAND-" will be displayed on the screen. Reentering "PRG" will restart execution. If desired, a record of all user commands can be sent to the printer at Battelle (Building 13) by entering

DISPOSE,TAPP99,PR=IAH.

If the session is complete enter LOGOUT to terminate the session.

#### ENTERING-PROGRAM COMMANDS

A summary of all IGOS program command options are listed in Table A-1. The commands are grouped into the following functional areas:

- AXIS GENERATION
- COVERAGE DISPLAYS
- VEHICLE PERFORMANCE
- RADIATION DISPLAY
- DECAY AND ORBITAL ACCURACY DISPLAY
- SUN-SYNCHRONOUS DISPLAY
- GRAPHICAL PLOT LABELING
- TABULAR DISPLAYS
- EXITTING PROGRAM
- MISCELLANEOUS

Whenever user input is required, the program issues a request by ringing the terminal bell and displaying two dashes (i.e., " - - ").

Associated with several commands are data variables that define the operation initiated by the command. The variable mnemonics and initialized values are given in columns 2 and 3 of Table A-1, respectively. Whenever a command request is executed, the current values of defined parameters are used to perform the operation. The parameter values can be changed in either of the following two ways

- (1) Individually - The parameter mnemonic is entered followed by the desired value. For example, the maximum inclination for operation code "A" would be changed by entering -

MAXINC=125.0. This modification capability can be used for the variables in Table A-1 marked with an "\*".

- (2) List - The parameters are included with the command entry as a list. Parameter values are separated by commas and the relative position in the command string determine which data values are modified. For example, the maximum inclination variable for operation code "A" is the fourth (4th) parameter in the list. Therefore, the maximum inclination value would be changed by entering - A,,,125.0.

Whenever a data parameter is specified, the parameter's value remains equal to that value until again modified. All values can be reset to their initialized value by entering the RESET command.

With a plot displayed on the screen, all commands are entered in a small rectangular box on the lower left of the screen. After the first command has been entered, it becomes difficult or impossible to read what has been typed. Therefore, the user must be attentive to his typing ability. If an error occurs and is detected in data entry, the user is informed by a multiple ring of the terminal bell. The command should then be reentered. No input entered by the user should cause abnormal program termination. However, if the error is not detected (i.e., a wrong numerical value entered for some parameter) which results in an incorrect plot, there is no capability to erase the results. The terminal, that the IGOS program uses is a "non-refresh" screen type. Whatever appears on the screen is permanent until the entire screen is erased. (See Page A-7, Terminal Hardware.) If an error does occur, the user should request a new axis and all other data (i.e., coverage, radiation, launch vehicle payload curves, etc.) to make the plot complete. The user only need enter the basis commands since all data parameters (except where the error occurred) are set from the previous plot.

The use of the above features are best illustrated in the example analysis session provided later in Appendix B, Sample Graphics Terminal Session.

TABLE A-1. IGOS COMMAND OPTIONS

OPERATION CODE	VARIABLE MNEMONIC	STRING POSITION	INITIALIZED VALUE	DESCRIPTION
<u>AXIS GENERATION</u>				
A	--*	--	--	Sets axis
	HMIN*	1	100.	Minimum circular altitude (N.M.)
	HMAX*	2	250.	Maximum circular altitude (N.M.)
	DIMIN*	3	0.	Minimum inclination (DEG.)
	DIMAX*	4	110.	Maximum inclination (DEG.)
<u>COVERAGE DISPLAY</u>				
COV	--	--	--	Performs coverage analysis
	LATMIN*	1	35.0	Minimum latitude to be viewed (DEG.)
	LATMAX*	2	35.0	Maximum latitude to be viewed (DEG.)
	DAYC*	3	50.0	Time for full coverage (DAYS)
	RNG*	4	1200.0	Maximum sensor range (N.M.)
	ELEMIN*	5	40.0	Minimum elevation (DEG.)
	FOV*	6	40.0	Sensor field of view (DEG.)
	ANGRES*	7	0.1	Resolution angle for sensor (DEG.)
HC	LINRES*	8	10.0	Linear resolution for sensor (N.M.)
	--	--	--	Adds cross-hatching to the coverage plot
	start	1	1.0	Starting line drawn
	skip	2	1.0	Number of lines skipped between lines

\* Value can be entered using the mnemonic code followed by the variable value.

TABLE A-1. IGOS COMMAND OPTIONS  
(Continued)

OPERATION CODE	VARIABLE MNEMONIC	STRING POSITION	INITIALIZED VALUE	DESCRIPTION
<u>VEHICLE PERFORMANCE</u>				
V	--	--	--	Selects launch vehicle
	Vehicle index	1	0	Vehicle index 1 = SCOUT D
	Launch Site	2-6		2 = DELTA
	specification			3 = DELTA
				4 = DELTA
				5 = SCOUT F
	Launch Site	2-6	SCOUT-WTR,	Launch sites can be specified by listing
	specification		WAL-S,	the desired ones to be considered using
			WAL-N, SM	the following mnemonics:
			DELTA-WTR,	ERT = Eastern Test Range
			ETR	WTR = Western Test Range
				SM = San Marco
				WAL-N = Wallops-North of the Bermuda
				Corridor
				WAL-S = Wallops-South of the Bermuda
				Corridor
P	--	--	--	Plots a payload contour
	Payload	1	0	
<u>RADIATION DISPLAY</u>				
RAD	--	--	--	Radiation model
	CMS*	1	.01	Density of aluminum shield (gm/cm <sup>2</sup> )
	FLUM*	2	5E12	Maximum fluence
	RDAY*	3	100.0	Number of days for allowable fluence
HR	--	--	--	Cross-hatches radiation curve

\* Same as previous page.



TABLE A-1. IGOS COMMAND OPTIONS  
(Continued)

OPERATION CODE	VARIABLE MNEMONIC	STRING POSITION	INITIALIZED VALUE	DESCRIPTION
<u>DECAY AND ORBITAL ACCURACY DISPLAY</u>				
DECAY	--	--	--	Decay model request. Also provides injection dispersion display (SCOUT only)
	ALTD*	1	175.0	Altitude of injection (n.mi.)
	DID*	2	37.0	Inclination of injection (deg.)
	BCD*	3	220.0	Ballistic coefficient (Kg/m <sup>2</sup> )
	YRD*	4	1976	Launch year parameter
	TMD*	5	1	Time in years for decay
<u>SUN-SYNCHRONOUS DISPLAY</u>				
SUN	--	--	--	Draws the sun synchronous lines
	DEGS*	1	0.	Allowable precession (degrees)
	DAYS*	2	0.	Time for allowable precession (days)
<u>GRAPHICAL PLOT LABELING</u>				
L	--	--	--	Provides capability to place labels on a plot. Cross-hairs appear on the screen. The user must position them. With the thumb wheels, strike the space bar, and enter the desired label. When finished position the cross-hairs in the command box and hit the space bar.

\* Same as previous page.

TABLE A-1. IGOS COMMAND OPTIONS  
(Continued)

OPERATION CODE	VARIABLE MNEMONIC	STRING POSITION	INITIALIZED VALUE	DESCRIPTION
<u>TABULAR DISPLAYS</u>				
T	--	--	--	Produces Tabular Output
	request code	1 & 2	0	Valid request codes are as follows:
	-See description -			1 = Vehicle table
				1,1 = Payload vs. altitude and inclination
				1,2 = Launch site vs. altitude and inclination
				1,3 = Launch azimuth vs. altitude and inclination
				2 = Payload table, altitude vs. payload and inclination
				4 = Sensor table
				5 = Vehicle library index.
<u>EXITTING PROGRAM</u>				
END	--	--	--	Exits program.
<u>MISCELLANEOUS</u>				
RESET	--	--	--	Returns all data to initialized values.

TEACH FEATURE

The Interactive Graphics Orbit Selection program has a feature referred to as "TEACH" to help the participating analyst use the interactive program. At any time in an exercise, all command options available at that current point are displayed merely by entering the "?" symbol. If questions then arise concerning the use of any specific command, instructions for that command can be called for by entering the command followed by the "?" symbol (i.e., COVER?). If a graphical display is currently on the screen, a page request to erase the screen will be issued. Permission is given by entering any character and striking the return key.

The teach feature is illustrated in Figures A-1 through A-3 which was taken directly from the terminal screen.

COMPUTER HARDWARE

The IGOS program was developed to use a Tektronix 4010/4012 series interactive graphics terminal. The display screen is a "non-refresh" type storage tube. The display area is 8.50 inches by 6.25 inches and consists of 1024 addressable points on the horizontal (X) axis and 781 points on the vertical (Y) axis. The terminal may operate in an alphanumeric (printing) mode or a graphic (plotting) mode.

The keyboard is a standard ASCII keyboard with several additions. There are extra keys for erasing the screen and for causing hard copy generation. There are also two thumbwheels for positioning the cross-hairs on the screen. Once positioned, striking any key on the keyboard will transmit the position of the intersection of the cross-hairs to the computer. The cross-hairs are turned on and off by the user's program (i.e., L COMMAND).

The hard copy unit is used to generate a permanent (paper) copy of what is displayed on the display screen. Approximately 5 seconds are required to generate a hard copy. The process does not affect what is displayed on the screen. However, while the screen is swept during the copy process, no information can be displayed. If any information comes from the computer during the sweep, it is lost.

```

--
VALID COMMANDS ARE AS FOLLOWS - (FORMAT- COMMAND (DESCRIPTION) )
A (AXIS)      V (VEHICLE)  P (PAYLOAD)  L (LABEL)
COV (COVER)   HC (HATCH)   T (TABLES)    RESET (RESET)
END (FINISH)  SUN (SUN-SYNC)              DECAY (DECAY)
RAD (RADIATION)      WR (WATCH- RAD)

FOR FURTHER INFORMATION ENTER THE COMMAND FOLLOWED BY A QUESTION MARK
***INITIALIZED VALUES ARE PRECEDED BY IV  EXAMPLE IV 100
--
A?
SETS AXIS - PARAMETERS      (1) HMIN - MINIMUM ALTITUDE (N M )  IV 100
                             (2) HMAX - MAXIMUM ALTITUDE (N M )  IV 250
                             (3) DIMIN - MINIMUM ALTITUDE (N M )  IV 0 0
                             (4) DIMAX - MAXIMUM INCLINATION (DEG) IV 110
                             EXAMPLE- A.100.100.28 5.50 .30
--
U?
SELECTS THE LAUNCH VEHICLE - REQUIRED PARAMETER- LV NUMBER
                           OPTIONAL PARAMETERS- LAUNCH SITES
AVAILABLE LAUNCH SITES- UTR - WESTERN TEST RANGE
                        ETR - EASTERN TEST RANGE
                        WAL-N - WALLOPS NORTH OF BERMUDA CORD
                        WAL-S - WALLOPS SOUTH OF BERMUDA CORD
                        SM - SAN MARCO

EXAMPLES-  V=1 OR U.2 OR V=1.UTR.SM OR U.2.ETR.UTR
--
P?
PLOTS A PAYLOAD CONTOUR - PARAMETER -(1) PAYLOAD
EXAMPLE  P.200 OR P=200
--
L?
COMMAND TO LABEL CURVES - THE CROSS HAIRS WILL APPEAR ON THE
SCREEN POSITION CROSS HAIRS AND HIT THE SPACE BAR. AT THE BEEP
OF THE BELL. ENTER THE DESIRED LABEL UPON COMPLETION. POSITION
THE CROSS HAIRS IN THE COMMAND BOX AND STRIKE THE SPACE BAR
--

```

FIGURE A-1. TEACH FEATURE OUTPUT

```

COV?
COMMAND TO PERFORM THE COVERAGE ANALYSIS AND INDICATE
ORBITS WHICH DO NOT SATISFY THE COVERAGE REQUIREMENTS
OPTIONAL PARAMETERS AS FOLLOWS -
  (1)MINLAT - MINIMUM LATITUDE TO BE VIEWED (DEG ) IV 35
  (2)MAXLAT - MAXIMUM LATITUDE TO BE VIEWED (DEG ) IV 35
  (3)DAYC - MAXIMUM TIME (DAYS) BETWEEN VIEWS OF ANY
            POINT IN THE INDICATED LATITUDE BAND IV 20
  (4)MAXRNG - SENSOR MAXIMUM RANGE (N MI ) IV 1200
  (5)MINELE - SENSOR MINIMUM ELEVATION (DEG ) IV 40
  (6)FOV - SENSOR FIELD OF VIEW (DEG ) IV 40 0
  (7)ANGRES - SENSOR ANGULAR RESOLUTION (DEG) IV 0.1
  (8)LINRES - REQUIRED LINEAR RESOLUTION (N MI ) IV 10.0
EXAMPLE- COV.30.60.5.10.1200.45.45.0 1.10 5
OR DAYC.10 FOLLOWED BY COV
-- HC?
--
ADDS CROSS HATCHING TO THE COVERAGE PLOT
OPTIONAL PARAMETERS- (1)IH1 - STARTING AT LINE IH1 - IV 1
                    (2)IH2 - SKIPPING IH2-1 LINES - IV 1
-- T?
--
COMMAND TO GENERATE TABULAR DISPLAYS OF THE COVERAGE DATA.
OPTIONS- 1 - VEHICLE TABLE
          1.1- PAYLOAD VERSES ALTITUDE AND INCLINATION
          1.2- LAUNCH SITE VERSES ALTITUDE AND INCLINATION
          1.3- LAUNCH AZIMUTH VERSES ALTITUDE AND INCLINATION
          2 - PAYLOAD TABLE, ALTITUDE VERSES PAYLOAD AND INCL.
          4 - SENSOR TABLE
          5 - VEHICLE TABLE
-- RESET?
--
COMMAND TO RESET ALL DATA TO THE DEFAULT VALUES.
-- END?
--
COMMAND TO END EXECUTION.
--

```

FIGURE A-2. TEACH FEATURE OUTPUT  
(Continued)

SUN?  
 COMMAND TO DRAW THE BAND OF NEAR SUN SYNCHRONOUS ORBITS  
 PARAMETERS - DEGS - ALLOWABLE PRECESSION (DEGS) IV 0  
 DAYS - TIME FOR ALLOWABLE PRECESSION (DAYS) IV 0  
 EXAMPLE- SUN.30 0.10  
 -- DECV?  
 COMMAND TO INCLUDE LAUNCH VEHICLE INJECTION DISPERSIONS (SCOUT ONLY)  
 AND ORBIT DECAY  
 PARAMETERS ALTD - ALTITUDE OF INJECTION (N MI) IV 175  
 DID - INCLINATION OF INJECTION (DEG) IV 37  
 BCD - BALLISTIC COEFFICIENT (KG/M2) IV 220  
 YRD - LAUNCH YEAR PARAMETER IV 1976  
 TMD - TIME TO BE CONSIDERED (YEARS) IV 1  
 EXAMPLE- DECAY.160 .35 5.220 .1977.2  
 -- HR?  
 COMMAND TO DRAW HATCH LINES TO SHADE RADIATION (SEE RAD) DISPLAY  
 -- RAD?  
 COMMAND TO INCLUDE ORBITS WITH EXCESSIVE RADIATION EXPOSURE  
 PARAMETERS- CMS - DENSITY OF ALUMINUM SHIELD (GM/CM2) IV 0.01  
 FLUM- MAXIMUM FLUENCE IV 5E12  
 \*DUE TO SIZE OF NUMBER, FLUM IS ENTERED AS  
 FOLLOWS - XX XEYV ENTERED AS XX.XX100.YY  
 OR 12.4E12 ENTERED AS 1240.12  
 OR 11 7E13 ENTERED AS 1170.13  
 RDAY- NUMBER OF DAYS FOR ALLOWABLE FLUENCE IV 100  
 EXAMPLE- RAD. 1.1240.12.3

FIGURE A-3. TEACH FEATURE OUTPUT  
 (Continued)

Although the IGOS program utilizes the Tektronix terminal, it is possible to modify the program to operate on other terminals with similar features with a minimum of effort. This has been done to give demonstrations on Computek 400/15 terminals located at NASA Headquarters.

The Battelle and NASA Headquarters terminals are currently driven by a Control Data CDC6400 computer system. A program version to use a Univac 1108 computer system has been developed and delivered to MSFC. The program is written in standard FORTRAN and should be adaptable to other computer systems with a minimum of conversion effort required.

APPENDIX B

SAMPLE IGOS WORK SESSION



## APPENDIX B

### SAMPLE GRAPHICS TERMINAL SESSION

The use of the Interactive Graphics Orbit Selection program is best illustrated by the following sample terminal session. All commands available to the analyst are used in this sample session. The displays shown were taken directly from the terminal screen. Table B-1 explains what each page illustrates and serves as an index to the work session.

TABLE B-1. ORBITAL DESIGN WORK SESSION GUIDE

PAGE	DESCRIPTION
B-4	Certain entries must be made to enter the program. Command EFL extends the field length, ETL extends the time limit, TERM defines the number of characters per line, and ATTACH connects the computer program. The PRG command initiates execution.
- B-5	The program is inquiring about the terminal being used. A "Y" response allows graphical output.
B-6	An axis request is made with altitudes ranging from 150 to 300 n mi and inclinations ranging from 10.0 to 120.0 degrees.
B-7	The resulting axis from the command request on page B-6.
B-8	A coverage model using the standard defaults is requested.
B-9	The coverage model is hatched.
B-10	Vehicle number 1 (i.e., SCOUT) is requested.
B-11	Payload curves for 225.0, 300.0, and 350.0 pounds are requested and labeled using the "L" command.
B-12	The coverage model from page B-8 is included with the payload curves shown on page B-11.
B-13	A sun synchronous line is requested.
B-14	The sun synchronous line is superimposed on the display created on page B-12.
B-15	The results of a radiation model request with .25 cm of aluminum shielding and a 2000 day exposure.
B-16	The results of the radiation model are cross-hatched.
B-17	The results of the radiation model, coverage model and payload curves are superimposed on a single axis display.
B-18	A "ZOOM" is done for altitudes 165.0 to 200 nautical miles and 50.0 to 75.0 degrees inclination. Then payload curves for 225.0, 300.0 and 350.0 pounds are superimposed. This region appears to represent a potential orbital area to view 35.0 degree latitudes at least once every 30 days.

TABLE B-1. ORBITAL DESIGN WORK SESSION GUIDE  
(Continued)

PAGE	DESCRIPTION
B-19	The results of the decay model for a 240 n mi altitude, 50 degree inclination, a ballistic coefficient of 220, a 1977 launch data, and a mission duration of 3 years.
B-20	The results of the decay model for a 240 n mi altitude, 65 degree inclination, a ballistic coefficient of 220, a 1977 launch date, and a mission duration of 1 year.
B-21	The results of the coverage model from page B-8 and the decay model on page B-20 superimposed. Some interesting conclusions can be drawn from this figure. First note that the initial altitude distribution (ticks to the left) indicate the possibility of inadequate coverage near + and $-2\sigma$ . Noting the decay of $+3\sigma$ and $+1\sigma$ it can be seen that an injection into the forbidden band would not decay out of the band for the entire mission. The lower forbidden band is much narrower and the decay rate much faster. Therefore, an injection in or above this band would result in a brief period of insufficient coverage. Attention should be paid to the fact that a $-3\sigma$ injection decays to 100 n.mi by May, 1977. These characteristics might warrant consideration of a slightly higher nominal altitude and lower inclination, for example 260 n.mi at $33^\circ$ .
B-22-23	Example of the payload vs. altitude and inclination data table.
B-24-25	Example of the launch site vs. altitude and inclination data table.
B-26-27	Example of the launch azimuth vs. altitude and inclination data table.
B-28-29	Example of the altitude vs. payload and inclination data table.
B-30-31	Sensor table illustration.
B-32	Vehicle library index.

COMMAND- EFL.50000  
COMMAND- ETL.100  
COMMAND- TERM.85  
COMMAND- ATTACH.PRG.COVER,ID-USPRE  
PF CYCLE NO \* 001  
COMMAND- PRG

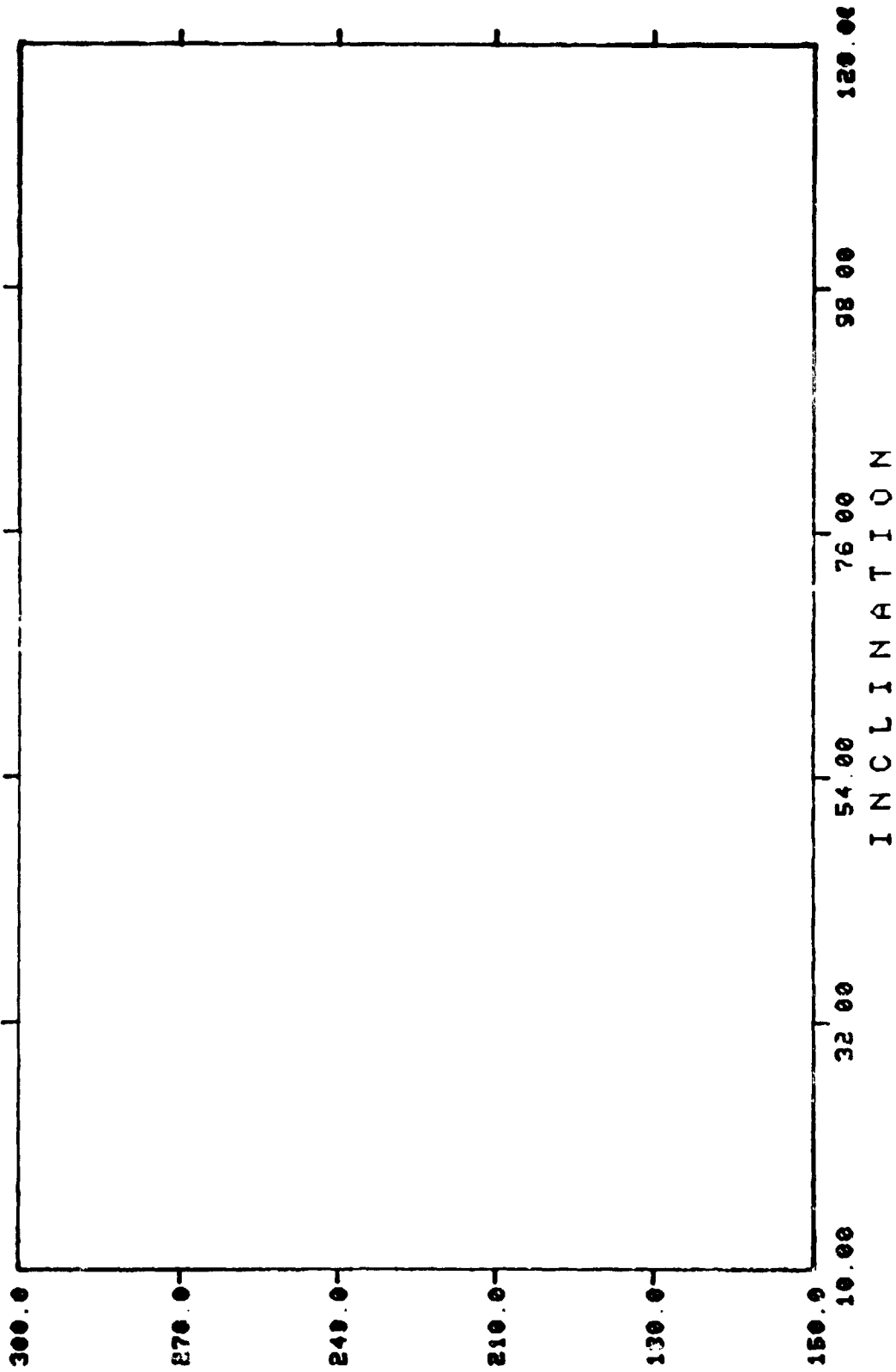
PROGRAM ORBIT (VER 2.0)

GRAPHICS TERMINAL (Y/N)

-- Y

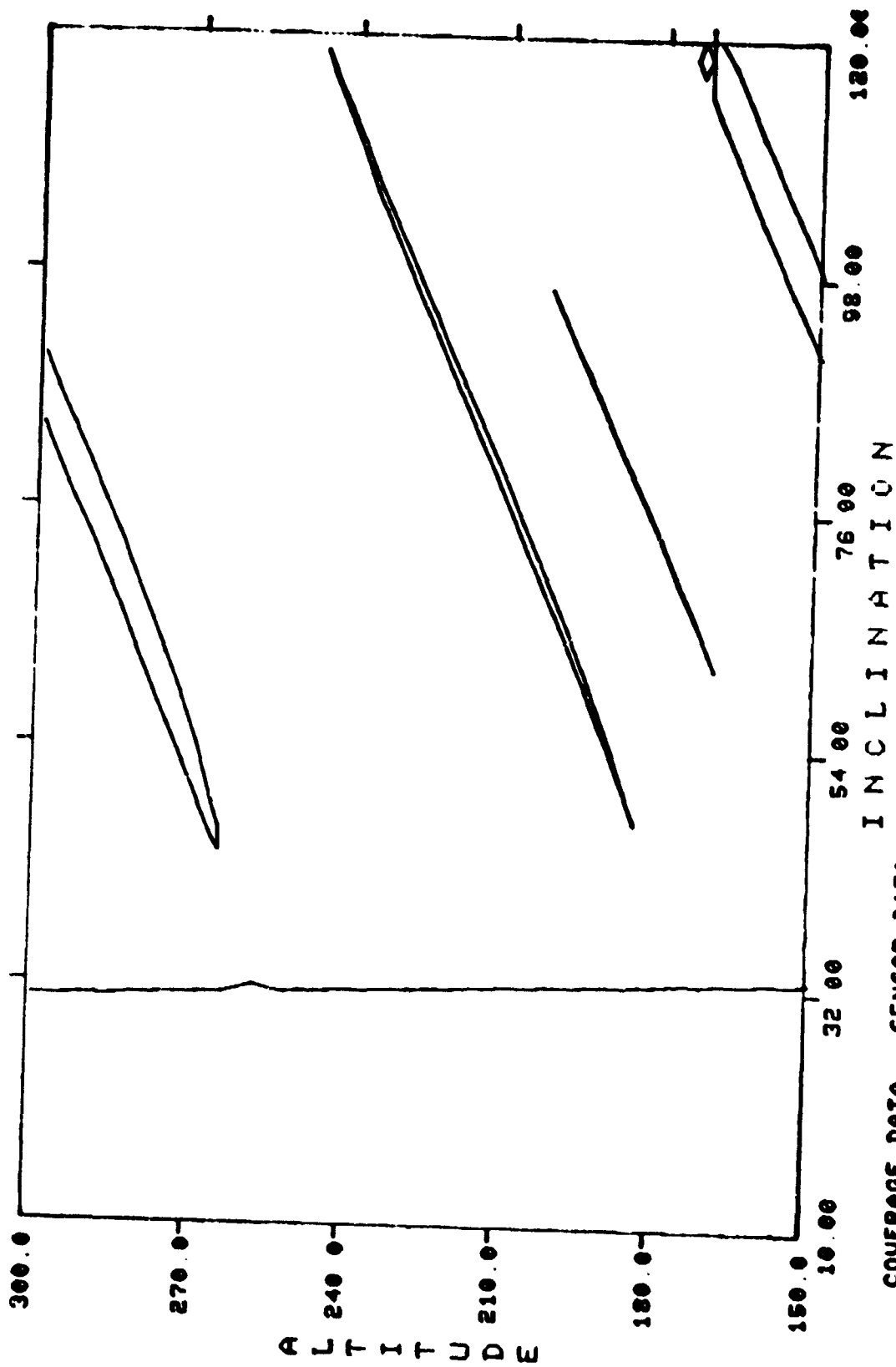
-- A.150.300.10.120

--



DEPTH



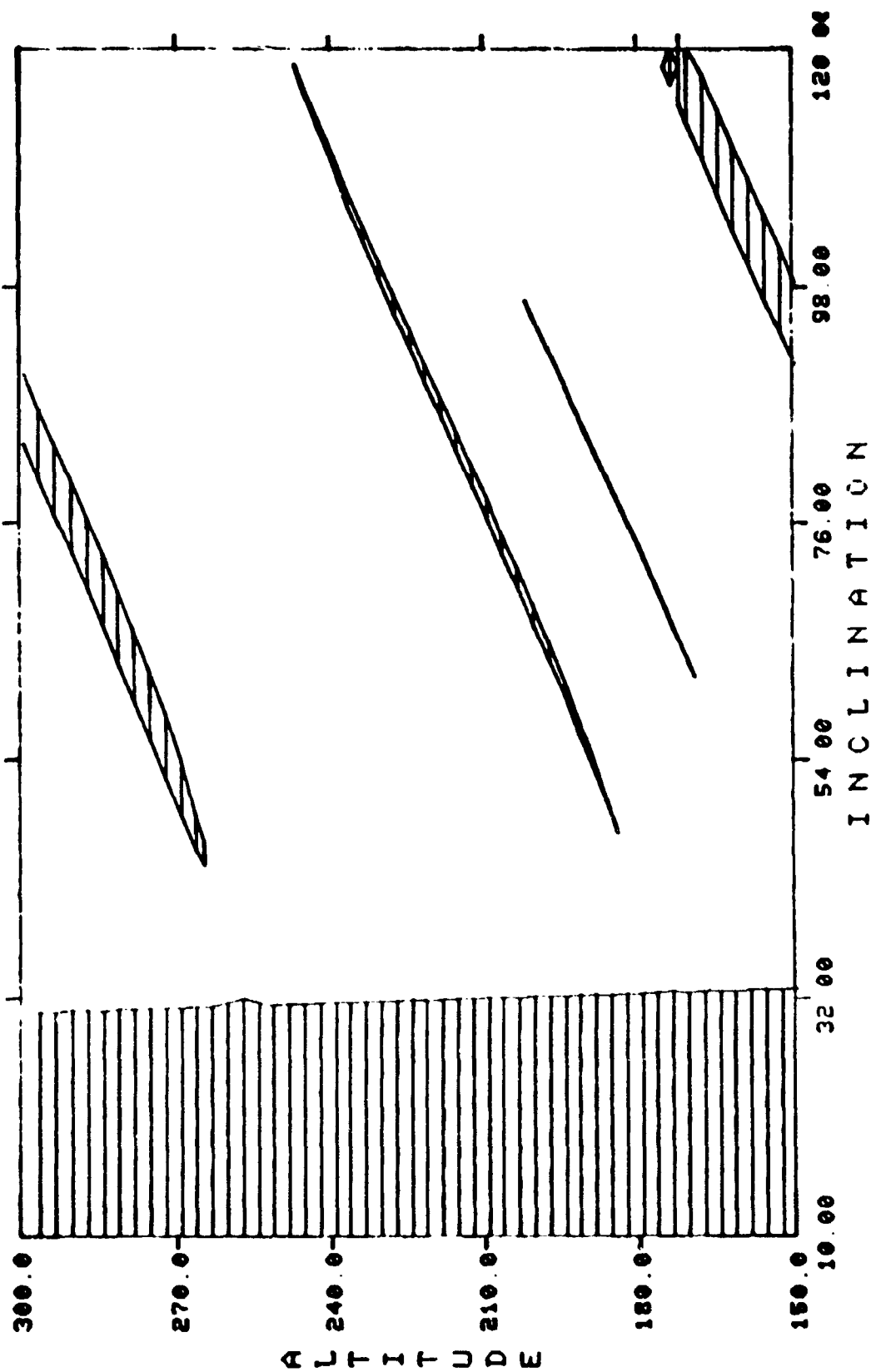


COVERAGE DATA SENSOR DATA

LATITUDES DAYS MAXRNG MINELE F.O.U. ANGRES LINRES  
 1 35.0- 35.0 30 1200.0 40.0 40.0 0.1 10.0

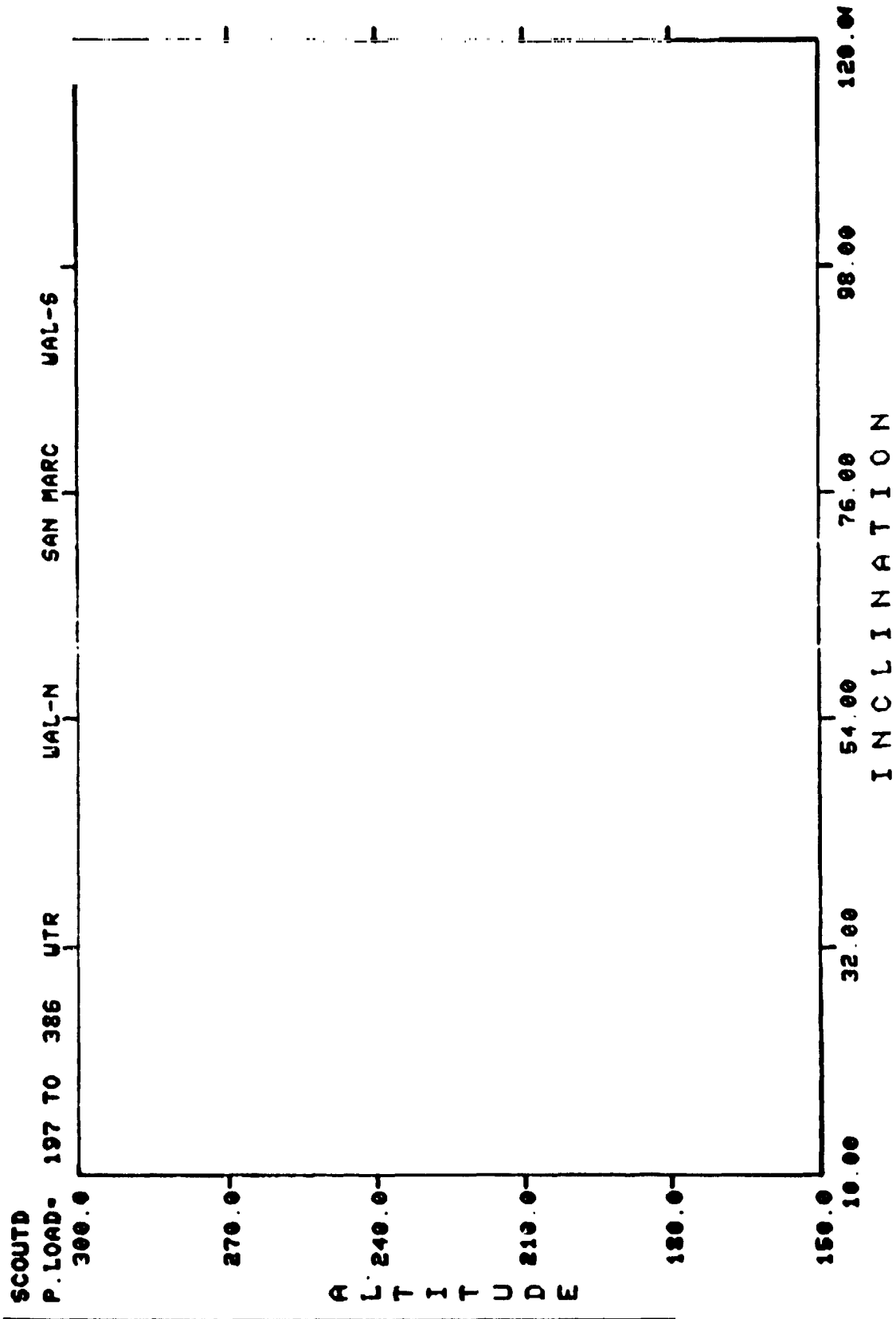
COV





COVERGE DATA SENSOR DATA  
 LATITUDES DAYS MAXRNG MINELE F.O U ANGRES LINRES  
 1 35.0- 35.0 30 1200.0 40 0 40.0 0.1 10 0

BOU

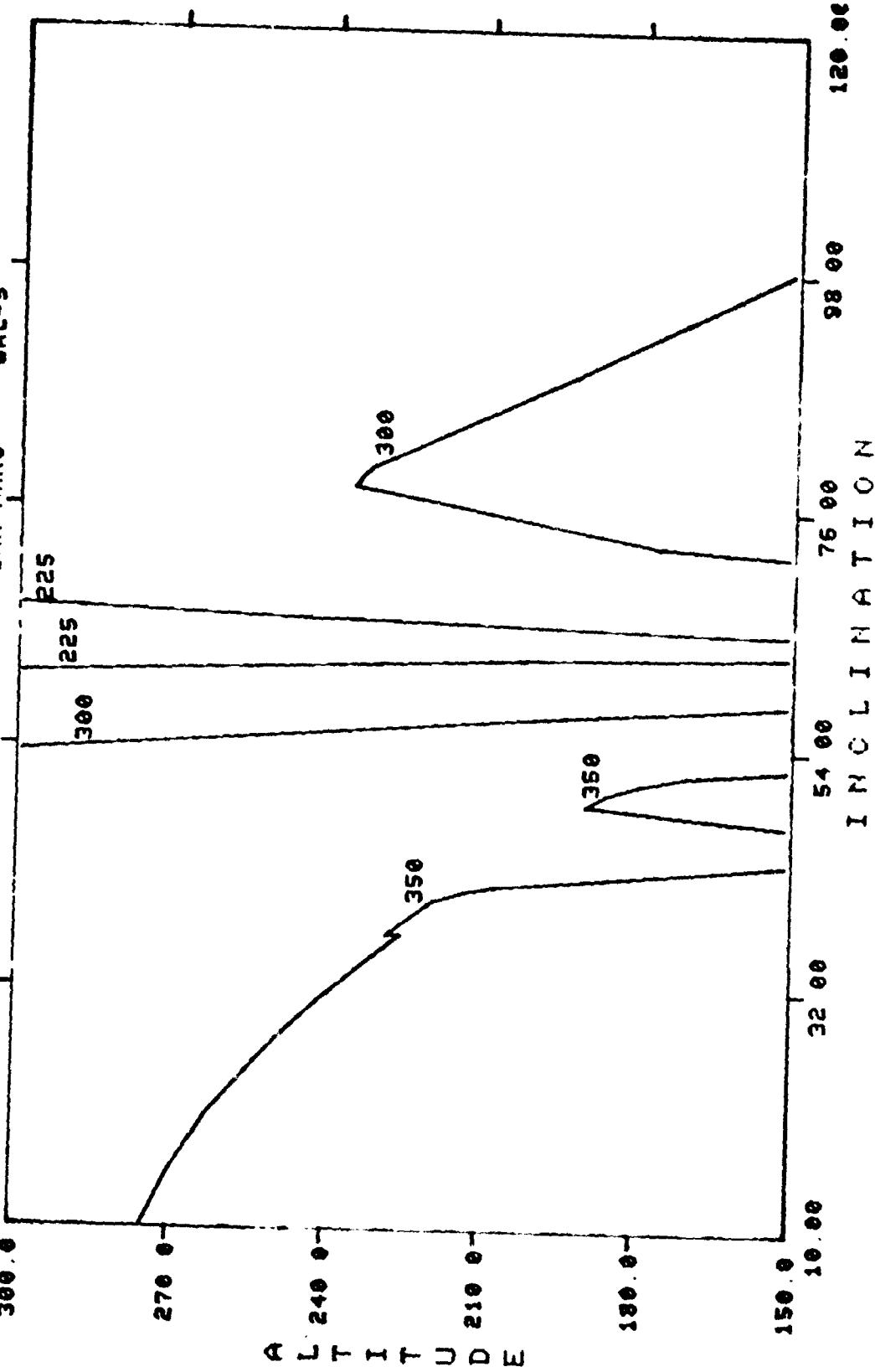


111

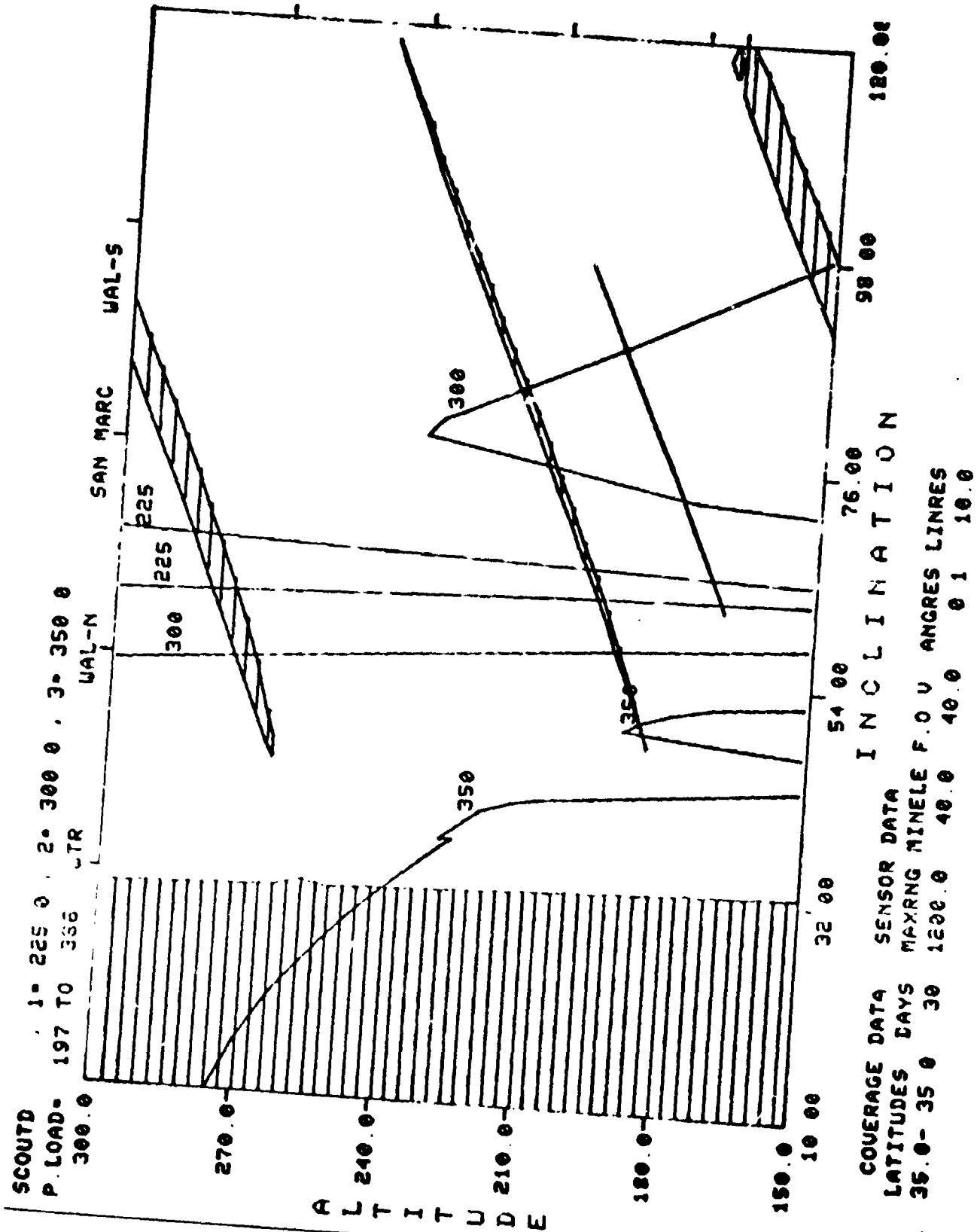
SCOUT  
P. LOAD- 197 TO 386 UTR  
300.0

1- 225 0 , 2- 300 0 , 3- 350 0

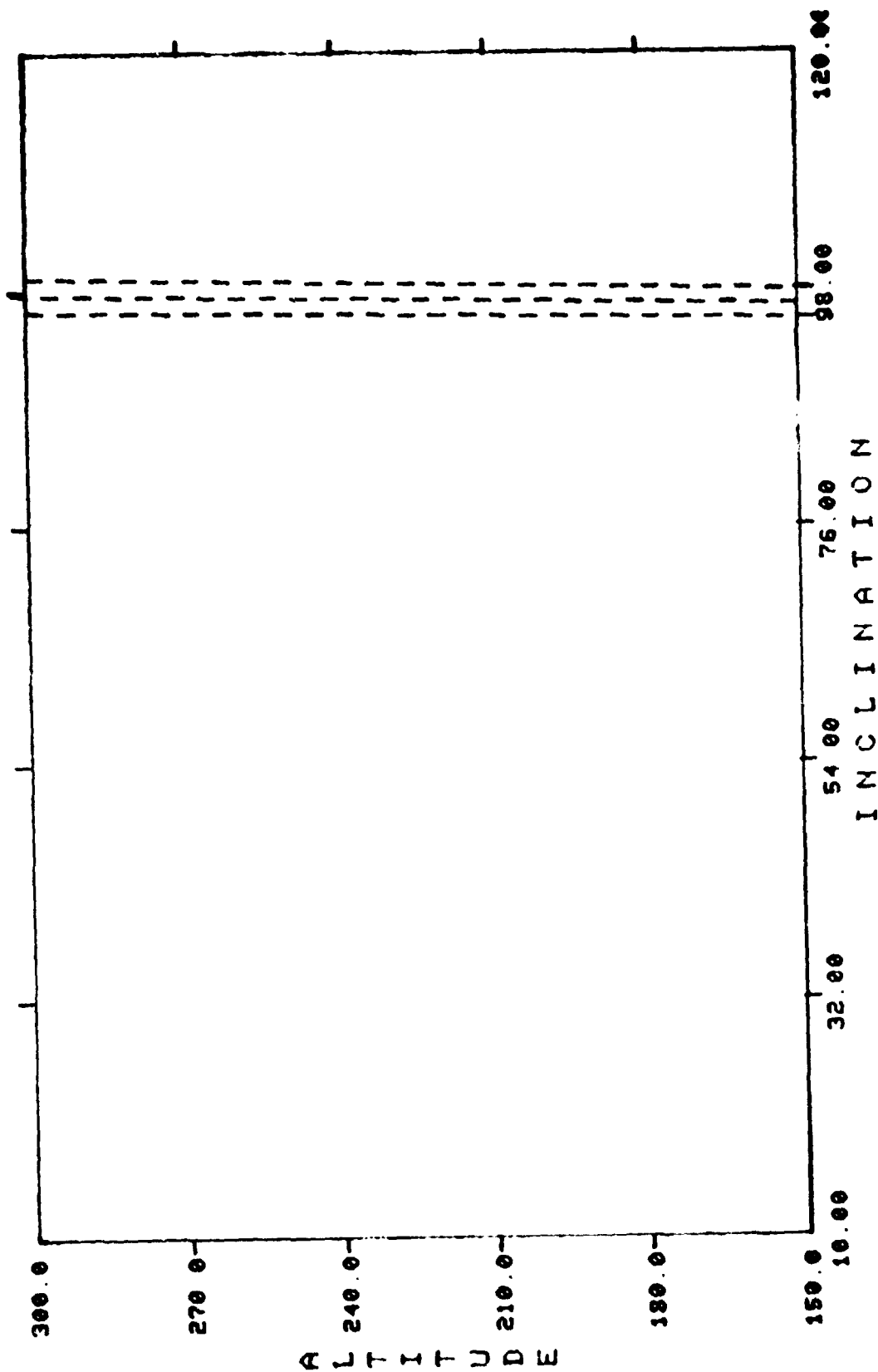
UAL-N SAN MARC UAL-S



203205

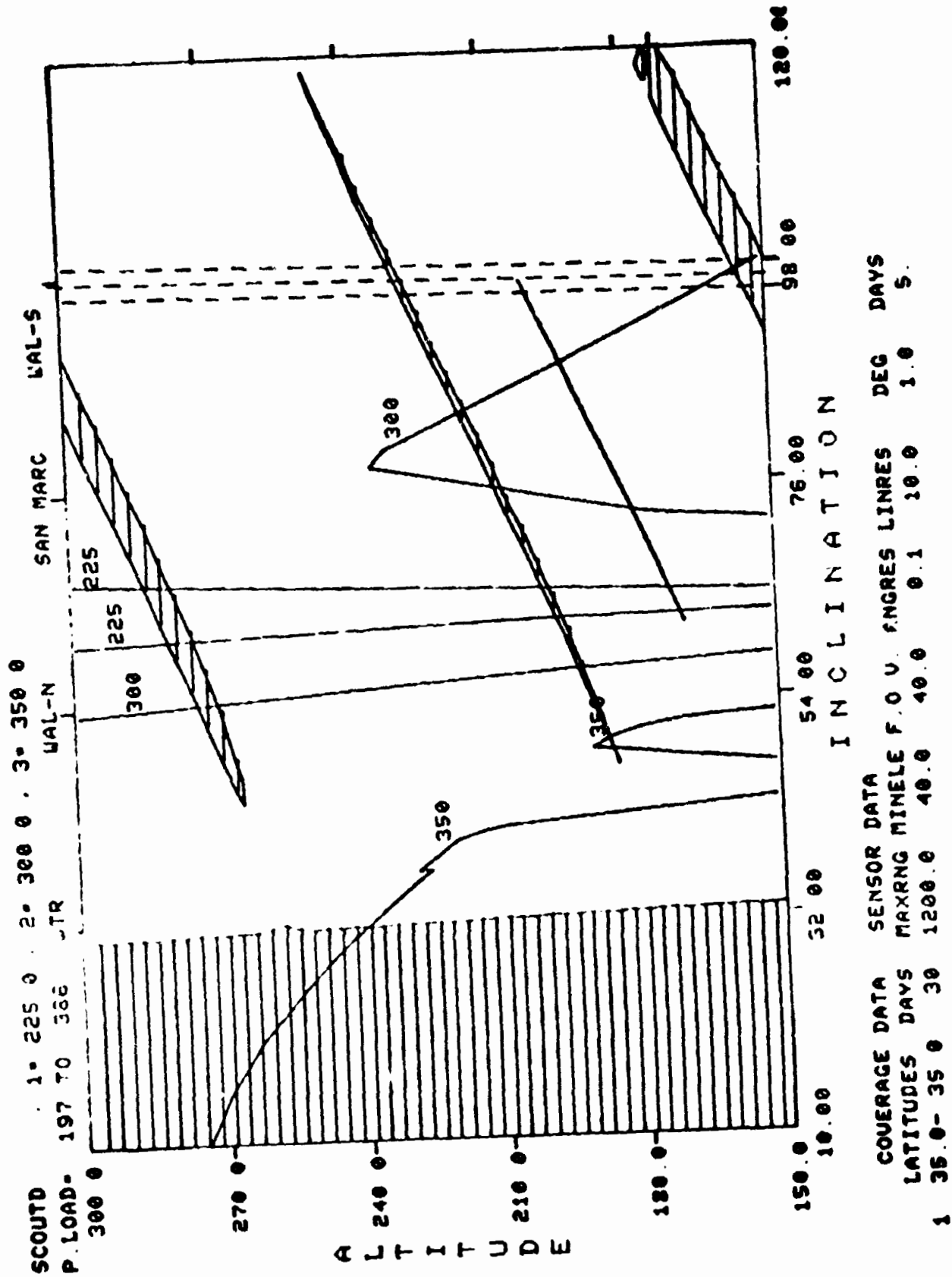


**5000**

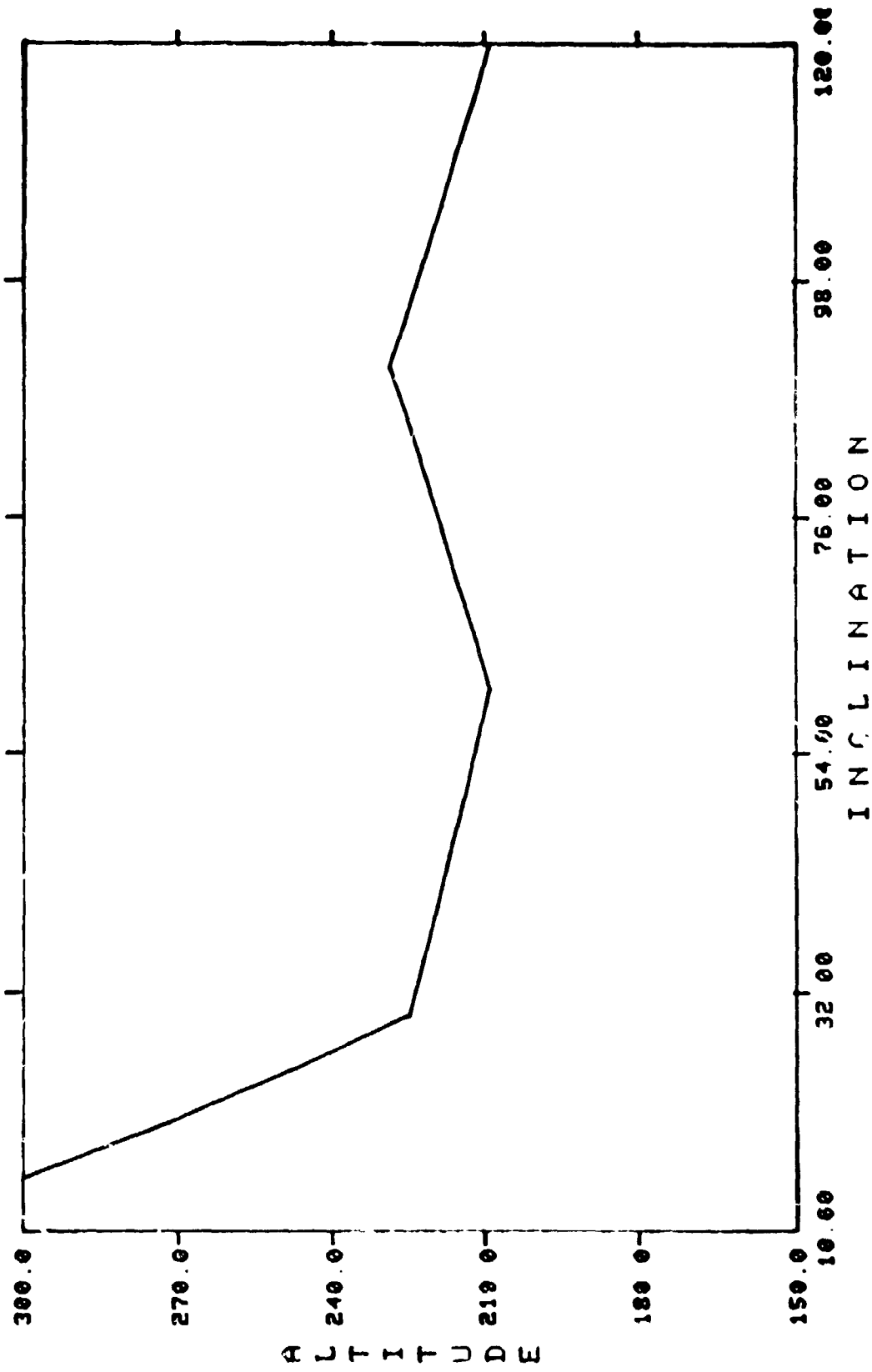


DEG DAYS  
1.0 5.

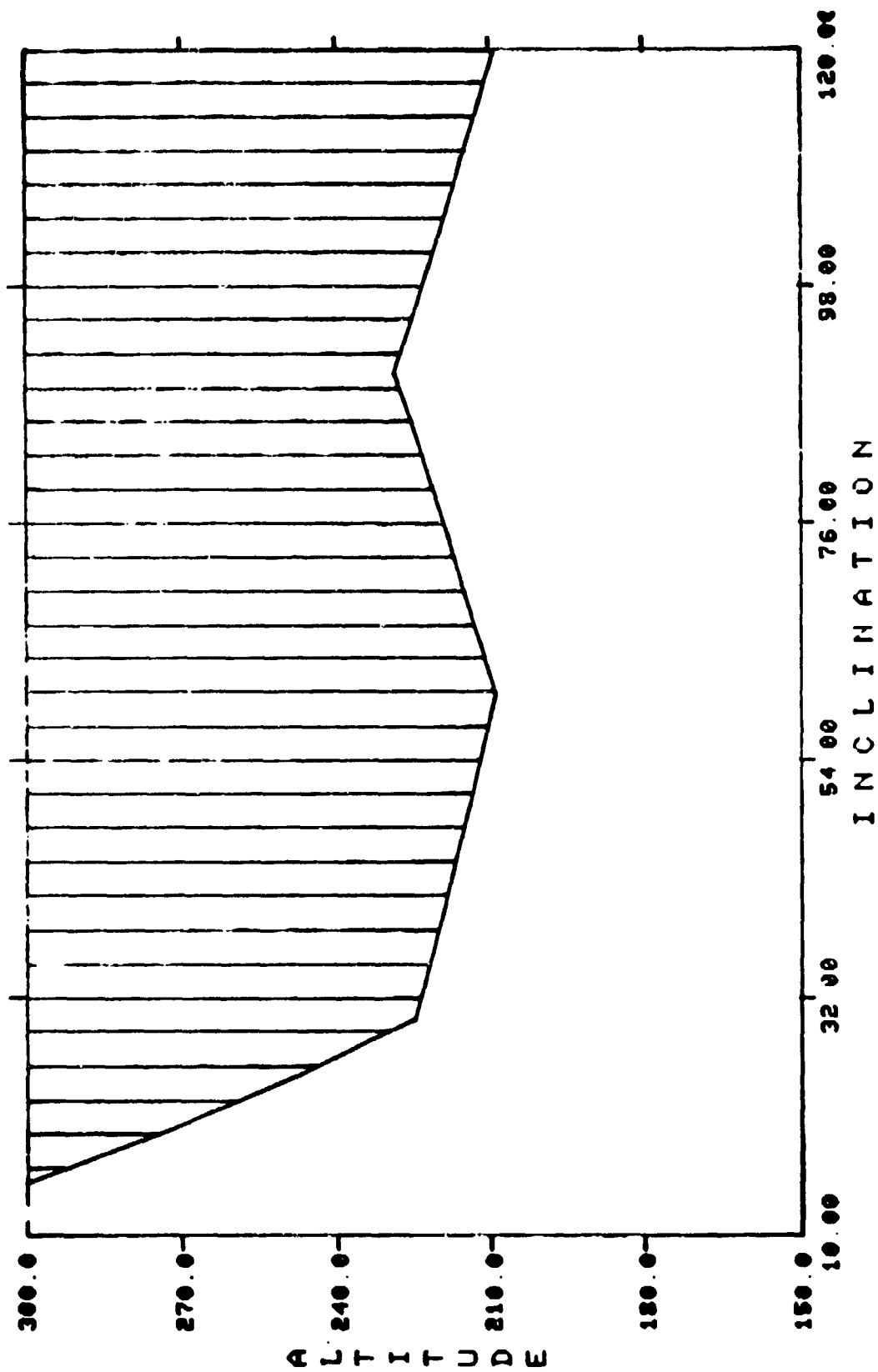
SUN.1.5



000051.5

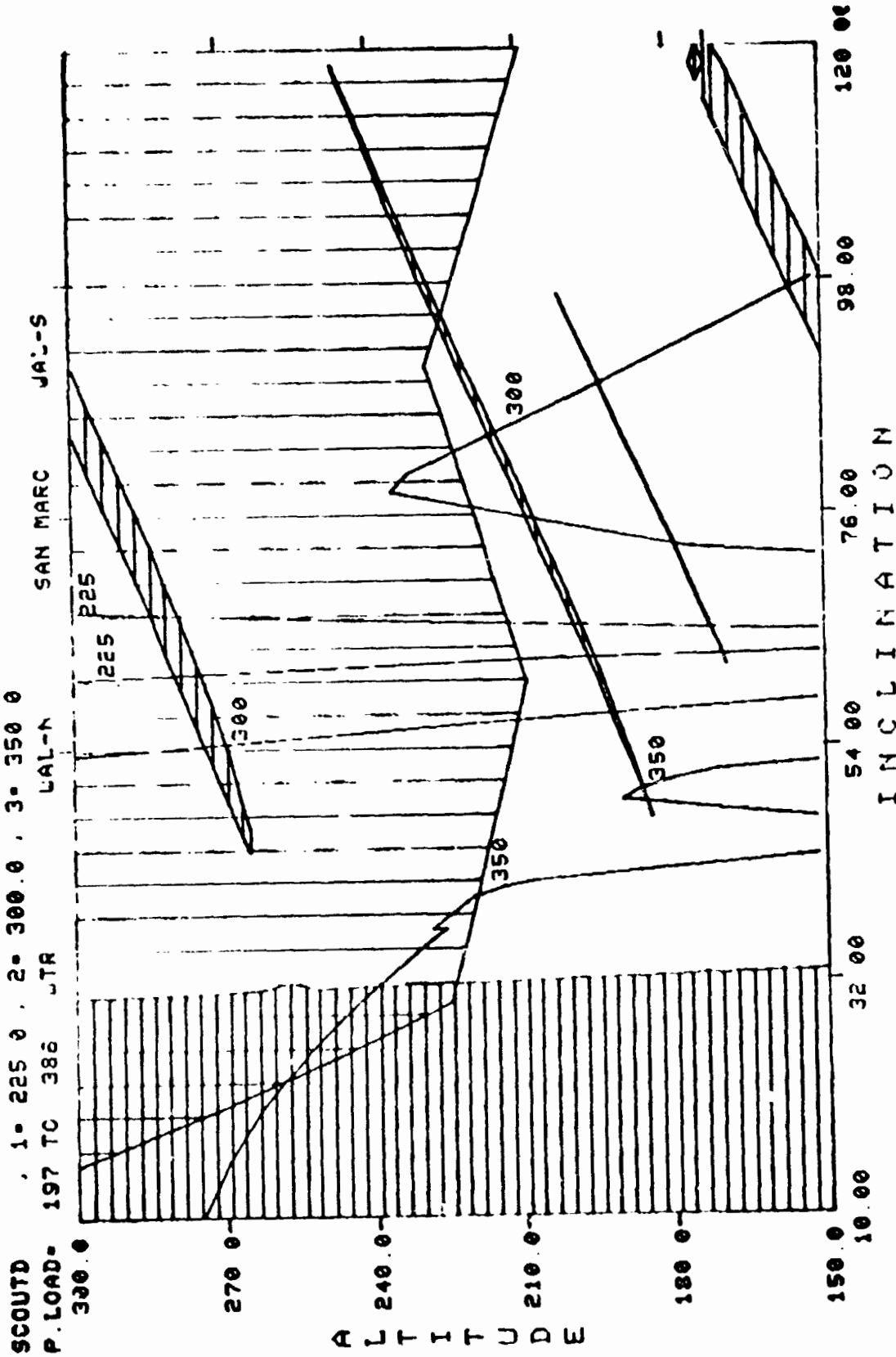


RAD. 25.2000



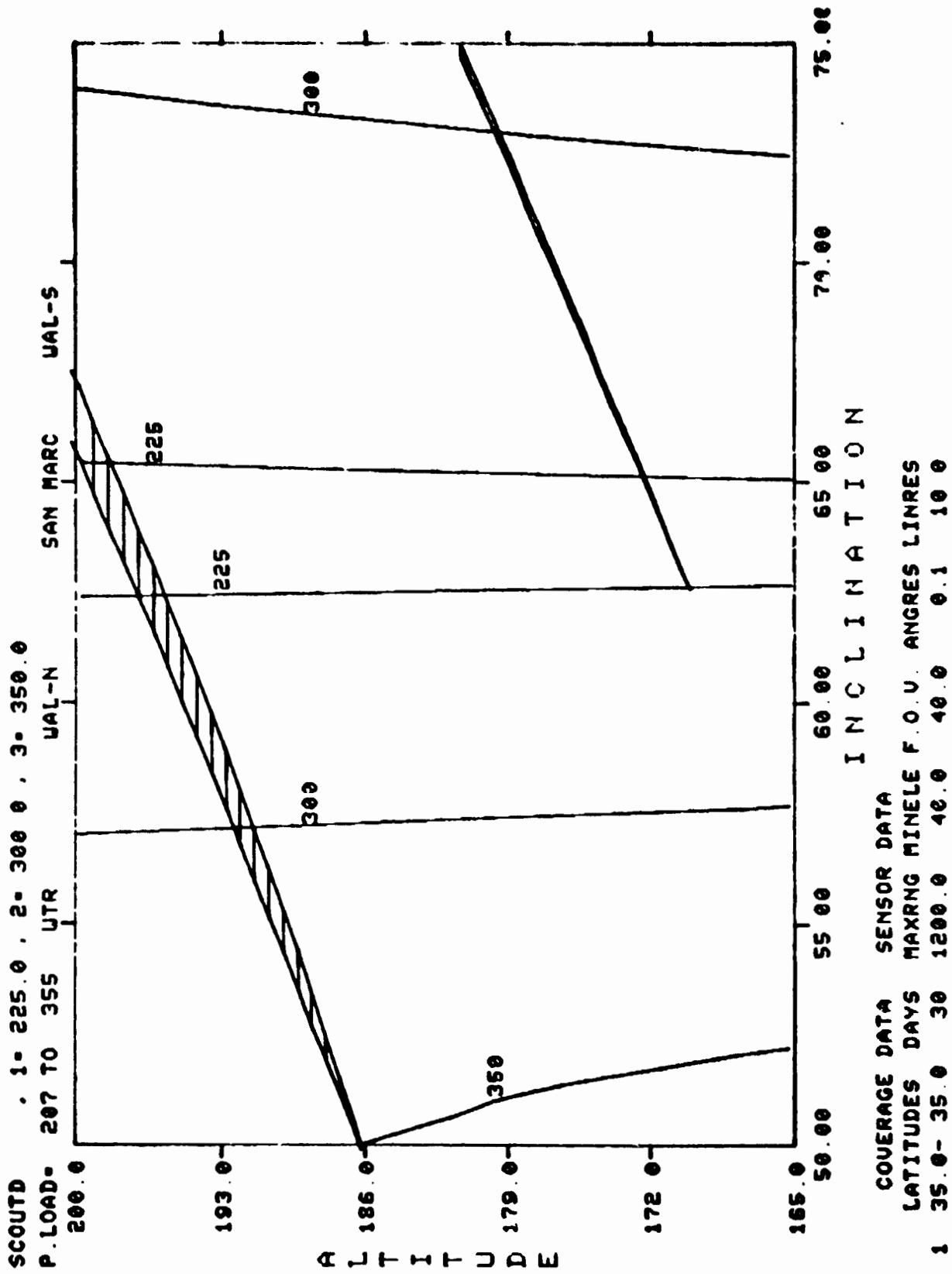
-- RAD. 25.2000



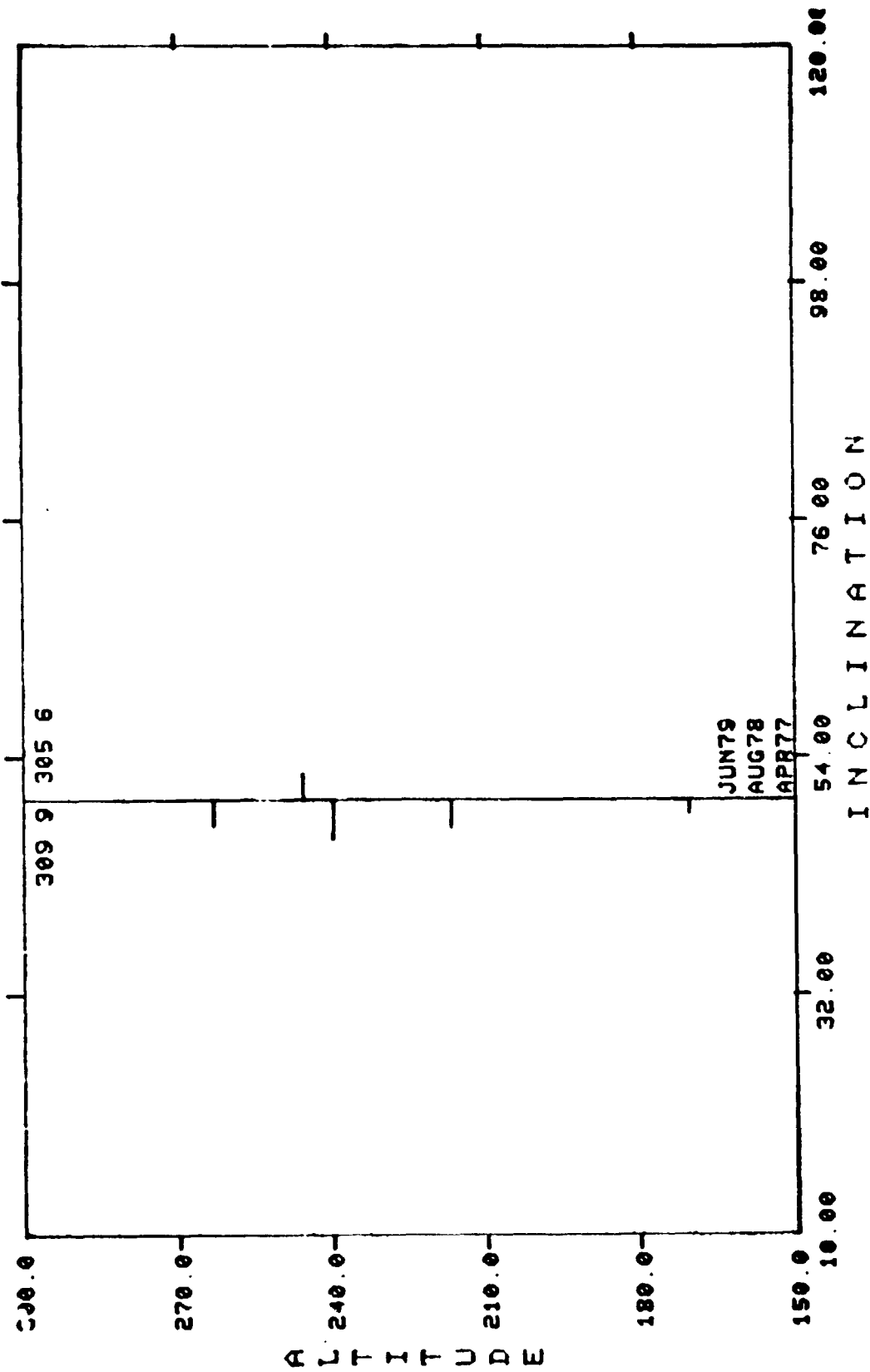


COVERAGE DATA SENSOR DATA  
LATITUDES DAYS MAXRNG HINELE F.O.U. ANGLES LINRES  
1 35.0- 35.0 30 1200.0 40.0 40.0 0.1 10.0

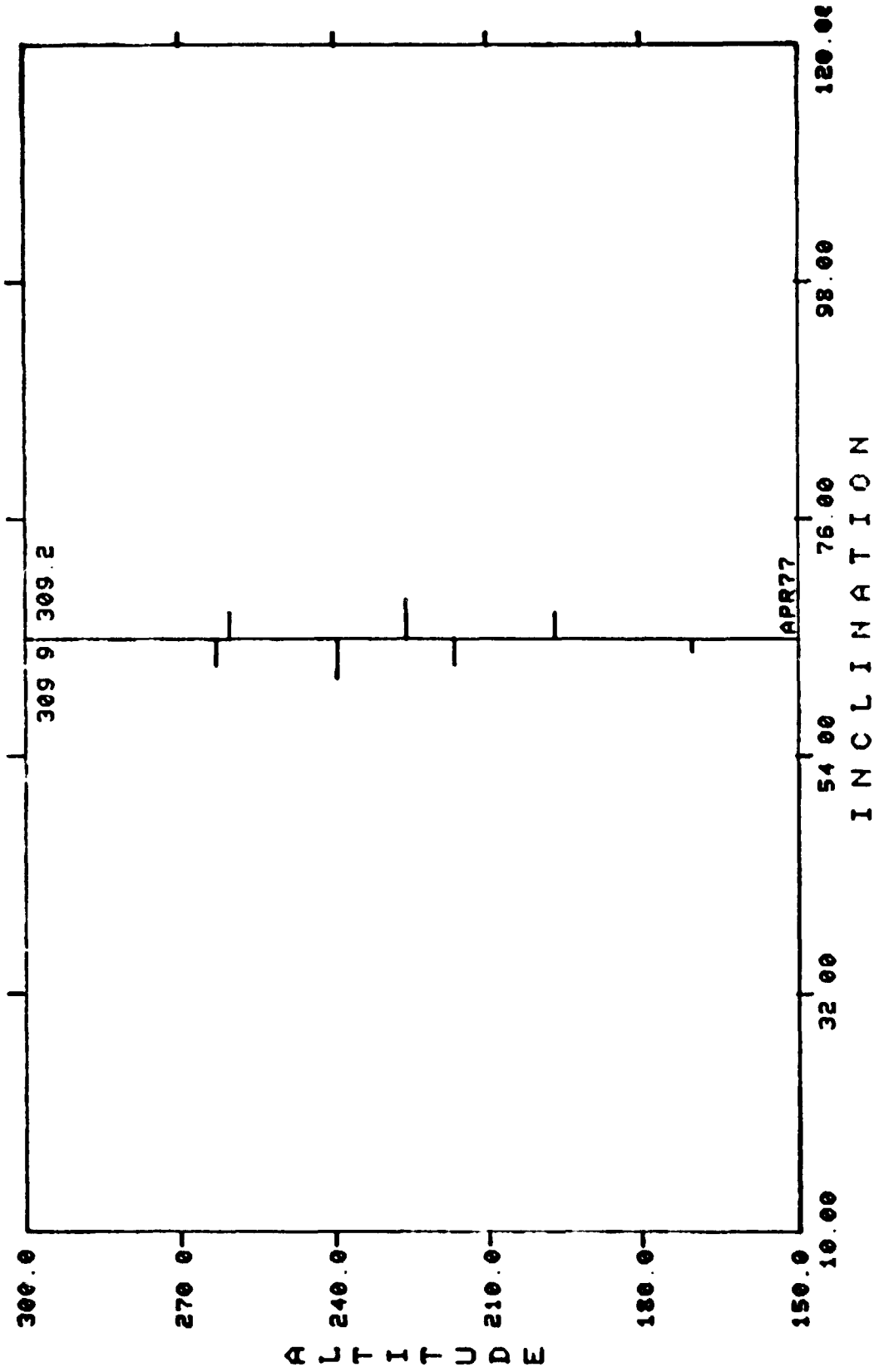
20000525..2000



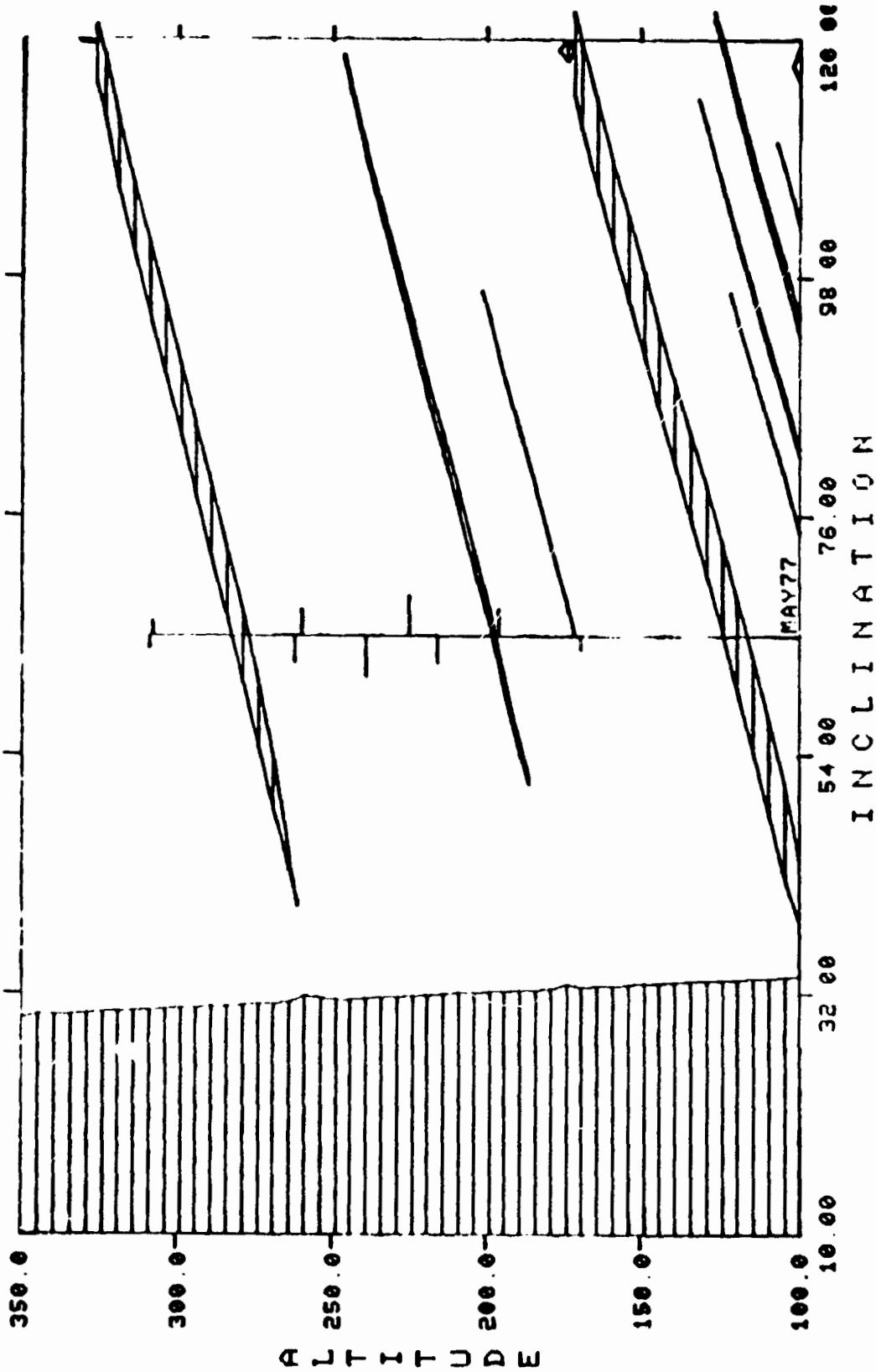
P 000025



-- DECAY.240.50.220.1977.3



-- DECAY, 240.65, 220.1977.1



COVERAGE DATA SENSOR DATA

LATITUDES	DAYS	MAXRNG	MINELE	F.O.U.	ANGRES	LINRES
1	35.0	30	1200.0	40.0	40.0	0.1 10.0

BB00AY.240.65.220.1977.1

## VEHICLE TABLE FOR SCOUTS

ALT. - INC	150.0	168.8	187.5	206.3	225.0	243.8	262.5	281.3	300.0
	PAYLOAD								
10.00	387.2	381.7	376.2	370.7	365.1	359.5	353.9	348.3	342.4
15.24	385.5	380.1	374.6	369.1	363.5	357.9	352.3	346.6	340.8
20.48	383.3	377.8	372.4	366.8	361.3	355.7	350.0	344.3	338.6
25.71	380.3	374.8	369.5	363.9	358.4	352.8	347.1	341.5	335.7
28.39	378.6	373.2	367.7	362.2	356.7	351.1	345.5	339.8	334.1
28.41	378.6	373.2	367.7	362.2	356.7	351.1	345.5	339.8	334.1
30.95	376.8	371.4	366.0	360.5	354.9	349.3	343.7	338.0	332.3
36.19	372.8	367.3	361.9	356.4	350.9	345.3	339.7	334.0	328.3
36.99	372.1	366.7	361.2	355.7	350.2	344.6	339.0	333.4	327.7
37.01	372.9	367.5	362.1	356.6	351.1	345.5	339.9	334.2	328.5
40.00	370.3	364.9	359.5	354.0	348.5	342.9	337.3	331.6	325.9
41.00	368.5	363.0	357.5	352.0	346.6	341.1	335.6	330.1	324.7
41.43	366.7	361.2	355.8	350.3	344.9	339.4	333.9	328.6	323.1
42.00	362.9	357.5	352.2	346.8	341.4	336.1	330.7	325.3	320.0
44.00	348.6	343.5	338.4	333.3	328.1	323.0	317.9	312.8	307.6
45.00	341.9	336.9	331.9	326.9	321.9	316.9	311.9	306.9	301.9
46.67	345.1	340.1	335.0	330.0	325.0	319.9	314.9	309.8	304.8
48.00	354.4	349.2	343.9	338.6	333.3	328.0	322.8	317.5	312.2
49.00	361.5	356.1	350.7	345.3	339.9	334.2	328.6	323.0	317.3
50.00	360.4	355.1	349.7	344.2	338.7	333.2	327.6	322.1	316.3
51.00	358.7	353.2	347.7	342.3	336.8	331.3	325.9	320.5	315.0
51.90	355.9	350.5	345.0	339.6	334.2	328.8	323.4	318.0	312.6
57.14	310.5	306.0	301.4	296.9	292.4	287.8	283.2	278.6	273.9
62.38	231.6	229.2	226.9	224.4	222.0	219.5	216.9	214.4	211.8
64.00	213.1	211.2	209.3	207.3	205.2	203.1	201.0	199.0	197.1
65.00	225.8	223.7	221.5	219.3	217.0	214.6	212.3	209.8	207.4
66.00	237.8	235.4	233.0	230.5	228.0	225.4	222.8	220.1	217.4
67.62	256.5	253.0	249.8	246.9	244.0	241.0	238.1	235.1	232.1
72.86	306.8	302.0	297.3	292.5	287.7	282.9	278.1	273.2	268.4
78.10	324.5	319.1	313.8	308.4	303.1	297.8	292.4	287.1	281.8

ALT.	150.0	168.8	187.5	206.3	225.0	243.8	262.5	281.3	300.0
INC.	----- PAYLOAD -----								
79.00	324.2	318.8	313.4	308.1	302.7	297.4	292.0	286.7	281.3
80.00	323.4	318.2	312.9	307.5	302.1	296.7	291.2	285.6	280.1
81.00	322.1	316.8	311.5	306.2	300.8	295.3	289.9	284.3	278.8
83.33	319.0	313.7	308.4	303.1	297.7	292.3	286.8	281.3	275.7
88.57	312.3	307.0	301.5	296.1	290.8	285.3	279.9	274.4	268.9
93.81	305.6	300.5	295.1	289.6	284.0	278.4	273.0	267.5	262.0
99.05	299.0	294.0	288.8	283.4	277.9	272.3	266.5	260.8	255.3
104.29	292.5	287.6	282.6	277.4	272.0	266.5	260.8	255.0	249.1
109.52	286.3	281.5	276.6	271.5	266.2	260.9	255.3	249.6	243.8
114.76	280.2	275.5	270.7	265.8	260.7	255.4	250.0	244.5	238.8
120.00	274.4	269.9	265.2	260.4	255.4	250.2	245.0	239.5	233.9

## VEHICLE TABLE FOR SCOUTE

ALT. -	150.0	168.8	187.5	206.3	225.0	243.8	262.5	281.3	300.0
INC.	----- SITE -----								
10.00	SAN	MARSAN	MARSAN	MARSAN	MARSAN	MARSAN	MARSAN	MARSAN	MARSAN
15.24	SAN	MARSAN	MARSAN	MARSAN	MARSAN	MARSAN	MARSAN	MARSAN	MARSAN
20.48	SAN	MARSAN	MARSAN	MARSAN	MARSAN	MARSAN	MARSAN	MARSAN	MARSAN
25.71	SAN	MARSAN	MARSAN	MARSAN	MARSAN	MARSAN	MARSAN	MARSAN	MARSAN
28.39	SAN	MARSAN	MARSAN	MARSAN	MARSAN	MARSAN	MARSAN	MARSAN	MARSAN
28.41	SAN	MARSAN	MARSAN	MARSAN	MARSAN	MARSAN	MARSAN	MARSAN	MARSAN
30.95	SAN	MARSAN	MARSAN	MARSAN	MARSAN	MARSAN	MARSAN	MARSAN	MARSAN
36.19	SAN	MARSAN	MARSAN	MARSAN	MARSAN	MARSAN	MARSAN	MARSAN	MARSAN
36.51	SAN	MARSAN	MARSAN	MARSAN	MARSAN	MARSAN	MARSAN	MARSAN	MARSAN
37.01	UAL-N	LAL-N	LAL-N	LAL-N	UAL-N	UAL-N	LAL-N	LAL-N	LAL-N
40.00	UAL-N	UAL-N	UAL-N	LAL-N	LAL-N	UAL-N	UAL-N	LAL-N	LAL-N
41.00	UAL-N	LAL-N	LAL-N	LAL-N	UAL-N	UAL-N	UAL-N	LAL-N	UAL-N
41.43	UAL-N	UAL-N	UAL-N	LAL-N	LAL-N	UAL-N	UAL-N	UAL-N	LAL-N
42.00	UAL-N	LAL-N	LAL-N	LAL-N	UAL-N	UAL-N	UAL-N	LAL-N	UAL-N
44.00	SAN	MARSAN	MARSAN	MARSAN	MARSAN	MARSAN	MARSAN	MARSAN	MARSAN
45.00	SAN	MARSAN	MARSAN	MARSAN	MARSAN	MARSAN	MARSAN	MARSAN	MARSAN
46.67	UAL-S	LAL-S	LAL-S	LAL-S	LAL-S	UAL-S	UAL-S	UAL-S	UAL-S
48.00	UAL-S	UAL-S	UAL-S	UAL-S	UAL-S	UAL-S	LAL-S	UAL-S	UAL-S
49.00	UAL-S	UAL-S	UAL-S	UAL-S	LAL-S	UAL-S	UAL-S	UAL-S	UAL-S
50.00	UAL-S	UAL-S	UAL-S	UAL-S	LAL-S	UAL-S	UAL-S	UAL-S	UAL-S
51.00	UAL-S	UAL-S	UAL-S	UAL-S	UAL-S	UAL-S	UAL-S	LAL-S	UAL-S
51.90	UAL-S	UAL-S	UAL-S	UAL-S	LAL-S	UAL-S	UAL-S	UAL-S	UAL-S
57.14	UAL-S	UAL-S	UAL-S	UAL-S	UAL-S	UAL-S	UAL-S	UAL-S	UAL-S
62.38	UAL-S	UAL-S	UAL-S	UAL-S	LAL-S	UAL-S	UAL-S	UAL-S	UAL-S
64.00	UTR	UTR	UTR	UTR	LTR	UTR	UTR	UTR	UTR
65.00	UTR	UTR	UTR	UTR	UTR	UTR	UTR	UTR	UTR
66.00	UTR	UTR	UTR	UTR	LTR	UTR	UTR	UTR	UTR
67.62	UTR	UTR	UTR	UTR	UTR	UTR	UTR	UTR	UTR
72.86	UTR	UTR	UTR	UTR	UTR	UTR	UTR	UTR	UTR
78.10	UTR	UTR	UTR	UTR	UTR	UTR	UTR	UTR	UTR









## PAYLOAD TABLE FOR SCOUTD

PAYLOAD- INC.	225 00	300 00	350 00	ALTITUDE
10.00	683.45	438.54	275.20	
15.24	678.57	433.44	269.93	
20.48	671.66	426.27	262.54	
25.71	662.82	417.10	253.02	
28.35	657.59	411.67	247.37	
28.41	657.55	411.63	247.33	
30.95	652.13	406.01	241.47	
36.19	639.67	393.08	227.93	
36.99	637.62	390.95	225.70	
37.01	640.42	393.75	228.57	
40.00	632.40	385.44	219.82	
41.00	643.15	385.02	213.21	
41.43	639.57	380.07	207.34	
42.00	632.62	369.53	195.06	
44.00	602.02	327.90	144.97	
45.00	587.52	307.14	119.72	
46.67	596.24	317.78	131.46	
48.00	610.26	343.46	165.75	
49.00	605.26	357.26	189.95	
50.00	601.95	353.86	186.32	
51.00	611.13	351.56	179.65	
51.90	604.63	343.79	170.37	
57.14	499.36	193.48	0.00	
62.38	201.88	0.00	0.00	
64.00	32.02	0.00	0.00	
65.00	157.30	0.00	0.00	
66.00	246.65	0.00	0.00	
67.62	344.06	0.00	0.00	
72.86	468.96	176.67	0.00	
78.10	500.39	235.85	61.01	

REPRODUCTION OF THIS  
COPY IS PROHIBITED

PAYLOAD- INC.	225.00	300.00	350.00	ALTITUDE
79.00	498.07	234.45	60.45	
80.00	485.52	232.23	55.45	
81.00	481.25	227.69	50.64	
83.33	471.24	216.98	40.01	
88.57	448.59	192.79	17.00	
93.81	425.87	170.34	0.00	
99.05	403.24	146.36	0.00	
104.29	375.83	121.51	0.00	
109.52	360.62	96.02	0.00	
114.76	345.32	70.11	0.00	
120.00	330.07	44.04	0.00	

## SENSOR TABLE

ALT (MM)	PSI-MN (DEG)	LIMIT	MAXRNG -----P S	MINELE S	F O U ( D E G )	ANGRES -----
100.0	1.41	F O U	13.65	1.85	1.41	5.11
100.5	1.42	F O U	13.68	1.90	1.42	5.13
101.0	1.43	F O U	13.72	1.91	1.43	5.15
101.5	1.43	F O U	13.75	1.92	1.43	5.17
102.0	1.44	F O U	13.78	1.93	1.44	5.20
102.5	1.45	F O U	13.82	1.94	1.45	5.23
103.0	1.46	F O U	13.85	1.95	1.46	5.24
103.5	1.46	F O U	13.88	1.96	1.46	5.26
104.0	1.47	F O U	13.91	1.96	1.47	5.28
104.5	1.48	F O U	13.95	1.97	1.48	5.30
105.0	1.48	F O U	13.95	1.98	1.48	5.32
105.5	1.49	F O U	14.01	1.95	1.49	5.34
106.0	1.50	F O U	14.04	2.00	1.50	5.37
106.5	1.51	F O U	14.08	2.01	1.51	5.39
107.0	1.51	F O U	14.11	2.03	1.51	5.41
107.5	1.52	F O U	14.14	2.03	1.52	5.43
108.0	1.53	F O U	14.17	2.04	1.53	5.45
108.5	1.53	F O U	14.20	2.04	1.53	5.47
109.0	1.54	F O U	14.24	2.05	1.54	5.49
109.5	1.55	F O U	14.27	2.06	1.55	5.51
110.0	1.56	F O U	14.30	2.07	1.56	5.53
110.5	1.56	F O U	14.33	2.08	1.56	5.55
111.0	1.57	F O U	14.36	2.09	1.57	5.57
111.5	1.58	F O U	14.39	2.10	1.58	5.59
112.0	1.58	F O U	14.43	2.11	1.58	5.61
112.5	1.59	F O U	14.46	2.12	1.59	5.64
113.0	1.60	F O U	14.49	2.13	1.60	5.66
113.5	1.61	F O U	14.52	2.13	1.61	5.68
114.0	1.61	F O U	14.55	2.14	1.61	5.70
114.5	1.62	F O U	14.58	2.15	1.62	5.72

ALT (NM)	PSI-MN (DEG)	LIMIT	MAXRNG -----P	MINELE S I	F O U ( D E G )	ANGRES -----
115 0	1 63	F O U	14 61	2 16	1 63	9 74
115 5	1 63	F O U	14 64	2 17	1 63	9 76
116 0	1 64	F O U	14 67	2 18	1 64	9 78
116 5	1 65	F O U	14 71	2 19	1 65	9 80
117 0	1 66	F O U	14 74	2 20	1 66	9 82
117 5	1 66	F O U	14 77	2 21	1 66	9 84
118 0	1 67	F O U	14 80	2 21	1 67	9 86
118 5	1 68	F O U	14 83	2 22	1 68	9 88
119 0	1 68	F O U	14 86	2 23	1 68	9 90
119 5	1 69	F O U	14 89	2 24	1 69	9 92
120 0	1 70	F O U	14 92	2 25	1 70	9 93

VEHICLE LIBRARY

1-SCOUTD  
2-DELTA2910  
3-DELTA2610  
4-DELTA2310  
5-SCOUTF